

Transfer Matrices and Partition-Function Zeros for Antiferromagnetic Potts Models

VI. Square Lattice with Extra-Vertex Boundary Conditions

Jesús Salas

Instituto Gregorio Millán

and

Grupo de Modelización, Simulación Numérica y Matemática Industrial

Universidad Carlos III de Madrid

Avda. de la Universidad, 30

28911 Leganés, SPAIN

JSALAS@MATH.UC3M.ES

Alan D. Sokal*

Department of Physics

New York University

4 Washington Place

New York, NY 10003 USA

SOKAL@NYU.EDU

February 19, 2010

revised June 6, 2011

Abstract

We study, using transfer-matrix methods, the partition-function zeros of the square-lattice q -state Potts antiferromagnet at zero temperature (= square-lattice chromatic polynomial) for the boundary conditions that are obtained from an $m \times n$ grid with free boundary conditions by adjoining one new vertex adjacent to all the sites in the leftmost column and a second new vertex adjacent to all the sites in the rightmost column. We provide numerical evidence that the partition-function zeros are becoming dense everywhere in the complex q -plane outside the limiting curve $\mathcal{B}_\infty(\text{sq})$ for this model with ordinary (e.g. free or cylindrical) boundary conditions. Despite this, the infinite-volume free energy is perfectly analytic in this region.

Key Words: Chromatic polynomial, chromatic roots, Tutte polynomial, Potts model, transfer matrix, Beraha–Kahane–Weiss theorem, planar graph, square lattice, extra-vertex boundary conditions.

*Also at Department of Mathematics, University College London, London WC1E 6BT, England.

Contents

1	Introduction	4
2	Preliminaries	7
2.1	Chromatic polynomials, Potts models, and all that	8
2.2	Transfer matrices	9
2.3	Beraha–Kahane–Weiss theorem	11
2.4	Chromatic roots of bi-fans and bipyramids	12
2.5	Chromatic roots of generalized theta graphs	14
3	Transfer-matrix theory for the family $\mathcal{S}_{m,n}$	15
3.1	Basic method	16
3.2	Block-diagonalization of the transfer matrix (I)	17
3.3	Block-diagonalization of the transfer matrix (II)	23
3.4	Relating the partition function to the transfer-matrix eigenvalues	25
3.5	Comparing $\mathcal{S}_{m,n}^\neq$ with $\mathcal{S}_{m,n}^=$	27
4	Numerical results I: Large-q expansion of the leading eigenvalue	29
4.1	Overview of method and results	29
4.2	Results for $\mathcal{S}_{m,n}^\neq$	32
4.3	Results for $\mathcal{S}_{m,n}^=$	35
4.4	Comparing $\mathcal{S}_{m,n}^\neq$ with $\mathcal{S}_{m,n}^=$	36
4.5	Summary of conjectured behavior	39
5	Thermodynamic limit $m \rightarrow \infty$ of the free energies	40
5.1	Generalities and finite-size-scaling theory	41
5.2	Overview of computations and results	43
5.3	Hand calculation of large- q expansion for the bulk, surface and corner free energies	44
5.4	Exact results for the bulk, surface and corner free energies	47
5.5	Families $\mathcal{S}_{m,n}^\neq$ and $\mathcal{S}_{m,n}^=$ via strip free energies	49
6	Numerical results II: Limiting curves \mathcal{B}_m	50
6.1	$m = 1$	51
6.2	$m = 2$	51
6.3	$m = 3$	53
6.4	$m = 4$	54
6.5	$m = 5$	54
6.6	$m = 6$	55
6.7	Comparison of $1 \leq m \leq 6$	55
7	Conjectures on the limiting curves \mathcal{B}_m as $m \rightarrow \infty$	56
7.1	Behavior at large $ q $ for each m	56
7.2	Uniformity in m and density of chromatic roots	58
7.3	Size of the discontinuity in the derivative of the free energy	60

7.4	Largest magnitude of a chromatic root	60
8	Discussion	61
8.1	Comparison with the work of Jacobsen, Saleur and Dubail	61
8.2	Density of zeros	62
8.3	Some concluding remarks	63
A	Proof of Proposition 3.5	64
B	Dimension of the transfer matrices	68
B.1	Catalan, Motzkin and Riordan numbers	68
B.2	Partitions on a circle modulo reflection	69
B.3	The dimensions $N_{\neq}(m)$ and $N_{=}(m)$	75
C	Chromatic polynomials for the family $\hat{S}_{m,n}$	76
	References	80

1 Introduction

It is well known that phase transitions do not occur in statistical-mechanical systems in finite volume, but occur only in the infinite-volume limit. One approach to studying phase transitions was introduced by Yang and Lee [72] in 1952, and involves investigating the zeros of the finite-volume partition function when one or more physical parameters (e.g. temperature or magnetic field) are allowed to take *complex* values. Lee and Yang showed, under mild conditions, that the accumulation points of these zeros in the infinite-volume limit constitute the only possible loci of phase transitions; away from such accumulation points of zeros, the infinite-volume free energy is analytic.

We would like to stress the word “possible” in the preceding sentence. The finite-volume free energy is of course singular at any zero of the finite-volume partition function (since $\log 0 = -\infty$); but it can happen that such a singularity disappears in the infinite-volume limit. To take a trivial example, suppose that the partition function in volume n is $Z_n(x) = x$, where x is a parameter; then the finite-volume free energy $f_n(x) = n^{-1} \log Z_n(x) = n^{-1} \log x$ is singular at $x = 0$, but the infinite-volume free energy $f(x) = \lim_{n \rightarrow \infty} f_n(x) = 0$ is analytic at $x = 0$.¹

In this paper we would like to give an extreme example of this phenomenon, in which the zeros of the finite-volume partition functions appear to be *dense* in a large region of the complex plane, while the infinite-volume free energy is perfectly analytic there.² Our example consists of the square-lattice Potts antiferromagnet at zero temperature — a model that we have studied in a series of previous papers [34–36, 38, 53, 54] — but with some unusual boundary conditions. We begin by reviewing the needed background on Potts models and chromatic polynomials.

The Potts model [47, 70, 71] on a regular lattice \mathcal{L} is characterized by two parameters: the number q of Potts spin states, and the nearest-neighbor coupling $v = e^{\beta J} - 1$.³ Initially q is a positive integer and v is a real number in the interval $[-1, +\infty)$, but the Fortuin–Kasteleyn representation (reviewed in Section 2.1 below) shows that the partition function $Z_G(q, v)$ of the q -state Potts model on any finite graph G is in fact a *polynomial* in q and v . This allows us to interpret q and v as taking arbitrary real or even complex values, and to study the phase diagram of the Potts model in the real (q, v) -plane or in complex

¹One could object that in this case we actually have

$$f(x) = \begin{cases} 0 & \text{for } x \neq 0 \\ -\infty & \text{for } x = 0 \end{cases}$$

which is not analytic at $x = 0$ (though the singularity at $x = 0$ is removable). Here is a variant that avoids this objection: $Z_n(x) = x - 1/n$. Then the finite-volume free energy $f_n(x) = n^{-1} \log Z_n(x)$ is singular at $x = 1/n$, but it is easy to see that $f(x) = \lim_{n \rightarrow \infty} f_n(x) = 0$ for all x (including $x = 0$).

²See also Section 8.2 for a brief discussion of the general question: When does an accumulation of partition-function zeros signal a nonanalyticity of the infinite-volume free energy?

³Here we are considering only the *isotropic* model, in which each nearest-neighbor edge is assigned the same coupling v . In a more refined analysis, one could put (for example) different couplings v_1, v_2 on the horizontal and vertical edges of the square lattice, different couplings v_1, v_2, v_3 on the three orientations of edges of the triangular or hexagonal lattice, etc.

(q, v) -space. In particular, by studying the zeros of $Z_G(q, v)$ in complex (q, v) -space for larger and larger pieces of the lattice \mathcal{L} , we can locate the possible loci of phase transitions in the real (q, v) -plane and more generally in complex (q, v) -space.

The partition function for $m \times n$ lattices can be efficiently computed using *transfer matrices*. Though the dimension of the transfer matrix (and thus the computational complexity) grows exponentially in the width m — thereby restricting us in practice to widths $m \lesssim 10$ – 30 — it is straightforward, by iterating the transfer matrix, to handle quite large lengths n . Indeed, by implementing the transfer-matrix method *symbolically* (i.e., as polynomials in q and/or v) and using the Beraha–Kahane–Weiss theorem (reviewed in Section 2.3), we can handle directly the limit $n \rightarrow \infty$ and compute the limiting curves \mathcal{B}_m of partition-function zeros. At a second stage we attempt to extrapolate these curves to $m = \infty$.

Since the problem of computing the phase diagram in complex (q, v) -space is difficult, it has proven convenient to study first certain “slices” through (q, v) -space, in which one parameter is fixed (usually at a real value) while the remaining parameter is allowed to vary in the complex plane. One very interesting special case is the chromatic polynomial ($v = -1$), which corresponds to the zero-temperature limit of the Potts antiferromagnet ($\beta J = -\infty$). In previous papers [34–36, 38, 53, 54] we have used symbolic transfer-matrix methods to study the square-lattice and triangular-lattice chromatic polynomials for free, cylindrical, cyclic and toroidal boundary conditions.^{4,5} Here we shall study the square-lattice model for the boundary conditions that are obtained from an $m_F \times n_F$ square grid (m columns, n rows, free boundary conditions in both directions) by adjoining one new vertex adjacent to all the sites in the leftmost column and a second new vertex adjacent to all the sites in the rightmost column (see Figure 1a).

The motivation for studying this family of graphs comes in part from work of one of the authors [63] on the *generalized theta graphs* [12]: namely, $\Theta^{(s,p)}$ is defined to be the graph consisting of p chains in parallel between a pair of endvertices, each chain consisting of s edges in series (Figure 2). For this family, the following result holds:

Theorem 1.1 [63, Theorems 1.1, 1.2 and 1.4] *The set of chromatic roots of all the graphs $\Theta^{(s,p)}$ is dense in the entire complex q -plane with the possible exception of the disc $|q - 1| < 1$.*

The proof of Theorem 1.1 proceeds in two steps: First, one fixes s , and shows that as $p \rightarrow \infty$ the chromatic roots of the graphs $\Theta^{(s,p)}$ accumulate densely on an explicitly computable real algebraic curve \mathcal{C}_s . This argument is a straightforward application of the Beraha–Kahane–Weiss theorem. Second, one shows that as $s \rightarrow \infty$ the curves \mathcal{C}_s become dense in $\mathbb{C} \setminus \{|q - 1| < 1\}$. This requires an *ad hoc* (but not terribly difficult) argument. See Section 2.5 for a slightly more detailed summary.

⁴See also the bibliographies of [34–36, 38, 53, 54] for reference to the important related works of Shrock and collaborators.

⁵We adopt Shrock’s [56] terminology for boundary conditions: free ($m_F \times n_F$), cylindrical ($m_P \times n_F$), cyclic ($m_F \times n_P$), toroidal ($m_P \times n_P$), Möbius ($m_F \times n_{TP}$) and Klein bottle ($m_P \times n_{TP}$). Here the first dimension (m) corresponds to the transverse (“short”) direction, while the second dimension (n) corresponds to the longitudinal (“long”) direction. The subscripts F, P and TP denote free, periodic and twisted-periodic boundary conditions, respectively.

The computations arising in the proof of Theorem 1.1 are based on the series and parallel reduction laws for the Potts-model partition function [63, 64]. This approach works because the graphs $\Theta^{(s,p)}$ are *series-parallel*: we can compute the partition function $Z_{\Theta^{(s,p)}}(q, v)$ by computing the “effective coupling” v_{eff} arising from putting s edges (each of weight v) in series and then placing p such chains in parallel.

No such simple approach can work for the graphs $S_{m,n}$, because they are not series-parallel. Still, the graphs $S_{m,n}$ and the generalized theta graphs are closely related: indeed, the generalized theta graph $\Theta^{(m+1,n)}$ is obtained from $S_{m,n}$ simply by deleting all the vertical edges. So it would not be surprising if the density-of-roots phenomenon observed for the generalized theta graphs occurred also for the family $S_{m,n}$. In this paper we would like to present some convincing evidence — which, however, falls short at present of a rigorous mathematical proof — that this is indeed the case (see in particular Conjecture 7.2 below).

As in the analysis [63] of the generalized theta graphs, we proceed in two steps. First we fix m , and show that as $n \rightarrow \infty$ the chromatic roots of the graphs $S_{m,n}$ accumulate densely on a real algebraic curve \mathcal{B}_m (as well as on certain isolated points). This argument is once again a straightforward application of the Beraha–Kahane–Weiss theorem. The more difficult problem is to compute the curves \mathcal{B}_m and to study their behavior as $m \rightarrow \infty$. In this paper we shall use the transfer-matrix formalism developed in [11, 34, 38, 53, 54] to compute the curves \mathcal{B}_m for $m \leq 6$ (see Figures 9–14 in Sections 6 and 7 below). We will see that the curve \mathcal{B}_m contains $2m$ outward branches running to infinity in the complex q -plane and equally spaced in asymptotic angle. Moreover, these branches appear to become dense as $m \rightarrow \infty$ everywhere in the complex q -plane outside the limiting curve $\mathcal{B}_\infty(\text{sq})$ for this model with ordinary (e.g. free or cylindrical) boundary conditions — a curve that we have estimated numerically in previous papers [34, 53] and which is entirely contained inside the disc $|q - 1| \leq 3$ (to give a crude bound). If this is indeed the case, it follows that the zeros of the chromatic polynomials of the graphs $S_{m,n}$ are likewise becoming dense everywhere outside $\mathcal{B}_\infty(\text{sq})$ and in particular everywhere in the region $|q - 1| > 3$.

As will be explained in Section 7 below (drawing on results from Section 4), these outward branches arise from the fact that the transfer matrix $T''(m)$ for this model has two eigenvalues — coming from two sectors in the block-diagonalization of $T''(m)$ — that are almost equal at large q , with a relative difference of order q^{-m} , and which compete for dominance: the outward branches of the curves \mathcal{B}_m are nothing other than the loci where these two eigenvalues are equal in modulus. On the other hand, the difference between these two eigenvalues disappears as $m \rightarrow \infty$ when $|q|$ is large enough, with the result that the infinite-volume free energy is perfectly analytic at large $|q|$.

A behavior of this type was observed recently by Jacobsen, Richard and Salas [33] for the Potts model with *cyclic* boundary conditions (i.e. *periodic* boundary conditions in the longitudinal direction) when q is fixed at a Beraha number and the temperature variable v is taken complex. On the square (resp. triangular) lattice, there are two eigenvalues — coming once again from two sectors in the block-diagonalization of the transfer matrix — that are almost equal at large v , with a relative difference of order v^{-m} (resp. $v^{-(2m-1)}$). This leads to $2m$ (resp. $4m - 2$) outward branches in the curve \mathcal{B}_m that appear to become dense as $m \rightarrow \infty$ everywhere outside a bounded region in the complex v -plane. These

same outward branches were observed earlier by Shrock and Chang for $m = 1, 2$ [55] and $m = 3$ [15] on the square lattice and for $m = 2$ on the triangular lattice [14]; they exist for *all* $q \neq 0, 1$, not only Beraha numbers.

The principle underlying all these examples is a general one: Suppose that the transfer matrix at some parameter value x_0 has two dominant eigenvalues of equal modulus, call them $\lambda_1(x_0)$ and $\lambda_2(x_0) = e^{i\theta}\lambda_1(x_0)$, and that for parameters $x \approx x_0$ we have $\lambda_2(x) - e^{i\theta}\lambda_1(x) = A(x - x_0)^k + o((x - x_0)^k)$ with $A \neq 0$ and some integer $k \geq 1$ [with the obvious modifications in case $x_0 = \infty$]. Then the curve \mathcal{B}_m contains $2k$ branches passing through x_0 , with an asymptotic angle π/k between neighboring branches. If $k = 1$ this is simply the generic situation for equimodular curves; if $k > 1$ it corresponds to a higher-order crossing. In particular, if k tends to infinity as $m \rightarrow \infty$, these branches are likely to become dense in a neighborhood of x_0 .

The plan of this paper is as follows: In Section 2 we review some needed background on chromatic and Tutte polynomials, transfer matrices, and the Beraha–Kahane–Weiss theorem. In Section 3 we present the transfer-matrix theory for the family $S_{m,n}$ and we prove some properties of the dominant diagonal elements and the dominant eigenvalues. In Section 4 we present the results of our transfer-matrix computation of the large- q expansion of the leading eigenvalues for $1 \leq m \leq 11$ and note some surprising properties. In Section 5 we study the thermodynamic limit $m \rightarrow \infty$ of the corresponding free energies. In Section 6 we present the numerically computed limiting curves \mathcal{B}_m for widths $1 \leq m \leq 6$. In Section 7 we present some conjectures on the behavior of these limiting curves as $m \rightarrow \infty$ and we relate these conjectures to the properties of the eigenvalues that were empirically observed in Section 4. Finally, in Section 8 we conclude with some brief discussion and suggestions for future research. In Appendix A we prove Proposition 3.5 concerning the dominant diagonal entries in the transfer matrix. In Appendix B we compute a general formula for the dimensions of our transfer matrices as a function of the width m . In Appendix C we present the transfer-matrix theory for the family $\hat{S}_{m,n}$ obtained by a 90° rotation of the grid; this plays an important role in checking the correctness of our transfer-matrix computations.

2 Preliminaries

In this section we review briefly some needed background on chromatic and Tutte polynomials (Section 2.1), transfer matrices (Section 2.2), and the Beraha–Kahane–Weiss theorem (Section 2.3). We also recall the easy analysis of the chromatic roots of bi-fans and bipyramids (Section 2.4) and briefly summarize the argument from [63] concerning the chromatic roots of generalized theta graphs (Section 2.5); both of these will serve as models for our analysis here of the graphs $S_{m,n}$.

2.1 Chromatic polynomials, Potts models, and all that

Let $G = (V, E)$ be a finite undirected graph, and let q be a positive integer. Then the q -state Potts-model partition function for the graph G is defined by the Hamiltonian

$$H_{\text{Potts}}(\boldsymbol{\sigma}) = - \sum_{e=ij \in E} J_e \delta(\sigma_i, \sigma_j) , \quad (2.1)$$

where the spins $\boldsymbol{\sigma} = \{\sigma_i\}_{i \in V}$ take values in $\{1, 2, \dots, q\}$, the J_e are coupling constants, and the δ is the Kronecker delta

$$\delta(a, b) = \begin{cases} 1 & \text{if } a = b \\ 0 & \text{if } a \neq b \end{cases} \quad (2.2)$$

The partition function can then be written as

$$Z_G^{\text{Potts}}(q, \mathbf{v}) = \sum_{\sigma: V \rightarrow \{1, 2, \dots, q\}} \prod_{e=ij \in E} [1 + v_e \delta(\sigma_i, \sigma_j)] , \quad (2.3)$$

where $v_e = e^{\beta J_e} - 1$. Please note, in particular, that if we set $v_e = -1$ for all edges e , then Z_G^{Potts} gives weight 1 to each proper coloring and weight 0 to each improper coloring, and so counts the proper colorings. Proper q -colorings ($v_e = -1$) thus correspond to the zero-temperature ($\beta \rightarrow +\infty$) limit of the antiferromagnetic ($J_e < 0$) Potts model.

It is far from obvious that $Z_G^{\text{Potts}}(q, \mathbf{v})$, which is defined separately for each positive integer q , is in fact the restriction to $q \in \mathbb{Z}_+$ of a *polynomial* in q . But this is in fact the case, and indeed we have:

Theorem 2.1 (Fortuin–Kasteleyn [27, 42] representation of the Potts model)

For integer $q \geq 1$,

$$Z_G^{\text{Potts}}(q, \mathbf{v}) = \sum_{A \subseteq E} q^{k(A)} \prod_{e \in A} v_e , \quad (2.4)$$

where $k(A)$ denotes the number of connected components in the subgraph (V, A) .

PROOF. In (2.3), expand out the product over $e \in E$, and let $A \subseteq E$ be the set of edges for which the term $v_e \delta(\sigma_i, \sigma_j)$ is taken. Now perform the sum over maps $\sigma: V \rightarrow \{1, 2, \dots, q\}$: in each component of the subgraph (V, A) the color σ_i must be constant, and there are no other constraints. We immediately obtain (2.4). \square

Historical Remark. The subgraph expansion (2.4) was discovered by Birkhoff [10] and Whitney [69] for the special case $v_e = -1$ (see also Tutte [67, 68]); in its general form it is due to Fortuin and Kasteleyn [27, 42] (see also [21]).

The foregoing considerations motivate defining the *multivariate Tutte polynomial* of the graph G :

$$Z_G(q, \mathbf{v}) = \sum_{A \subseteq E} q^{k(A)} \prod_{e \in A} v_e , \quad (2.5)$$

where q and $\mathbf{v} = \{v_e\}_{e \in E}$ are commuting indeterminates. If we set all the edge weights v_e equal to the same value v , we obtain a two-variable polynomial that is equivalent to the standard Tutte polynomial $T_G(x, y)$ after a simple change of variables (see [64]). If we set all the edge weights v_e equal to -1 , we obtain the *chromatic polynomial* $P_G(q) = Z_G(q, -1)$.

Further information on the multivariate Tutte polynomial $Z_G(q, \mathbf{v})$ can be found in a recent survey article [64].

2.2 Transfer matrices

For any family of graphs $G_n = (V_n, E_n)$ consisting of n identical “layers” with identical connections between adjacent layers, the multivariate Tutte polynomials of the G_n (with edge weights likewise repeated from layer to layer) can be written in terms of a transfer matrix [11, 53]. Here we briefly summarize the needed formalism [53] specialized to the case of an $m \times n$ square lattice with free boundary conditions in both directions. The modifications needed to handle the extra sites at left and right in the graphs $S_{m,n}$ will be discussed in Section 3.

Consider the $m \times n$ square grid with edge weights $v_{i,i+1}$ on the horizontal edges ($1 \leq i \leq m-1$) and v_i on the vertical edges ($1 \leq i \leq m$). We fix the “width” m and consider the family of graphs G_n obtained by varying the “length” n ; our goal is to calculate the multivariate Tutte polynomials $Z_{G_n}(q, \mathbf{v})$ for this family by building up the graph G_n layer by layer. What makes this a bit tricky is the nonlocality of the factor $q^{k(A)}$ in (2.5). At the end we will need to know the number of connected components in the subgraph (V_n, A) ; in order to be able to compute this, we shall keep track, as we go along, of which sites in the current “top” layer are connected to which other sites in that layer by a path of occupied edges (i.e. edges of A) in lower layers. Thus, we shall work in the basis of connectivities of the top layer, whose basis elements $\mathbf{e}_{\mathcal{P}}$ are indexed by partitions \mathcal{P} of the single-layer vertex set $\{1, \dots, m\}$. The elementary operators we shall need are:

- The *join operators*

$$J_{ij} \mathbf{e}_{\mathcal{P}} = \mathbf{e}_{\mathcal{P} \bullet ij}, \quad (2.6)$$

where $\mathcal{P} \bullet ij$ is the partition obtained from \mathcal{P} by amalgamating the blocks containing i and j (if they were not already in the same block). Note that all these operators commute.

- The *detach operators*

$$D_i \mathbf{e}_{\mathcal{P}} = \begin{cases} \mathbf{e}_{\mathcal{P} \setminus i} & \text{if } \{i\} \notin \mathcal{P} \\ q \mathbf{e}_{\mathcal{P}} & \text{if } \{i\} \in \mathcal{P} \end{cases} \quad (2.7)$$

where $\mathcal{P} \setminus i$ is the partition obtained from \mathcal{P} by detaching i from its block (and thus making it a singleton). Note that these operators commute as well.

Note, finally, that D_k commutes with J_{ij} whenever $k \notin \{i, j\}$.

The horizontal transfer matrix, which adds a row of horizontal edges, is

$$H = \prod_{i=1}^{m-1} (1 + v_{i,i+1} J_{i,i+1}) \quad (2.8)$$

(note that all the operators in the product commute). The vertical transfer matrix, which adds a new row of sites along with the corresponding vertical edges, is

$$\mathbf{V} = \prod_{i=1}^m (v_i I + \mathbf{D}_i) \quad (2.9)$$

(note once again that all the operators commute). The multivariate Tutte polynomial for G_n is then given [53] by the formula

$$Z_{G_n}(q, \mathbf{v}) = \boldsymbol{\omega}^T \mathbf{H} (\mathbf{V} \mathbf{H})^{n-1} \mathbf{e}_{\text{id}} , \quad (2.10)$$

where “id” denotes the partition in which each site $i \in \{1, \dots, m\}$ is a singleton, and the “end vector” $\boldsymbol{\omega}^T$ is defined by

$$\boldsymbol{\omega}^T \mathbf{e}_{\mathcal{P}} = q^{|\mathcal{P}|} . \quad (2.11)$$

The transfer matrix is thus

$$\mathbf{T} = \mathbf{V} \mathbf{H} . \quad (2.12)$$

In what follows we shall use a convenient shorthand notation for the basis vectors $\mathbf{e}_{\mathcal{P}}$: namely, we denote by $\mathbf{1}$ the basis element \mathbf{e}_{id} corresponding to the partition in which each site is a singleton, and we denote the action on \mathbf{e}_{id} of a join operator \mathbf{J}_{ij} by the Kronecker deltas δ_{ij} . Thus, for instance, for $m = 3$ we have the five basis vectors

$$\mathbf{e}_{\text{id}} \equiv \mathbf{e}_{\{\{1\}, \{2\}, \{3\}\}} = \mathbf{1} \quad (2.13a)$$

$$\mathbf{e}_{\{\{1,2\}, \{3\}\}} = \delta_{12} \quad (2.13b)$$

$$\mathbf{e}_{\{\{1,3\}, \{2\}\}} = \delta_{13} \quad (2.13c)$$

$$\mathbf{e}_{\{\{1\}, \{2,3\}\}} = \delta_{23} \quad (2.13d)$$

$$\mathbf{e}_{\{\{1,2,3\}\}} = \delta_{123} \equiv \delta_{12}\delta_{13}\delta_{23} = \delta_{12}\delta_{13} = \delta_{12}\delta_{23} = \delta_{13}\delta_{23} \quad (2.13e)$$

For $m \geq 4$ we also have basis vectors that are products of deltas, such as $\delta_{13}\delta_{24}$ and so forth. This notation allows describing partitions and their corresponding basis vectors in a fairly compact way.

In principle we are working here in the space spanned by the basis vectors $\mathbf{e}_{\mathcal{P}}$ for all partitions \mathcal{P} of $\{1, \dots, m\}$; the dimension of this space is given by the Bell number B_m [18, 61, 65, 66]. However, it is easy to see, on topological grounds (thanks to the planarity of the G_n), that only *non-crossing* partitions can arise. (A partition is said to be *non-crossing* if $a < b < c < d$ with a, c in the same block and b, d in the same block imply that a, b, c, d are all in the same block.) The number of non-crossing partitions of $\{1, \dots, m\}$ is given by the Catalan number [61, 66]

$$C_m = \frac{(2m)!}{m!(m+1)!} = \frac{1}{m+1} \binom{2m}{m} . \quad (2.14)$$

When the horizontal couplings $v_{i,i+1}$ are all equal to -1 (which is the case for the chromatic polynomial), then the horizontal operator \mathbf{H} is a *projection*, and we can work

in its image subspace by using the modified transfer matrix $\mathbf{T}' = \mathbf{H}\mathbf{V}\mathbf{H}$ in place of $\mathbf{T} = \mathbf{V}\mathbf{H}$, and using the basis vectors

$$\mathbf{f}_{\mathcal{P}} = \mathbf{H}\mathbf{e}_{\mathcal{P}} \quad (2.15)$$

in place of $\mathbf{e}_{\mathcal{P}}$. Please note that $\mathbf{f}_{\mathcal{P}} = 0$ if \mathcal{P} has any pair of nearest neighbors in the same block. We thus work in the space spanned by the basis vectors $\mathbf{f}_{\mathcal{P}}$ where \mathcal{P} is a non-crossing non-nearest-neighbor partition of $\{1, \dots, m\}$. The dimension of this space is given [60, Proposition 3.6] [45] by the Motzkin number M_{m-1} , where [9, 19, 29, 51, 61, 66]⁶

$$M_n = \sum_{j=0}^{\lfloor n/2 \rfloor} \binom{n}{2j} C_j. \quad (2.16)$$

Finally, spatial symmetries further restrict the subspace whenever the couplings $v_{i,i+1}$ and v_i are invariant under the symmetry. Here the relevant symmetry is reflection in the center line of the strip. For reflection-invariant couplings, we can work in the space of equivalence classes of non-crossing non-nearest-neighbor partitions modulo reflection. We denote the corresponding symmetry-reduced transfer matrix by \mathbf{T}'' , and its dimension $\text{SqFree}(m)$ is then given by the number of these equivalence classes. The exact expression for $\text{SqFree}(m)$ was obtained in [13, Theorem 2]:

$$\text{SqFree}(m) = \frac{1}{2}M_{m-1} + \frac{(m'-1)!}{2} \sum_{j=0}^{\lfloor m'/2 \rfloor} \frac{m'-j}{(j!)^2(m'-2j)!} \quad (2.17)$$

where

$$m' = \left\lfloor \frac{m+1}{2} \right\rfloor \quad (2.18)$$

and $\lfloor p \rfloor$ stands for the largest integer $\leq p$. (We give a new proof of this formula in Appendix B.) The asymptotic behavior of $\text{SqFree}(m)$ is given by [13, Corollary 1]

$$\text{SqFree}(m) \sim \frac{\sqrt{3}}{4\sqrt{\pi}} 3^m m^{-3/2} \left[1 + O\left(\frac{1}{m}\right) \right] \quad \text{as } m \rightarrow \infty \quad (2.19)$$

The values of all these dimensions for $m \leq 16$ are displayed in Table 1.

Some further structural properties of the transfer matrices can be found in Ref. [54].

2.3 Beraha–Kahane–Weiss theorem

A central role in our work is played by a theorem on analytic functions due to Beraha, Kahane and Weiss [5–8] and generalized slightly by one of us [63]. The situation is as follows: Let D be a domain (connected open set) in the complex plane, and let $\alpha_1, \dots, \alpha_M, \lambda_1, \dots, \lambda_M$ ($M \geq 2$) be analytic functions on D , none of which is identically zero. For each integer $n \geq 0$, define

$$f_n(z) = \sum_{k=1}^M \alpha_k(z) \lambda_k(z)^n. \quad (2.20)$$

⁶ *Warning:* Several references use the notation m_n to denote what we call M_n ; and one reference [19] writes M_n to denote a *different* sequence.

We are interested in the zero sets

$$\mathcal{Z}(f_n) = \{z \in D: f_n(z) = 0\} \quad (2.21)$$

and in particular in their limit sets as $n \rightarrow \infty$:

$$\liminf \mathcal{Z}(f_n) = \{z \in D: \text{every neighborhood } U \ni z \text{ has a nonempty intersection with all but finitely many of the sets } \mathcal{Z}(f_n)\} \quad (2.22)$$

$$\limsup \mathcal{Z}(f_n) = \{z \in D: \text{every neighborhood } U \ni z \text{ has a nonempty intersection with infinitely many of the sets } \mathcal{Z}(f_n)\} \quad (2.23)$$

Let us call an index k *dominant at z* if $|\lambda_k(z)| \geq |\lambda_l(z)|$ for all l ($1 \leq l \leq M$); and let us write

$$D_k = \{z \in D: k \text{ is dominant at } z\}. \quad (2.24)$$

Then the limiting zero sets can be completely characterized as follows:

Theorem 2.2 [5–8, 63] *Let D be a domain in \mathbb{C} , and let $\alpha_1, \dots, \alpha_M, \lambda_1, \dots, \lambda_M$ ($M \geq 2$) be analytic functions on D , none of which is identically zero. Let us further assume a “no-degenerate-dominance” condition: there do not exist indices $k \neq k'$ such that $\lambda_k \equiv \omega \lambda_{k'}$ for some constant ω with $|\omega| = 1$ and such that $D_k (= D_{k'})$ has nonempty interior. For each integer $n \geq 0$, define f_n by*

$$f_n(z) = \sum_{k=1}^M \alpha_k(z) \lambda_k(z)^n.$$

Then $\liminf \mathcal{Z}(f_n) = \limsup \mathcal{Z}(f_n)$, and a point z lies in this set if and only if either

- (a) *There is a unique dominant index k at z , and $\alpha_k(z) = 0$; or*
- (b) *There are two or more dominant indices at z .*

Note that case (a) consists of isolated points in D ; we refer to these as *isolated limiting points*. Case (b) consists of curves (plus possibly isolated points where all the λ_k vanish simultaneously); we call these *limiting curves* or *dominant equimodular curves*. Henceforth we shall denote by \mathcal{B} the locus of points satisfying condition (b).

We shall often refer to the functions λ_k as “eigenvalues”, because that is how they arise in the transfer-matrix formalism.

2.4 Chromatic roots of bi-fans and bipyramids

The simplest case of the graphs $S_{m,n}$ is width $m = 1$: the graphs $S_{1,n}$ are called *bi-fans* (Figure 3a), and their chromatic polynomials can be easily computed. Here we would like to recall this computation and to discuss the behavior of the chromatic roots as $n \rightarrow \infty$. Similar methods apply to a closely related class of graphs called *bipyramids* (Figure 3b).

We recall that the *join* $G + H$ of two graphs is the graph obtained from the disjoint union of G and H by adding one edge connecting each pair of vertices $i \in V(G)$, $j \in V(H)$.

Let \bar{K}_2 be the graph with two vertices and no edges, and let G be any graph. Then the chromatic polynomial of the join $G + \bar{K}_2$ is given in terms of the chromatic polynomial of G by the easy formula

$$P_{G+\bar{K}_2}(q) = qP_G(q-1) + q(q-1)P_G(q-2). \quad (2.25)$$

Indeed, the first (resp. second) term on the right-hand side of (2.25) counts the proper q -colorings of $G + \bar{K}_2$ in which the two vertices of \bar{K}_2 are colored the same (resp. different).

Using the well-known chromatic polynomials of the n -vertex path P_n and the n -vertex cycle C_n ,

$$P_{P_n}(q) = q(q-1)^{n-1} \quad (2.26)$$

$$P_{C_n}(q) = (q-1)^n + (q-1)(-1)^n \quad (2.27)$$

we obtain the chromatic polynomials of the bi-fan $P_n + \bar{K}_2$ and the bipyramid $C_n + \bar{K}_2$:

$$P_{P_n+\bar{K}_2}(q) = q(q-1)(q-2)^{n-1} + q(q-1)(q-2)(q-3)^{n-1} \quad (2.28)$$

$$P_{C_n+\bar{K}_2}(q) = q(q-2)^n + q(q-1)(q-3)^n + q(q^2-3q+1)(-1)^n \quad (2.29)$$

Using the Beraha–Kahane–Weiss theorem, we see immediately that the chromatic roots of the bi-fans accumulate as $n \rightarrow \infty$ on the curve $|q-2| = |q-3|$, i.e. the vertical line $\operatorname{Re} q = 5/2$ [58]. (There are also isolated limiting points at $q = 0, 1, 2$.) The analysis for the bipyramids is slightly more complicated, because there are three “eigenvalues” ($q-2$, $q-3$ and -1) that need to be compared. Elementary computations show [50, 57] that the limiting curve \mathcal{B} consists of the pair of semi-infinite vertical line segments $\operatorname{Re} q = 5/2$, $|\operatorname{Im} q| \geq \sqrt{3}/2$ together with the pair of circular arcs $q = 2 + e^{i\theta}$ and $q = 3 - e^{i\theta}$ for $-\pi/3 \leq \theta \leq \pi/3$.⁷

It is worth remarking that if one plots the chromatic roots of the bi-fans or bipyramids, one finds a large number of roots accumulating on the parts of \mathcal{B} fairly close to the real axis, together with a few roots at large imaginary part lying *far to the right* of the line $\operatorname{Re} q = 5/2$.⁸ (In Figure 4 we depict the chromatic roots of the $n = 100$ bi-fan. The rightmost zeros are located at $q \approx 21.8463758923 \pm 14.9443992222i$.) This behavior is at first surprising (at least it was to us), but after some thought one realizes that it is perfectly consistent with the Beraha–Kahane–Weiss theorem: the limiting curve $\operatorname{Re} q = 5/2$ contains the point at infinity, and roots can tend to infinity in the topology of the Riemann sphere (which turns out to be the relevant sense) in many different ways; in particular, their real parts need not tend to $5/2$. In fact, it turns out that the rightmost root has

$$q = \frac{n}{\log n - \log \log n} \left[1 \pm \frac{\pi i}{\log n} + O\left(\frac{\log \log n}{\log^2 n}\right) \right], \quad (2.30)$$

⁷Read and Royle’s formula for the chromatic polynomial of the bipyramids [50, p. 1017] has a typographical error: $z^2 - 3z + 3$ should be $z^2 - 3z + 1$.

⁸For the bipyramids this was noticed already two decades ago by Read and Royle [50, pp. 1019–1020]. It was further observed by Shrock and Tsai [58, Sections III.A and III.B] for some classes of graphs that generalize the bi-fans and bipyramids.

so that its real and imaginary parts *both* tend to infinity as $n \rightarrow \infty$. This asymptotic formula can be proven by a minor modification of the analysis given in [12, Section 5] for the chromatic roots of the complete bipartite graphs $K_{2,n} \simeq \bar{K}_n + \bar{K}_2$.

2.5 Chromatic roots of generalized theta graphs

Let us now summarize briefly the argument from [63] concerning the chromatic roots of the generalized theta graphs.

The chromatic polynomial of $\Theta^{(s,p)}$ is [12, 59, 63]

$$P_{\Theta^{(s,p)}}(q) = q\lambda_{=,s}(q)^p + q(q-1)\lambda_{\neq,s}(q)^p \quad (2.31)$$

where

$$\lambda_{=,s}(q) = \frac{(q-1)^s + (q-1)(-1)^s}{q} \quad (2.32)$$

$$\lambda_{\neq,s}(q) = \frac{(q-1)^s - (-1)^s}{q} \quad (2.33)$$

Indeed, $\lambda_{=,s}(q)$ [resp. $\lambda_{\neq,s}(q)$] is the number of ways of coloring the internal vertices of one s -edge path when the two endvertices are colored the same (resp. different). Please note that the leading large- q term in both $\lambda_{=,s}(q)$ and $\lambda_{\neq,s}(q)$ is $q^{s-1} \equiv q^m$, and that they start to differ at order q^0 : indeed, we have the curious formula

$$\lambda_{=,s}(q) - \lambda_{\neq,s}(q) = (-1)^s. \quad (2.34)$$

Let us begin by fixing s and considering the limit $p \rightarrow \infty$. Using the Beraha–Kahane–Weiss theorem, we see immediately that the chromatic roots of the graphs $\Theta^{(s,p)}$ accumulate as $p \rightarrow \infty$ on the real algebraic curve \mathcal{C}_s defined by $|\lambda_{=,s}(q)| = |\lambda_{\neq,s}(q)|$, or equivalently

$$\mathcal{C}_s: \quad |1 + (q-1)(1-q)^{-s}| = |1 - (1-q)^{-s}|. \quad (2.35)$$

To handle the limit $s \rightarrow \infty$, we use the following lemma:

Lemma 2.3 [63, Lemma 1.6] *Let F_1, F_2, G be analytic functions on a disc $|z| < R$ satisfying $|G(0)| \leq 1$ and $G \not\equiv \text{constant}$. Then, for each $\epsilon > 0$, there exists $s_0 < \infty$ such that for all integers $s \geq s_0$ the equation*

$$|1 + F_1(z)G(z)^s| = |1 + F_2(z)G(z)^s| \quad (2.36)$$

has a solution in the disc $|z| < \epsilon$.

This lemma immediately implies that the curves \mathcal{C}_s accumulate as $s \rightarrow \infty$ at every point in the region $|q-1| \geq 1$. A strengthened version of this lemma is proven in [63, Theorem 4.1].

In Figure 5a we show the curve \mathcal{C}_s together with the chromatic roots of $\Theta^{(s,p)}$ for $s = 5$ and $p = 25, 100, 400$. Just as for the bi-fans, we see clearly the accumulation of roots on the inner parts of the curve \mathcal{C}_s , together with a few points at larger $|q|$ lying far off this curve. All this can presumably be explained by a generalization of the analysis

given in [12, Section 5] for the special case $s = 2$. In particular, we expect that the root of largest modulus grows like $(p/\log p)^{1/(s-1)}$ as $p \rightarrow \infty$.⁹ This explains the extremely slow convergence of the roots to the outer parts of the curve \mathcal{C}_s in Figure 5a. Note in particular that a naive computational approach, without the insight provided by the Beraha–Kahane–Weiss theorem, would give little indication that the roots are in fact unbounded as $p \rightarrow \infty$.

In Figure 5b we show the curves \mathcal{C}_s for $s = 5, 10, 15$. We see clearly how these curves are becoming dense in the entire complex plane with the exception of the disc $|q - 1| < 1$. The curves \mathcal{C}_s do enter this disc, but as $s \rightarrow \infty$ they retreat to its boundary, so that no point of the open disc is a limit point of the curves \mathcal{C}_s .

Finally, let us note, for future reference, the formula for the multivariate Tutte polynomial of $\Theta^{(s,p)}$ when the *same* weights v_1, \dots, v_s (but not necessarily $v_1 = \dots = v_s = -1$) are assigned to each path [63]:

$$Z_{\Theta^{(s,p)}}(q, \mathbf{v}) = q\lambda_{=,s}(q, \mathbf{v})^p + q(q-1)\lambda_{\neq,s}(q, \mathbf{v})^p \quad (2.37)$$

where

$$\lambda_{=,s}(q, \mathbf{v}) = \frac{1}{q} \left[\prod_{i=1}^s (q + v_i) + (q-1) \prod_{i=1}^s v_i \right] \quad (2.38)$$

$$\lambda_{\neq,s}(q, \mathbf{v}) = \frac{1}{q} \left[\prod_{i=1}^s (q + v_i) - \prod_{i=1}^s v_i \right] \quad (2.39)$$

We have the curious formula

$$\lambda_{=,s}(q, \mathbf{v}) - \lambda_{\neq,s}(q, \mathbf{v}) = \prod_{i=1}^s v_i, \quad (2.40)$$

which generalizes (2.34).

3 Transfer-matrix theory for the family $S_{m,n}$

In Section 2.2 we explained the transfer-matrix formalism for computing the multivariate Tutte polynomial of an $m \times n$ square lattice with free boundary conditions in both directions. In this section we begin (Section 3.1) by discussing the modifications needed to handle the extra sites at left and right in the graphs $S_{m,n}$. We then (Section 3.2) go on to prove some structural properties of the transfer matrix for the family $S_{m,n}$, by analogy with what was done in Ref. [54] for free and cylindrical boundary conditions; in particular we show that the transfer matrix \mathbf{T} can be decomposed into two independent blocks $\mathbf{T}_=$ and \mathbf{T}_\neq . Next (Section 3.3) we introduce the families of graphs $S_{m,n}^=$ and $S_{m,n}^\neq$, which shed further light on the block-diagonalization of the transfer matrix for the family $S_{m,n}$. Then (Section 3.4) we prove that the large- $|q|$ expansion for the dominant eigenvalue of

⁹Brown, Hickman, Sokal and Wagner [12, Theorem 1.3] proved that the roots are bounded in modulus by $\text{const} \times p/\log p$, uniformly in s and p . But this bound is presumably far from sharp when $s > 2$.

the transfer matrix $T_ =$ or $T_ \neq$ holds uniformly in the strip width m (throughout the antiferromagnetic regime), by invoking results from [62]. Finally (Section 3.5), we prove a key identity concerning the difference between the dominant eigenvalues $\lambda_{*,=}(m, q, \mathbf{v})$ and $\lambda_{*,\neq}(m, q, \mathbf{v})$ corresponding to $S_{m,n}^ =$ and $S_{m,n}^ \neq$.

3.1 Basic method

We want to compute the chromatic polynomial $P_{S_{m,n}}(q)$ — or more generally, the multivariate Tutte polynomial $Z_{S_{m,n}}(q, \mathbf{v})$ with periodically repeated edge weights — for the graph $S_{m,n}$ that is obtained from a square-lattice strip of width m and length n (with free boundary conditions in both directions) by connecting every site in the leftmost (resp. rightmost) column to an extra site s (resp. s'). Thus, the number of sites of this strip is $mn + 2$ (see Figure 1a).

We shall also denote the strip $S_{m,n}$ as $m_{F++} \times n_F$: here the subscript F denotes free boundary conditions, while the subscript $F++$ denotes free boundary conditions with the two extra sites attached at left and right. A square-lattice strip with standard free boundary conditions in both directions will be denoted as $m_F \times n_F$.

In the strip $S_{m,n}$ we assign weight $v_{0,1}$ to all the edges connecting the leftmost site (which we can think of as “column 0”) to the sites of column 1, weights $v_{i,i+1}$ to the horizontal edges linking column i to column $i + 1$ ($1 \leq i \leq m - 1$), weight $v_{m,m+1}$ to all the edges connecting the sites of column m to the rightmost site (which we can think of as “column $m + 1$ ”), and weight v_i to the vertical edges in column i ($1 \leq i \leq m$). Of course, for the chromatic polynomial all these weights will be taken to be -1 .

The computation of the multivariate Tutte polynomial for this strip family can be achieved by using a minor modification of the transfer-matrix method explained in Section 2.2. As before, we fix the “width” m and consider the family of graphs $S_{m,n}$ obtained by varying the “length” n ; our goal is to calculate the multivariate Tutte polynomials $Z_{S_{m,n}}(q, \mathbf{v})$ for this family by building up the graphs $S_{m,n}$ layer by layer.

One way of constructing the transfer matrix $T(m)$ for the family $S_{m,n}$ is to treat this family as a special case of a square-lattice strip $(m + 2)_F \times n_F$: see Figure 1b. Thus, we choose to work in the space of connectivities $\{\mathbf{e}_{\mathcal{P}}\}$ associated to the non-crossing partitions \mathcal{P} of the set $\{0, 1, 2, \dots, m, m + 1\}$. The dimension of this space is the Catalan number C_{m+2} .

On the edges of the $(m + 2)_F \times n_F$ strip that correspond to the edges of the starting graph $S_{m,n}$, we simply use the desired weights $v_{i,i+1}$ ($0 \leq i \leq m$) and v_i ($1 \leq i \leq m$). On the vertical edges in the first and last columns (depicted with dashed lines in Figure 1b), we associate a weight $v_e \rightarrow +\infty$, which corresponds to contracting all the sites in each of these columns into a single site. In other words, we use two different vertical-bond operators depending on which column we are in:

$$P_i = \begin{cases} v_i I + D_i & \text{for } 1 \leq i \leq m \\ I & \text{for } i = 0, m + 1 \end{cases} \quad (3.1)$$

Therefore, the horizontal transfer matrix is given by

$$H = \prod_{i=0}^m (1 + v_{i,i+1} J_{i,i+1}) \quad (3.2)$$

[compare (2.8)] and the vertical transfer matrix is given by

$$\mathbf{V} = \prod_{i=1}^m (v_i I + \mathbf{D}_i) . \quad (3.3)$$

Note that the formula for \mathbf{V} is *identical* to the formula (2.9) for an ordinary $m_F \times n_F$ grid; the only difference is that here the operators act on the space of partitions of $\{0, 1, 2, \dots, m, m+1\}$ rather than $\{1, 2, \dots, m\}$.

The full transfer matrix is then $\mathbf{T} = \mathbf{V}\mathbf{H}$, and the multivariate Tutte polynomial $Z_{S_{m,n}}(q, \mathbf{v})$ is given by

$$Z_{S_{m,n}}(q, \mathbf{v}) = \boldsymbol{\omega}^T \mathbf{H} \mathbf{T}^{n-1} \mathbf{e}_{\text{id}} , \quad (3.4)$$

where \mathbf{e}_{id} denotes the basis vector associated to the partition

$$\text{id} = \{\{0\}, \{1\}, \dots, \{m\}, \{m+1\}\} \quad (3.5)$$

and the left vector $\boldsymbol{\omega}$ acts on a connectivity state as in (2.11).

When the horizontal couplings $v_{i,i+1}$ are all equal to -1 (as is the case for the chromatic polynomial), the horizontal operator \mathbf{H} is a *projection*, so that (as explained in Section 2.2) we can work in its image subspace by using the modified transfer matrix $\mathbf{T}' = \mathbf{H}\mathbf{V}\mathbf{H}$ and the basis vectors $\mathbf{f}_{\mathcal{P}} = \mathbf{H}\mathbf{e}_{\mathcal{P}}$, where \mathcal{P} runs over the non-crossing non-nearest-neighbor partitions of $\{0, \dots, m+1\}$. The dimension of this space is the Motzkin number M_{m+1} [cf. (2.16)]. We then write the chromatic polynomial for $S_{m,n}$ as

$$P_{S_{m,n}}(q) = \boldsymbol{\omega}^T (\mathbf{T}')^{n-1} \mathbf{f}_{\text{id}} . \quad (3.6)$$

Finally, when the couplings are also reflection-symmetric (e.g., when they are all -1), we can work in the space of equivalence classes of non-crossing non-nearest-neighbor partitions modulo reflection. The dimension of this space is given by $\text{SqFree}(m+2)$ [cf. (2.17)]. Hereafter, we will denote by $\mathbf{T}''(m)$ this symmetry-reduced transfer matrix.

3.2 Block-diagonalization of the transfer matrix (I)

One important property of the transfer matrix \mathbf{T} (or \mathbf{T}' or \mathbf{T}'') for the family $S_{m,n}$ is that it can be decomposed into two independent transfer matrices of a lower dimension. To see this, it suffices to note that the projection $\mathbf{J}_{0,m+1}$ commutes with both \mathbf{H} and \mathbf{V} : it commutes with \mathbf{H} because all join operators commute with each other, and it commutes with \mathbf{V} because (3.3) does not contain the detach operators \mathbf{D}_0 or \mathbf{D}_{m+1} . Therefore, \mathbf{T} (or \mathbf{T}' or \mathbf{T}'') block-diagonalizes if we choose a basis in which the first group of basis elements corresponds to the range of $\mathbf{J}_{0,m+1}$, and the second group corresponds to the range of $I - \mathbf{J}_{0,m+1}$. We call these two blocks $\mathbf{T}_=$ and \mathbf{T}_{\neq} , respectively. Indeed, this block-diagonalization holds for any transfer matrix built out of operators of the general form

$$\mathbf{H} = \sum_{A \subseteq \{0, \dots, m\}} c_A \prod_{i \in A} \mathbf{J}_{i,i+1} \quad (3.7a)$$

$$\mathbf{V} = \sum_{B \subseteq \{1, \dots, m\}} d_B \prod_{i \in B} \mathbf{D}_i \quad (3.7b)$$

irrespective of the coefficients $\{c_A\}$ and $\{d_B\}$. The point, once again, is simply that V does not contain the detach operators D_0 or D_{m+1} .

Let us now recall that id denotes the partition of $\{0, \dots, m+1\}$ in which each element is a singleton, and that $\text{id} \bullet (0, m+1)$ denotes the partition in which $\{0, m+1\}$ is a block and all the other elements are singletons. Let us call a partition \mathcal{P} of $\{0, \dots, m+1\}$ *non-trivial* if it is neither id nor $\text{id} \bullet (0, m+1)$.

Proposition 3.1 *For any operators H and V of the form (3.7), we can write*

$$VH J_{0,m+1} \mathbf{e}_{\text{id}} = t_{=} J_{0,m+1} \mathbf{e}_{\text{id}} + \sum_{\mathcal{P} \text{ non-trivial}} a_{\mathcal{P}}^- J_{0,m+1} \mathbf{e}_{\mathcal{P}} \quad (3.8a)$$

$$VH (I - J_{0,m+1}) \mathbf{e}_{\text{id}} = t_{\neq} (I - J_{0,m+1}) \mathbf{e}_{\text{id}} + \sum_{\mathcal{P} \text{ non-trivial}} a_{\mathcal{P}}^{\neq} (I - J_{0,m+1}) \mathbf{e}_{\mathcal{P}} \quad (3.8b)$$

for some coefficients $t_{=}$, t_{\neq} , $\{a_{\mathcal{P}}^-\}$ and $\{a_{\mathcal{P}}^{\neq}\}$ that are polynomials in q , $\{c_A\}$ and $\{d_B\}$. Furthermore, these coefficients satisfy the identity

$$t_{=} - t_{\neq} = c_{\{0,\dots,m\}} d_{\{1,\dots,m\}} \quad (3.9)$$

reminiscent of (2.34)/(2.40).

PROOF. Let us begin by considering the quantity $H\mathbf{e}_{\text{id}}$:

$$H\mathbf{e}_{\text{id}} = \sum_{A \subseteq \{0,\dots,m\}} c_A \left(\prod_{i \in A} J_{i,i+1} \right) \mathbf{e}_{\text{id}}. \quad (3.10)$$

Let us now apply the operator V to (3.10). It is clear that we obtain three types of terms: a) terms that contain non-trivial partitions \mathcal{P} , b) terms that contain the trivial partition id , and c) a single term that contains the trivial partition $\text{id} \bullet (0, m+1)$. Indeed, this latter term can arise in only one way: first we must join all the sites $\{0, \dots, m+1\}$ into a single block (i.e., take $A = \{0, \dots, m\}$ in H), and then we must detach all the inner sites (i.e., take $B = \{1, \dots, m\}$ in V). It follows that

$$VH\mathbf{e}_{\text{id}} = c_{\{0,\dots,m\}} d_{\{1,\dots,m\}} J_{0,m+1} \mathbf{e}_{\text{id}} + a_{\text{id}} \mathbf{e}_{\text{id}} + \sum_{\mathcal{P} \text{ non-trivial}} a_{\mathcal{P}} \mathbf{e}_{\mathcal{P}} \quad (3.11)$$

for some coefficients a_{id} and $\{a_{\mathcal{P}}\}$ that will clearly be polynomials in q , $\{c_A\}$ and $\{d_B\}$. From this equation is easy to derive (3.8), as the join operator $J_{0,m+1}$ commutes with all the join and detach operators arising in (3.11). Indeed, using $J_{0,m+1}^2 = J_{0,m+1}$ we find

$$t_{=} = a_{\text{id}} + c_{\{0,\dots,m\}} d_{\{1,\dots,m\}} \quad (3.12a)$$

$$t_{\neq} = a_{\text{id}} \quad (3.12b)$$

From this relation, (3.9) follows immediately. \square

When \mathbf{H} and \mathbf{V} are the transfer matrices (3.2)/(3.3) for the multivariate Tutte polynomial, we have $c_{\{0,\dots,m\}} = \prod_{i=0}^m v_{i,i+1}$ and $d_{\{1,\dots,m\}} = 1$, so that (3.9) becomes

$$t_{=} - t_{\neq} = \prod_{i=0}^m v_{i,i+1} . \quad (3.13)$$

Note that this formula holds irrespective of the values of the vertical couplings v_i . In particular, it holds when $v_i = 0$; this explains the “curious formula” (2.40) for the generalized theta graphs.¹⁰ When all the horizontal couplings $v_{i,i+1}$ equal -1 , we have

$$t_{=} - t_{\neq} = (-1)^{m+1} , \quad (3.14)$$

which includes (2.34) as a special case.

The next result is similar to Proposition 3.1 in [54].

Proposition 3.2 *Consider operators \mathbf{H} and \mathbf{V} of the form (3.7) where the coefficients $\{c_A\}$ and $\{d_B\}$ are numbers (i.e., independent of q). Then, using the notation of Proposition 3.1,*

$$t_{=} = c_{\emptyset} d_{\{1,\dots,m\}} q^m + \text{terms of order at most } q^{m-1} \quad (3.15a)$$

$$t_{\neq} = c_{\emptyset} d_{\{1,\dots,m\}} q^m + \text{terms of order at most } q^{m-1} \quad (3.15b)$$

Furthermore, all the coefficients $\{a_{\overline{p}}\}$ and $\{a_{\overline{p}}^{\neq}\}$ defined in Proposition 3.1 are polynomials in q of degree at most $m-1$.

PROOF. First of all, it is obvious that each entry in the transfer matrix $\mathbf{T} = \mathbf{V}\mathbf{H}$ is a polynomial in q . Indeed, from (2.7) it is clear that we get a factor of q every time we apply the operator \mathbf{D}_i to a partition in which i is a singleton. Indeed, we can *maximize* the number of factors of q by applying the vertical transfer matrix \mathbf{V} to a partition in

¹⁰There is a small missing step here, because (3.13) refers to the dominant diagonal entries of the transfer matrix, while (2.40) refers to the transfer-matrix eigenvalues. But in the case of the generalized theta graphs $\Theta^{(s,p)}$ these two quantities coincide, as can easily be seen by expressing $Z_{\Theta^{(s,p)}}(q, \mathbf{v})$ using a transfer-matrix formalism. Labelling the vertices along each of the p chains from 0 to s , it is not hard to see that the partition function can be written in the basis $\{\mathbf{1}, \delta_{0,s}\}$ as follows:

$$Z_{\Theta^{(s,p)}}(q, \mathbf{v}) = \begin{pmatrix} q^2 \\ q \end{pmatrix}^T \cdot \begin{pmatrix} \lambda_{\neq,s}(q, \mathbf{v}) & 0 \\ \prod_{i=0}^{s-1} v_{i,i+1} & \lambda_{=,s}(q, \mathbf{v}) \end{pmatrix}^p \cdot \begin{pmatrix} 1 \\ 0 \end{pmatrix} .$$

Since the transfer matrix is lower-triangular, the leading diagonal entries of the transfer matrix coincide with its eigenvalues.

Let us remark that if we choose the basis $\{\delta_{0,s}, \mathbf{1} - \delta_{0,s}\} = \{\mathbf{J}_{0s}, (\mathbf{I} - \mathbf{J}_{0s})\} \mathbf{e}_{\text{id}}$, then the above expression simplifies to

$$Z_{\Theta^{(s,p)}}(q, \mathbf{v}) = q \begin{pmatrix} 1 \\ q-1 \end{pmatrix}^T \cdot \begin{pmatrix} \lambda_{=,s}(q, \mathbf{v}) & 0 \\ 0 & \lambda_{\neq,s}(q, \mathbf{v}) \end{pmatrix}^p \cdot \begin{pmatrix} 1 \\ 1 \end{pmatrix} ,$$

and we obtain (2.37).

which every site $1, \dots, m$ is a singleton, i.e. either \mathbf{e}_{id} or $\mathbf{J}_{0,m+1}\mathbf{e}_{\text{id}}$. In particular, from (3.7b) we have

$$\mathbf{V}\mathbf{e}_{\text{id}} = \sum_{B \subseteq \{1, \dots, m\}} d_B q^{|B|} \mathbf{e}_{\text{id}} \quad (3.16a)$$

$$= (d_{\{1, \dots, m\}} q^m + \text{terms of order at most } q^{m-1}) \mathbf{e}_{\text{id}} \quad (3.16b)$$

and analogously for $\mathbf{J}_{0,m+1}\mathbf{e}_{\text{id}}$. If we apply the vertical transfer matrix to any non-trivial partition, we get a polynomial in q of degree at most $m-1$. Now let M denote any linear combination of $\mathbf{J}_{0,m+1}$ and $I - \mathbf{J}_{0,m+1}$, and consider

$$\mathbf{H}M\mathbf{e}_{\text{id}} = \sum_{A \subseteq \{0, \dots, m\}} c_A \left(\prod_{i \in A} \mathbf{J}_{i,i+1} \right) \mathbf{e}_{\text{id}} \quad (3.17a)$$

$$= c_{\emptyset} M\mathbf{e}_{\text{id}} + \sum_{\mathcal{P} \text{ non-trivial}} b_{\mathcal{P}} M\mathbf{e}_{\mathcal{P}} \quad (3.17b)$$

for some quantities $b_{\mathcal{P}}$ that are polynomials in $\{c_A\}$ (and of course independent of q). Using (3.16)/(3.17) it is obvious that

$$\mathbf{V}\mathbf{H}M\mathbf{e}_{\text{id}} = c_{\emptyset} \sum_{B \subseteq \{1, \dots, m\}} d_B q^{|B|} M\mathbf{e}_{\text{id}} + \sum_{\mathcal{P}} b'_{\mathcal{P}}(q) \mathbf{e}_{\mathcal{P}} \quad (3.18)$$

where the coefficients $b'_{\mathcal{P}}(q)$ are polynomials in q of degree at most $m-1$. \square

In view of Proposition 3.2, we shall henceforth refer to $t_{=}$ and t_{\neq} as the “dominant diagonal terms” in the transfer matrix, as they are indeed dominant at large $|q|$. Furthermore, we can deduce from Propositions 3.1 and 3.2 the leading large- $|q|$ behavior of the eigenvalues. We begin with a simple perturbation lemma proved in Ref. [54]:

Lemma 3.3 [54, Lemma 3.2] *Consider an $N \times N$ matrix $M(\xi) = (M_{ij}(\xi))_{i,j=1}^N$ whose entries are analytic functions of ξ in some disc $|\xi| < R$. Suppose that $M_{11} = 1$ and that $M_{ij} = O(\xi)$ for $(i, j) \neq (1, 1)$. Then, in some disc $|\xi| < R'$, $M(\xi)$ has a simple leading eigenvalue $\mu_{\star}(\xi)$ that is given by a convergent expansion*

$$\mu_{\star}(\xi) = 1 + \sum_{k=2}^{\infty} \alpha_k \xi^k \quad (3.19)$$

[note that $\alpha_1 = 0$] with associated eigenvector

$$\mathbf{v}_{\star}(\xi) = \mathbf{e}_1 + \sum_{k=1}^{\infty} \mathbf{v}_k \xi^k, \quad (3.20)$$

while all other eigenvalues are $O(\xi)$.

Remarks. 1. The key fact here is that the eigenvalue shift in (3.19) begins at order ξ^2 , not order ξ .

2. The “small” eigenvalues need not be analytic in ξ . For instance,

$$M(\xi) = \begin{pmatrix} 1 & 0 & 0 \\ 0 & 0 & \xi \\ 0 & \xi^2 & 0 \end{pmatrix} \quad (3.21)$$

has eigenvalues $\mu = 1$ and $\mu = \pm \xi^{3/2}$. \square

To apply Lemma 3.3 to our transfer matrix $\mathsf{T}_=$ (resp. T_\neq), we set $\xi = q^{-1}$ and $M = \mathsf{T}_=/t_=$ (resp. T_\neq/t_\neq). We then have:¹¹

Corollary 3.4 *Consider operators H and V of the form (3.7) where the coefficients $\{c_A\}$ and $\{d_B\}$ are numbers (i.e., independent of q) and $c_\emptyset d_{\{1,\dots,m\}} \neq 0$. Then $\mathsf{T}_=$ and T_\neq each have a single eigenvalue that is analytic for large $|q|$ and behaves there like $\text{const} \times q^m$: more precisely, these eigenvalues have convergent expansions*

$$\frac{\lambda_{*,=}}{t_=} = 1 + \sum_{k=2}^{\infty} \alpha_k^- q^{-k} \quad (3.22a)$$

$$\frac{\lambda_{*,\neq}}{t_\neq} = 1 + \sum_{k=2}^{\infty} \alpha_k^\neq q^{-k} \quad (3.22b)$$

so that in particular

$$\lambda_{*,=} - t_ = O(|q|^{m-2}) \quad (3.23a)$$

$$\lambda_{*,\neq} - t_\neq = O(|q|^{m-2}) \quad (3.23b)$$

All other eigenvalues are $O(|q|^{m-1})$.

Let us now return to the case of main interest, in which H and V are the transfer matrices (3.2)/(3.3) for the chromatic polynomial (i.e., $v_{i,i+1} = -1$ for $0 \leq i \leq m$, and $v_i = -1$ for $1 \leq i \leq m$). In this case we can sharpen (3.15) by providing explicit expressions for the lower-order terms:¹²

Proposition 3.5 *Let H and V be the transfer matrices (3.2)/(3.3) for the chromatic polynomial $v_{i,i+1} = v_i = -1$. Then for $m \geq 1$, we have that*

$$t_\neq(m) = \sum_{k=0}^m (-1)^k a_k(m) q^{m-k} \quad (3.24a)$$

$$t_=(m) = \sum_{k=0}^m (-1)^k a_k(m) q^{m-k} + (-1)^{m+1} \quad (3.24b)$$

¹¹This Corollary is similar to Corollary 3.3 in [54].

¹²This Proposition is similar to Propositions 3.4 and 3.6 in [54].

where each $a_k(m)$ is, for fixed $k \geq 0$, the restriction to integers $m \geq \max(1, k)$ of a polynomial in m of degree k given by

$$a_k(m) = \sum_{p=0}^k (-1)^p \binom{m-p}{p} \sum_{q=0}^{k-p} 3^q \binom{m-2p}{q} \binom{p}{k-p-q}. \quad (3.25)$$

The first few coefficients $a_k(m)$ are

$$a_0(m) = 1 \quad (3.26a)$$

$$a_1(m) = 2m + 1 \quad (3.26b)$$

$$a_2(m) = 2m^2 + m - 2 \quad (3.26c)$$

$$a_3(m) = \frac{4}{3}m^3 - \frac{16}{3}m + 1 \quad (3.26d)$$

The proof of Proposition 3.5 is given in Appendix A; it is based on computing the partition function for a special one-dimensional polymer model.

Since we have proven that $a_k(m)$ is a polynomial in m of degree k , it is also of interest to obtain explicit expressions for the coefficients of this polynomial, which we write as

$$a_k(m) = \sum_{\ell=0}^k \frac{(-1)^\ell 2^{k-2\ell+1}}{(k-\ell)!(\ell+2)!} a_{k,\ell} m^{k-\ell}; \quad (3.27)$$

here the prefactors have been chosen to make many (though not all) of the coefficients $a_{k,\ell}$ integers (in fact, they are all integers for $\ell \leq 5$ but not for $\ell = 6$, see below). Now we use the well-known expansion of the falling powers in terms of Stirling cycle numbers [30],

$$x^{\underline{r}} = \sum_{c \geq 0} \begin{bmatrix} r \\ c \end{bmatrix} (-1)^{r-c} x^c, \quad (3.28)$$

and expand all the binomials in (3.25) involving m . We arrive after some algebra at the following expression:

$$a_{k,\ell} \equiv \frac{(k-\ell)!(\ell+2)!}{(-1)^\ell 2^{k-2\ell+1}} [m^{k-\ell}] a_k(m) \quad (3.29a)$$

$$\begin{aligned} &= \frac{(k-\ell)!(\ell+2)!(-1)^k}{2^{k-2\ell+1}} \sum_{p=0}^k \sum_{q=0}^{k-p} \binom{p}{k-p-q} \frac{(-3)^q}{p!q!} \\ &\quad \times \sum_{a=0}^p \sum_{c=0}^q \begin{bmatrix} p \\ a \end{bmatrix} \begin{bmatrix} q \\ c \end{bmatrix} \sum_{d=0}^{k-\ell} \binom{a}{k-\ell-d} \binom{c}{d} 2^{c-d} p^{a+c-k+\ell} \end{aligned} \quad (3.29b)$$

By computing (3.29b) for integers $k \geq \ell \geq 0$, we find *empirically* that $a_{k,\ell}$ is in fact, for each fixed ℓ , (the restriction of) a *polynomial* in k of degree ℓ . The first few of these

polynomials are:

$$a_{k,0} = 1 \quad (3.30a)$$

$$a_{k,1} = 3k - 9 \quad (3.30b)$$

$$a_{k,2} = 6k^2 - 62k + 4 \quad (3.30c)$$

$$a_{k,3} = 10k^3 - 220k^2 + 410k + 0 \quad (3.30d)$$

$$a_{k,4} = 15k^4 - 570k^3 + 3245k^2 + 1662k + 2872 \quad (3.30e)$$

$$a_{k,5} = 21k^5 - 1225k^4 + 14245k^3 - 6111k^2 + 9982k + 70560 \quad (3.30f)$$

$$a_{k,6} = 28k^6 - 2324k^5 + 45780k^4 - \frac{1166396}{9}k^3 - \frac{653968}{3}k^2 - \frac{3313360}{9}k + \frac{1935488}{3} \quad (3.30g)$$

Full disclosure. We did not begin by proving Propositions 3.1–3.5. Rather, we computed the transfer matrices for small widths m and noticed some patterns. Only then did we try to provide proofs.

3.3 Block-diagonalization of the transfer matrix (II)

This block-diagonalization can be explained in another way, without reference to transfer matrices. We begin by observing that the addition-contraction relation (which is a variant of the deletion-contraction relation) for multivariate Tutte polynomials gives

$$Z_{S_{m,n}}(q, \mathbf{v}) = Z_{S_{m,n}^=} (q, \mathbf{v}) + Z_{S_{m,n}^{\neq}} (q, \mathbf{v}) \quad (3.31)$$

where $S_{m,n}^=$ is the graph obtained from $S_{m,n}$ by contracting the two extra vertices into one, while $S_{m,n}^{\neq}$ is the graph obtained from $S_{m,n}$ by adding a $v = -1$ edge between the two extra vertices. Indeed, (3.31) simply says, in coloring language, that the two extra vertices in $S_{m,n}$ must receive either the same color or different colors. The block-diagonalization of T into $\mathsf{T}_=$ and T_{\neq} simply corresponds to carrying out separate transfer-matrix calculations for the two families $S_{m,n}^=$ and $S_{m,n}^{\neq}$ and observing that

$$Z_{S_{m,n}^=}(q, \mathbf{v}) = \boldsymbol{\omega}^{\mathsf{T}} \mathsf{T}_=(m)^{n-1} \mathbf{e}_{\text{id}} \quad (3.32a)$$

$$Z_{S_{m,n}^{\neq}}(q, \mathbf{v}) = \boldsymbol{\omega}^{\mathsf{T}} \mathsf{T}_{\neq}(m)^{n-1} \mathbf{e}_{\text{id}} \quad (3.32b)$$

Note also that $S_{m,n}^=$ is equivalent to a lattice of width $m+1$ with *cylindrical* boundary conditions in which m of the columns have the ordinary vertical edges v_i while one column (corresponding to the contracted extra sites) has $v \rightarrow +\infty$; the horizontal edges are given by the $v_{i,i+1}$ as usual (see Figure 6). Likewise, $S_{m,n}^{\neq}$ is equivalent to a lattice of width $m+2$ with cylindrical boundary conditions in which m of the columns have the ordinary vertical edges v_i while two adjacent columns (corresponding to the two extra sites) have $v \rightarrow +\infty$; the horizontal edges are given by the $v_{i,i+1}$ as usual except that the horizontal edges between the two adjacent special columns are set to -1 (see Figure 7).

For the chromatic polynomials $P_{S_{m,n}^=}(q)$ and $P_{S_{m,n}^{\neq}}(q)$, we can use the modified transfer matrix $\mathbf{T}' = \mathbf{H}\mathbf{V}\mathbf{H}$ because all the horizontal weights are $v = -1$:

$$P_{S_{m,n}^=}(q) = \boldsymbol{\omega}^T \mathbf{T}'_{=}(m)^{n-1} \mathbf{f}_{\text{id}} \quad (3.33a)$$

$$P_{S_{m,n}^{\neq}}(q) = \boldsymbol{\omega}^T \mathbf{T}'_{\neq}(m)^{n-1} \mathbf{f}_{\text{id}} \quad (3.33b)$$

The transfer matrix $\mathbf{T}'_{=}(m)$ acts on the space of non-crossing non-nearest-neighbor partitions of the set $\{0, \dots, m\}$ with periodic boundary conditions (i.e., 0 and m are also considered to be nearest neighbors). However, because of the reflection symmetry, we can work in the space of equivalence classes modulo reflection (with respect a diameter passing through the vertex 0) of non-crossing non-nearest-neighbor partitions of the set $\{0, \dots, m\}$ on a circle. We write $N_{=} = \dim \mathbf{T}''_{=}(m)$ for the dimension of this space, where $\mathbf{T}''_{=}(m)$ is the symmetry-reduced transfer matrix for the family $S_{m,n}^=$. Likewise, the transfer matrix $\mathbf{T}'_{\neq}(m)$ acts on the space of non-crossing non-nearest-neighbor partitions of the set $\{0, \dots, m+1\}$ with periodic boundary conditions. Once again exploiting the reflection symmetry, we can work in the space of equivalence classes modulo reflection (with respect a diameter passing between the vertices 0 and $m+1$) of non-crossing non-nearest-neighbor partitions of the set $\{0, \dots, m+1\}$ on a circle. We write $N_{\neq} = \dim \mathbf{T}''_{\neq}(m)$ for the dimension of this space. In Table 1 we quote the dimensionalities $N_{=}(m)$ and $N_{\neq}(m)$ for $1 \leq m \leq 14$.

In Appendix B we compute the following general formulae for $N_{=}(m)$ and $N_{\neq}(m)$:

Theorem 3.6 *The number $N_{=}(m)$ of equivalence classes, modulo reflection with respect an axis going through vertex 0, of non-crossing non-nearest-neighbor partitions of the set $\{0, 1, \dots, m\}$ on a circle is given by*

$$N_{=}(m) = \frac{1}{2}R_{m+1} + \frac{1}{2} \sum_{k=0}^{\lfloor m'/2 \rfloor} \binom{m'}{k} \binom{m'-k}{k + I[m \text{ is even}]} \quad (3.34)$$

where $m' = \lfloor (m+1)/2 \rfloor$ and

$$I[\text{condition}] \equiv \begin{cases} 1 & \text{if condition is true} \\ 0 & \text{if condition is false} \end{cases} \quad (3.35)$$

The generating function for this sequence is

$$G_{=}(z) = \frac{1}{z} \left[-1 - \frac{1}{4z} \sqrt{\frac{1-3z}{1+z}} + \frac{1+2z-z^2}{4z\sqrt{(1+z^2)(1-3z^2)}} \right]. \quad (3.36)$$

In the above theorem, R_m denotes the m th Riordan number (see Appendix B.1 for the main properties of the Riordan numbers [9]). We remark that the sequence $N_{=}(m)$ coincides with sequence A005218 in [61] shifted by two units.

Theorem 3.7 *The number $N_{\neq}(m)$ of equivalence classes, modulo reflection with respect an axis going between the vertices 0 and $m+1$, of non-crossing non-nearest-neighbor partitions of the set $\{0, 1, \dots, m, m+1\}$ on a circle is given by*

$$N_{\neq}(m) = \frac{1}{2}R_{m+2} + \frac{1}{2} \sum_{k=0}^{\lfloor m'/2 \rfloor} \binom{m'}{k} \binom{m'-k}{k + I[m \text{ is odd}]} \quad (3.37)$$

where $m' = \lfloor (m+1)/2 \rfloor$. The generating function for this sequence is

$$G_{\neq}(z) = \frac{1}{4z^3} \left[\frac{2z^3 - z^2 + 1}{\sqrt{(1+z^2)(1-3z^2)}} - \sqrt{\frac{1-3z}{1+z}} - 2z(1+2z^2) \right]. \quad (3.38)$$

It follows that the dimension of the full symmetry-reduced transfer matrix $\mathsf{T}''(m)$ is

$$\dim \mathsf{T}''(m) = \text{SqFree}(m+2) = N_{\neq}(m) + N_{=}(m). \quad (3.39)$$

In particular, by using Theorems 3.6 and 3.7 we have rederived formula (2.17) and have found a few equivalent expressions:

Corollary 3.8 *The number $\dim \mathsf{T}''(m) = \text{SqFree}(m+2)$ of equivalence classes, modulo reflection in the center of the strip, of non-crossing non-nearest-neighbor partitions of the set $\{0, 1, \dots, m, m+1\}$ is given by*

$$\text{SqFree}(m+2) = \frac{1}{2}M_{m+1} + \frac{1}{2} \sum_{k=0}^{\lfloor m'/2 \rfloor} \binom{m'}{k} \binom{m'-k+1}{k+1} \quad (3.40a)$$

$$= \frac{1}{2}M_{m+1} + \frac{1}{2} \sum_{k=0}^{\lfloor m'/2 \rfloor} \binom{m'}{k} \binom{m'-k+1}{k} \quad (3.40b)$$

$$= \frac{1}{2}M_{m+1} + \frac{1}{4} \sum_{k=0}^{\lfloor m'/2 \rfloor} \binom{m'}{k} \binom{m'-k+2}{k+1} \quad (3.40c)$$

where $m' = \lfloor (m+1)/2 \rfloor$. The generating function for this sequence is

$$G(z) = \frac{1}{2z^2} \left[\frac{1+z}{z} \sqrt{\frac{1+z^2}{1-3z^2}} - \frac{\sqrt{(1+z)(1-3z)}}{z} - (1+2z+2z^2) \right] \quad (3.41)$$

We defer to Appendix B the detailed proof of this Corollary and the fact that (3.40a,b,c) and (2.17) do in fact coincide.

3.4 Relating the partition function to the transfer-matrix eigenvalues

For each boundary condition \sharp ($=$ or \neq), the partition function $Z_{S_{m,n}^{\sharp}}(q, \mathbf{v})$ can be expanded in the form

$$Z_{S_{m,n}^{\sharp}}(q, \mathbf{v}) = \sum_k \alpha_{k,\sharp}(m, q, \mathbf{v}) \lambda_{k,\sharp}(m, q, \mathbf{v})^n, \quad (3.42)$$

where $\lambda_{k,\sharp}(m, q, \mathbf{v})$ are the eigenvalues (labelled arbitrarily) of the transfer matrix $T_{\sharp}(m, q, \mathbf{v})$, and $\alpha_{k,\sharp}(m, q, \mathbf{v})$ are the corresponding amplitudes. Please note that the $\alpha_{k,\sharp}$ and $\lambda_{k,\sharp}$ are algebraic functions of q and \mathbf{v} , but we have to be careful about labels as we go around branch points.

For large $|q|$ everything becomes simple. By Corollary 3.4 there exists, for each m and \mathbf{v} , a value $Q(m, \mathbf{v})$ such that (for both boundary conditions) the dominant eigenvalue $\lambda_{\star,\sharp}(m, q, \mathbf{v})$ is analytic in the region $|q| > Q(m, \mathbf{v})$ and has there a convergent expansion in powers of q^{-1} ,

$$\lambda_{\star,\sharp}(m, q, \mathbf{v}) = \sum_{k=0}^{\infty} (-1)^k b_k^{\sharp}(m, \mathbf{v}) q^{m-k}, \quad (3.43)$$

with all other eigenvalues being strictly smaller in modulus. We have $b_0^{\sharp}(m, \mathbf{v}) = 1$ by Proposition 3.2 specialized to the particular operators H and V given by (3.2)/(3.3). By increasing $Q(m, \mathbf{v})$ if necessary, we may also suppose that the amplitude $\alpha_{\star,\sharp}(m, q, \mathbf{v})$ corresponding to the dominant eigenvalue is nonvanishing for $|q| > Q(m, \mathbf{v})$. Inserting these facts into (3.42), we conclude that for $|q| > Q(m, \mathbf{v})$ we have

$$\lim_{n \rightarrow \infty} \left(\frac{Z_{S_{m,n}^{\sharp}}(q, \mathbf{v})}{q^{|V(S_{m,n}^{\sharp})|}} \right)^{1/n} = q^{-m} \lambda_{\star,\sharp}(m, q, \mathbf{v}) \quad (3.44a)$$

$$= 1 + \sum_{k=1}^{\infty} (-1)^k b_k^{\sharp}(m, \mathbf{v}) q^{-k} \quad (3.44b)$$

uniformly on compact subsets of $|q| > Q(m, \mathbf{v})$. [Here we used $\lim_{n \rightarrow \infty} |V(S_{m,n}^{\sharp})|/n = m$.] It follows from this that (3.44) also holds order-by-order as a power series in $1/q$.

Unfortunately, the foregoing argument does not control the dependence of $Q(m, \mathbf{v})$ on m and \mathbf{v} . However, the uniformity in m (and \mathbf{v}) can be proven, at least for the antiferromagnetic case $-1 \leq v_e \leq 0$, by invoking the following result:¹³

Theorem 3.9 [62, Theorem 6.3] *Let $G = (V, E)$ be a loopless finite undirected graph in which all vertices have degree $\leq \Delta'$ except perhaps for an N -clique y_1, \dots, y_N . Let G be equipped with edge weights $\{v_e\}_{e \in E}$ satisfying $-1 \leq v_e \leq 0$ for all e and $v_{\langle y_i, y_j \rangle} = -1$ for all $i \neq j$. Then all the zeros of $Z_G(q, \mathbf{v})$ lie in the disc $|q| < 7.963907\Delta' + N$.*

For the family $S_{m,n}^=$ we have $\Delta' = 4$ and $N = 1$, where y_1 is the extra site; therefore, all zeros of $P_{S_{m,n}^=}(q)$ lie within the disc $|q| < 7.963907\Delta' + 1 = 32.855628$. For the family $S_{m,n}^{\neq}$ we have $\Delta' = 4$ and $N = 2$, where the 2-clique is formed by the two extra sites; therefore, all zeros of $P_{S_{m,n}^{\neq}}(q)$ lie within the slightly larger disc $|q| < 7.963907\Delta' + 2 = 33.855628$.

Using the Beraha–Kahane–Weiss theorem (Theorem 2.2) we can conclude that, outside such a disc, the transfer matrix $T_{\sharp}(m, q, \mathbf{v})$ for each width m and each antiferromagnetic coupling \mathbf{v} must have one and only one eigenvalue of largest modulus $\lambda_{\star,\sharp}(m, q, \mathbf{v})$. Since this dominant eigenvalue cannot collide with any other eigenvalue of the same transfer matrix, it must be an analytic function of q (and nonvanishing) outside the given disc;

¹³Actually, [62, Theorem 6.3] also gives a more general result applicable to *complex* edge weights in the “complex antiferromagnetic regime” $|1 + v_e| \leq 1$, albeit with slightly weaker bounds.

and the series (3.43) must be convergent outside the given disc. That is, we can take $Q(m, \mathbf{v}) = 33.855628$ for all m and all antiferromagnetic \mathbf{v} .

In summary, the transfer matrix for a square-lattice strip of width m and with $=$ or \neq boundary conditions has a single dominant eigenvalue $\lambda_{*,=}(m, q, \mathbf{v})$ or $\lambda_{*,\neq}(m, q, \mathbf{v})$ that is a nonvanishing analytic function of q (in fact, q^m times an analytic function of q^{-1}) whenever $|q| > 33.855628$, uniformly in m and in \mathbf{v} belonging to the antiferromagnetic regime.

3.5 Comparing $S_{m,n}^{\neq}$ with $S_{m,n}^=$

A *2-terminal graph* (G, s, t) is a (loopless and connected) graph $G = (V, E)$ with two distinguished vertices s and t ($s \neq t$), called the *terminals*. We define the partial partition functions of (G, s, t) as follows [63, Section 2.1]:

$$Z_G^{(s \nleftrightarrow t)}(q, \mathbf{v}) = \sum_{\substack{A \subseteq E \\ A \text{ does not connect } s \text{ to } t}} q^{k(A)} \prod_{e \in A} v_e \quad (3.45a)$$

$$Z_G^{(s \leftrightarrow t)}(q, \mathbf{v}) = \sum_{\substack{A \subseteq E \\ A \text{ connects } s \text{ to } t}} q^{k(A)} \prod_{e \in A} v_e \quad (3.45b)$$

From (2.4) it follows trivially that

$$Z_G(q, \mathbf{v}) = Z_G^{(s \leftrightarrow t)}(q, \mathbf{v}) + Z_G^{(s \nleftrightarrow t)}(q, \mathbf{v}). \quad (3.46)$$

We define $G \bullet st$ to be the graph in which s and t are contracted into a single vertex. (Note that if G contains one or more edges st , then these edges are *not* deleted, but become loops in $G \bullet st$.) Then from (2.4) it also follows [63] that

$$Z_{G \bullet st}(q, \mathbf{v}) = Z_G^{(s \leftrightarrow t)}(q, \mathbf{v}) + q^{-1} Z_G^{(s \nleftrightarrow t)}(q, \mathbf{v}). \quad (3.47)$$

Finally, let $G + st$ define the graph G with an extra edge st . Then it also follows from (2.4) that

$$Z_{G+st}(q, \mathbf{v}) = (1 + v_{st}) Z_G^{(s \leftrightarrow t)}(q, \mathbf{v}) + \left(1 + \frac{v_{st}}{q}\right) Z_G^{(s \nleftrightarrow t)}(q, \mathbf{v}), \quad (3.48)$$

which equals $Z_G(q, \mathbf{v}) + v_{st} Z_{G \bullet st}(q, \mathbf{v})$ in agreement with the deletion-contraction formula.

Both $Z_G^{(s \nleftrightarrow t)}(q, \mathbf{v})$ and $Z_G^{(s \leftrightarrow t)}(q, \mathbf{v})$ are polynomials in q and \mathbf{v} . At large $|q|$, the leading behavior of $Z_G^{(s \leftrightarrow t)}$ and $Z_G^{(s \nleftrightarrow t)}$ is

$$Z_G^{(s \nleftrightarrow t)}(q, \mathbf{v}) = q^{|V(G)|} + \dots \quad (3.49a)$$

$$Z_G^{(s \leftrightarrow t)}(q, \mathbf{v}) = q^{|V(G)| - d_G(s, t)} \sum_{\substack{\text{shortest paths} \\ s \rightarrow t}} \prod_{e \in \text{path}} v_e + \dots \quad (3.49b)$$

where $d_G(s, t)$ is the length of the shortest path from s to t using edges having $v_e \neq 0$.

Let us now specialize these general formulae to the case $G = S_{m,n}$, with the terminals s, t taken to be the two special vertices. Then

$$G \bullet st = S_{m,n}^- \quad (3.50a)$$

$$G + st = S_{m,n}^\neq \quad (3.50b)$$

so that

$$Z_{S_{m,n}^-}(q, \mathbf{v}) = Z_{S_{m,n}}^{(s \leftrightarrow t)}(q, \mathbf{v}) + q^{-1} Z_{S_{m,n}}^{(s \nleftrightarrow t)}(q, \mathbf{v}) \quad (3.51a)$$

$$Z_{S_{m,n}^\neq}(q, \mathbf{v}) = (1 - q^{-1}) Z_{S_{m,n}}^{(s \nleftrightarrow t)}(q, \mathbf{v}) \quad (3.51b)$$

We have $|V(G)| = mn + 2$, $|V(G \bullet st)| = mn + 1$ and $|V(G + st)| = mn + 2$. Furthermore, we have $d_G(s, t) = m + 1$, and there are n shortest paths from s to t : each of them consists of the $m - 1$ horizontal edges in a row of $S_{m,n}$ together with the two additional edges joining this row to the vertices s, t . Therefore

$$\sum_{\substack{\text{shortest paths} \\ s \rightarrow t}} \prod_{e \in \text{path}} v_e = n \prod_{i=0}^m v_{i,i+1}. \quad (3.52)$$

Finally, in the graph $G + st = S_{m,n}^\neq$ we have $v_{st} = -1$.

For $|q| > Q(m, \mathbf{v})$, using (3.44) applied to $S_{m,n}^\neq$ together with (3.51b), we see that

$$\lambda_{*,\neq}(m, q, \mathbf{v}) = \lim_{n \rightarrow \infty} \left(Z_{S_{m,n}}^{(s \nleftrightarrow t)}(q, \mathbf{v}) \right)^{1/n} \quad (3.53a)$$

$$= q^m \left[1 + \sum_{k=1}^{\infty} (-1)^k b_k^\neq(m, \mathbf{v}) q^{-k} \right]. \quad (3.53b)$$

Likewise, using (3.44) applied to $S_{m,n}^-$ together with (3.51a), (3.49) and (3.52), we see that

$$\lambda_{*,=}(m, q, \mathbf{v}) = \lim_{n \rightarrow \infty} \left(Z_{S_{m,n}}^{(s \leftrightarrow t)}(q, \mathbf{v}) + q^{-1} Z_{S_{m,n}}^{(s \nleftrightarrow t)}(q, \mathbf{v}) \right)^{1/n} \quad (3.54a)$$

$$= \lambda_{*,\neq}(m, q, \mathbf{v}) \lim_{n \rightarrow \infty} \left[1 + q \frac{Z_{S_{m,n}}^{(s \leftrightarrow t)}(q, \mathbf{v})}{Z_{S_{m,n}}^{(s \nleftrightarrow t)}(q, \mathbf{v})} \right]^{1/n} \quad (3.54b)$$

$$= \lambda_{*,\neq}(m, q, \mathbf{v}) \lim_{n \rightarrow \infty} \left[1 + q^{-m} n \prod_{i=0}^m v_{i,i+1} + O(q^{-m-1}) \right]^{1/n} \quad (3.54c)$$

$$= \lambda_{*,\neq}(m, q, \mathbf{v}) \left[1 + q^{-m} \prod_{i=0}^m v_{i,i+1} + O(q^{-m-1}) \right] \quad (3.54d)$$

$$= \lambda_{*,\neq}(m, q, \mathbf{v}) + \prod_{i=0}^m v_{i,i+1} + O(q^{-1}). \quad (3.54e)$$

Please note the logic in the step from (3.54c) to (3.54d): we know from (3.44) that the limit exists order-by-order as a power series in q^{-1} ; so the term of order q^{-m} is indeed as claimed, and everything else is of order q^{-m-1} or smaller. We do not need to have any explicit bounds on the n -dependence of the $O(q^{-m-1})$ terms in (3.54c). We have therefore proven:

Proposition 3.10 *The difference at large $|q|$ between the leading eigenvalues $\lambda_{*,=}(m, q, \mathbf{v})$ and $\lambda_{*,\neq}(m, q, \mathbf{v})$ of the transfer matrices $\mathbb{T}''_{=}(m, q, \mathbf{v})$ and $\mathbb{T}''_{\neq}(m, q, \mathbf{v})$ for $m \geq 1$ satisfies*

$$\lambda_{*,=}(m, q, \mathbf{v}) - \lambda_{*,\neq}(m, q, \mathbf{v}) = \prod_{i=0}^m v_{i,i+1} + O(q^{-1}). \quad (3.55)$$

In particular, for the chromatic-polynomial case $v_e = -1$ we have

$$\lambda_{*,=}(m, q) - \lambda_{*,\neq}(m, q) = (-1)^{m+1} + O(q^{-1}). \quad (3.56)$$

The formula (3.55) generalizes the result (2.40) for theta graphs [which corresponds to setting the vertical couplings $v_i = 0$]. It has the same form as the result (3.13) for the dominant diagonal entries — the only difference being that (3.13) is exact, while (3.55) is for the leading term only.

4 Numerical results I: Large- q expansion of the leading eigenvalue

In this section we compute the large- q expansion of the leading eigenvalues $\lambda_{*,=}(m)$ and $\lambda_{*,\neq}(m)$ and determine empirically some of their remarkable properties. In Section 5 we shall provide theoretical explanations of some (but not all!) of these empirical observations.

4.1 Overview of method and results

In Proposition 3.5 (proven in Appendix A) we computed in closed form the dominant diagonal entry in the transfer matrix, $t_{=}$ or t_{\neq} , for a strip of width $m \geq 1$ with either $=$ or \neq boundary conditions. We found that this entry is in each case a polynomial in q of degree m :

$$t_{\neq}(m) = \sum_{k=0}^m (-1)^k a_k(m) q^{m-k} \quad (4.1a)$$

$$t_{=}(m) = \sum_{k=0}^m (-1)^k a_k(m) q^{m-k} + (-1)^{m+1} \quad (4.1b)$$

We furthermore computed in closed form the coefficients $a_k(m)$, which are in fact, for each fixed $k \geq 0$, the restriction to integers $m \geq \max(1, k)$ of polynomials in m of degree k [cf. (3.25)].

In this section we want to carry out an analogous (though ultimately less explicit) computation for the leading *eigenvalue* of the transfer matrix, which we call $\lambda_{*,=}$ or $\lambda_{*,\neq}$. From Section 3.4 we recall that each $\lambda_*(m)$ has, for large $|q|$, a convergent expansion in powers of q^{-1} ,

$$\lambda_{*,\sharp}(m) = \sum_{k=0}^{\infty} (-1)^k b_k^{\sharp}(m) q^{m-k}, \quad (4.2)$$

where \sharp denotes $=$ or \neq . It is also illuminating to pass from the eigenvalue $\lambda_*(m)$ to its logarithm, which is a free energy, and define

$$\log \frac{\lambda_{*,\sharp}(m)}{q^m} = \sum_{k=1}^{\infty} c_k^{\sharp}(m) q^{-k}. \quad (4.3)$$

Corollary 3.4 guarantees that the first two terms in the expansion of the leading eigenvalue coincide with those in the dominant diagonal entry:

$$b_k^-(m) = b_k^{\neq}(m) = a_k(m) \quad \text{for } k = 0, 1 \quad (4.4)$$

(with $m \geq 2$ required for b_1^- in order to avoid the $(-1)^{m+1}$ term), or more specifically

$$b_0^-(m) = b_0^{\neq}(m) = 1 \quad (4.5a)$$

$$b_1^-(m) = b_1^{\neq}(m) = 2m + 1 \quad \text{for } m \geq 2 \quad (4.5b)$$

Here we shall go further and compute the coefficients $b_k^-(m)$ and $b_k^{\neq}(m)$ for $1 \leq m \leq 12$ and $1 \leq m \leq 11$, respectively, with $0 \leq k \leq 40$.¹⁴ We shall find empirically that the agreement between the eigenvalue and the dominant diagonal entry extends one term beyond that guaranteed by Corollary 3.4: namely, we have¹⁵

$$b_2^{\neq}(m) = a_2(m) \quad \text{for } m \geq 2 \quad (4.6a)$$

$$b_2^-(m) = a_2(m) \quad \text{for } m \geq 3 \quad (4.6b)$$

Beyond this, the eigenvalues deviate from the dominant diagonal terms. However, from Proposition 3.10 we know — and our computations of course confirm — that the deviations of the eigenvalues from the dominant diagonal terms are the *same* for $=$ and \neq boundary conditions, all the way down to order 1, so that the *difference* between the two eigenvalues has the same leading behavior as the difference between the two dominant diagonal terms:

$$\lambda_{*,=}(m) - \lambda_{*,\neq}(m) = (-1)^{m+1} + O(q^{-1}) \quad (4.7)$$

as compared with

$$t_=(m) - t_{\neq}(m) = (-1)^{m+1}. \quad (4.8)$$

¹⁴It would not be difficult to extend this computation to much larger values of k , if we really cared. Extension to larger values of m is, however, an extremely demanding computational task. The dimensions of the transfer matrices $\mathbf{T}''_{=}(13)$ and $\mathbf{T}''_{\neq}(12)$ are 15465 and 15339, respectively, which are beyond the capabilities of our current computer facilities.

¹⁵In [54] we found, for free and cylindrical boundary conditions, an agreement extending *two* terms beyond that guaranteed by Corollary 3.4.

In terms of the coefficients, this says that

$$b_k^-(m) - b_k^\neq(m) = \begin{cases} 0 & \text{for } 0 \leq k \leq m-1 \\ -1 & \text{for } k = m \end{cases} \quad (4.9)$$

and

$$c_k^-(m) - c_k^\neq(m) = \begin{cases} 0 & \text{for } 1 \leq k \leq m-1 \\ (-1)^{m+1} & \text{for } k = m \end{cases} \quad (4.10)$$

This amazing behavior suggests that we look more closely at the differences between $=$ and \neq boundary conditions for orders $k \geq m$. We therefore define coefficients $d_\ell(m)$ by

$$(-1)^{m+1}[\lambda_{*,=(m)} - \lambda_{*,\neq(m)}] = 1 + \sum_{\ell=1}^{\infty} (-1)^\ell d_\ell(m) q^{-\ell} \quad (4.11)$$

or equivalently

$$d_\ell(m) = -[b_{m+\ell}^-(m) - b_{m+\ell}^\neq(m)] . \quad (4.12)$$

It furthermore turns out to be interesting to look at the *logarithm* of this difference of eigenvalues:

$$\log\{(-1)^{m+1}[\lambda_{*,=(m)} - \lambda_{*,\neq(m)}]\} = \sum_{\ell=1}^{\infty} e_\ell(m) q^{-\ell} . \quad (4.13)$$

The following variant is also of interest:

$$-\log\left[(-1)^{m+1}q^m \log\left(\frac{\lambda_{*,=(m)}}{\lambda_{*,\neq(m)}}\right)\right] = \sum_{\ell=1}^{\infty} f_\ell(m) q^{-\ell} . \quad (4.14)$$

We shall obtain empirical formulae for the coefficients $d_\ell(m)$, $e_\ell(m)$ and $f_\ell(m)$ for $1 \leq \ell \leq 13$.

In this section we shall proceed as follows (imitating what we did in [54, Section 4] for free and cylindrical boundary conditions): First we shall compute the transfer matrices for strips of width $m \leq 11$ (resp. $m \leq 12$) for \neq (resp. $=$) boundary conditions, using the methods of [34, 53] as modified for the family $S_{m,n}$ (see Section 3 above). From these matrices we then extract the dominant eigenvalue as a power series in q^{-1} , i.e. for each available m we compute as many coefficients $b_k^\neq(m)$ and $c_k^\neq(m)$ as we please.¹⁶ We then observe *empirically* that, for each $k \geq 0$, the coefficients $b_k^-(m)$ and $b_k^\neq(m)$ [resp. $c_k^-(m)$ and $c_k^\neq(m)$] are *equal* and are represented by a polynomial $B_k(m)$ [resp. $C_k(m)$] of degree k [resp. degree 1] in m , *provided that we restrict to integers $m \geq m_{\min}(k)$* , where

$$m_{\min}^\neq(k) = \max(k, 1) \quad (4.15a)$$

$$m_{\min}^-(k) = k + 1 \quad (4.15b)$$

¹⁶To compute the dominant eigenvalue as a power series in q^{-1} , we have used the power method [28, Section 7.3.1] *in symbolic form*. Each iteration gives one additional term in the expansion of the dominant eigenvalue in powers of q^{-1} . We can therefore compute the *exact* expansion up to any desired order in a *finite* number of steps.

for the two boundary conditions.¹⁷ *Assuming* that this empirical observation is accurate (i.e., that the polynomial behavior observed for $m \leq 11, 12$ persists to all larger m), we can infer the exact expressions for the polynomials B_k and C_k for $k \leq 17$ for \neq and $=$ boundary conditions. The fact that the polynomials C_k are of degree 1 in m — hence consist of a bulk term $\alpha_k m$ and a surface term β_k — can be explained (non-rigorously) by finite-size-scaling theory: see Section 5 below and especially the discussion around eqns. (5.7)/(5.9) and at the beginning of Section 5.5.

Analogously — and rather more surprisingly — we find that the coefficients $d_\ell(m)$, $e_\ell(m)$ and $f_\ell(m)$ are also represented by polynomials $D_\ell(m)$, $E_\ell(m)$ and $F_\ell(m)$, of degrees ℓ , 1 and 1, respectively, provided that we restrict to integers $m \geq \ell + 1$. This behavior — in which the difference of two eigenvalues (which are essentially free energies) behaves *like a partition function* in the sense that its *logarithm* grows asymptotically linearly in the strip length — is wholly unexpected, at least to us.

4.2 Results for $S_{m,n}^\neq$

Using the methods just described, we have obtained the leading eigenvalue $\lambda_{*,\neq}(m)$ for $1 \leq m \leq 11$ as a power series in q^{-1} [cf. (3.43)] through order $k = 40$. The resulting coefficients $b_k^\neq(m)$ are displayed for $0 \leq k \leq 15$ in Table 2, and the corresponding coefficients $c_k^\neq(m)$ [cf. (4.3)] are displayed in Table 3. (The complete data set for $0 \leq k \leq 40$ is contained in the MATHEMATICA file `data_Neq.m` that is included in the on-line version of this paper at arXiv.org.) It is interesting to note that for all pairs (k, m) that we have computed (namely, $1 \leq m \leq 11$ and $0 \leq k \leq 40$), the coefficients $b_k^\neq(m)$ and $kc_k^\neq(m)$ are integers. Furthermore, we observe *empirically* that, for each fixed k , the coefficients $b_k^\neq(m)$ [resp. $c_k^\neq(m)$] are the restriction to integers m of a polynomial $B_k(m)$ [resp. $C_k(m)$] of degree k (resp. degree 1) in m , *provided that we restrict attention to $m \geq m_{\min}^\neq(k)$* with

$$m_{\min}^\neq(k) = \max(k, 1) . \quad (4.16)$$

Below this threshold $m_{\min}^\neq(k)$, the coefficients deviate from polynomial behavior. With our available data together with a few tricks described below, we are able to determine these polynomials for $0 \leq k \leq 17$.

First we start by trying to fit the coefficients $b_k^\neq(m)$ with $m \geq m_{\min}^\neq(k)$ to a polynomial $B_k(m)$ of degree k . As we need $k + 1$ coefficients for such a polynomial, we are able to obtain these polynomials when $m_{\min}^\neq(k) + k \leq 11$, i.e. $k \leq 5$. Please observe that in all cases we have at least one data point more than the number of unknowns, so that every

¹⁷By contrast, for the dominant diagonal entry we have *proven* in Proposition 3.5 that $a_k(m)$ are polynomials in m of degree k ; and in this case the polynomial form holds for *all* allowable integers m , i.e. $m \geq \max(k, 1)$.

fit can be tested on at least one extra data point.¹⁸ Our results are:

$$B_0(m) = 1 \quad (4.17a)$$

$$B_1(m) = 2m + 1 \quad (4.17b)$$

$$B_2(m) = 2m^2 + m - 2 \quad (4.17c)$$

$$B_3(m) = \frac{4}{3}m^3 - \frac{16}{3}m + 3 \quad (4.17d)$$

$$B_4(m) = \frac{2}{3}m^4 - \frac{2}{3}m^3 - \frac{37}{6}m^2 + \frac{61}{6}m - 3 \quad (4.17e)$$

$$B_5(m) = \frac{4}{15}m^5 - \frac{2}{3}m^4 - \frac{13}{3}m^3 + \frac{91}{6}m^2 - \frac{343}{30}m - 2 \quad (4.17f)$$

We see that the three highest-order coefficients in these polynomials agree with those of the corresponding polynomial $a_k(m)$ [cf. (3.25)/(3.26)], i.e.

$$B_k(m) = \begin{cases} a_k(m) & \text{for } 0 \leq k \leq 2 \\ a_k(m) + O(m^{k-3}) & \text{for } k \geq 3 \end{cases} \quad (4.18)$$

There is, however, a better way of extracting the desired information from our numerical data: instead of using the coefficients $b_k^\neq(m)$ as our basic quantities, we can use the related coefficients $c_k^\neq(m)$ [cf. (4.3)]. The latter coefficients are empirically found to be, for each fixed k , the restriction to integer m of a polynomial $C_k(m)$ of degree 1, i.e.

$$C_k(m) = \alpha_k m + \beta_k, \quad (4.19)$$

provided again that we restrict attention to $m \geq$ the same $m_{\min}^\neq(k)$ defined in (4.16). As we now need only the *two* coefficients α_k and β_k to specify such a polynomial, we are able to obtain these polynomials up to $k = 9$ (if we want at least one extra data point to test the fit) or $k = 10$ (if we don't). The first polynomials C_k are given by

$$C_1(m) = -2m - 1 \quad (4.20a)$$

$$C_2(m) = -m - \frac{5}{2} \quad (4.20b)$$

$$C_3(m) = \frac{1}{3}m - \frac{16}{3} \quad (4.20c)$$

$$C_4(m) = \frac{5}{2}m - \frac{41}{4} \quad (4.20d)$$

$$C_5(m) = \frac{28}{5}m - \frac{81}{5} \quad (4.20e)$$

and the results for $6 \leq k \leq 10$ are shown in Table 4. The polynomials B_k for $k \leq 10$ can then be determined from the C_k using (3.43)/(4.3).

¹⁸In our view this test is important, because the formula (4.16) for $m_{\min}^\neq(k)$ is only empirical; and if it were to be mistaken by one unit (i.e. the real threshold for polynomial behavior were one unit higher than we thought), then a fit with no extra data points would give a definite result (one can *always* fit $k + 1$ points to a polynomial of degree k) *but this result would be total nonsense*.

Actually, we can do better than this. We believe (or at least conjecture!) that the coefficients $c_k^\neq(m)$ are, for each fixed $k \geq 0$, the restriction to integers $m \geq m_{\min}^\neq(k)$ of a polynomial $C_k(m)$ of degree 1. If we now compute the difference

$$\Delta_k^\neq(m) = c_k^\neq(m) - C_k(m) \quad (4.21)$$

between the numerical coefficients $c_k^\neq(m)$ and the corresponding polynomials $C_k(m)$, we find, not surprisingly, that these differences are nonzero whenever $m < m_{\min}^\neq(k)$: see Table 5, where we initially know $\Delta_k^\neq(m)$ only for $k \leq 10$ (or $k \leq 9$ if we wish to be conservative). If we could somehow guess an analytic form for at least some of these coefficients $\Delta_k^\neq(m)$, we could then define “improved” coefficients $\widehat{c}_k^\neq(m)$ by

$$\widehat{c}_k^\neq(m) = c_k^\neq(m) - \Delta_k^\neq(m), \quad (4.22)$$

so that these coefficients $\widehat{c}_k^\neq(m)$ would be, for each fixed k , the restriction to integers $m \geq \widehat{m}_{\min}^\neq(k)$ of the same polynomial $C_k(m)$, but with a *smaller* threshold $\widehat{m}_{\min}^\neq(k) < m_{\min}^\neq(k)$. The important point here is that a smaller threshold $\widehat{m}_{\min}^\neq(k)$ implies that we can obtain more polynomials C_k with the same raw data.

By inspecting Table 5, it is not difficult to realize that there are some patterns in $\Delta_k^\neq(m)$ just below the threshold $m_{\min}^\neq(k)$, and more specifically along diagonals $m = k - \ell$ with fixed integer $\ell \geq 1$. For instance, for $\ell = 1$ we see that $\Delta_k^\neq(k - 1) = (-1)^{k+1}$ for $2 \leq k \leq 10$; and it is reasonable to *conjecture* that this holds also for larger k , i.e.

$$\Delta_k^\neq(k - 1) = (-1)^{k+1} \quad \text{for all } k \geq 2. \quad (4.23)$$

Likewise, for $\ell = 2, 3$ we find for $k \leq 10$ — and conjecture for all larger k — that $\Delta_k^\neq(k - \ell)$ can be written as $(-1)^{k+1}$ times a polynomial in k of degree $\ell - 1$, provided that $k \geq 2\ell - 1$:

$$\Delta_k^\neq(k - 2) = (-1)^{k+1} (k - 7) \quad \text{for } k \geq 3 \quad (4.24a)$$

$$\Delta_k^\neq(k - 3) = (-1)^{k+1} \left(\frac{1}{2}k^2 - \frac{27}{2}k + 57 \right) \quad \text{for } k \geq 5 \quad (4.24b)$$

Each of these fits can be tested on at least three additional data points. [We can also obtain a fit for $\Delta_k^\neq(k - 4)$ for $k \geq 7$, but at this stage we would have no extra data points to test it.]

Then, assuming the correctness of (4.23)/(4.24), we can infer the polynomials C_k for $k = 11, 12$ (if we demand at least one extra data point to test the fit) and $k = 13$ (if we don't). In turn, knowing the polynomials C_{11} and C_{12} , we can obtain a fit for $\Delta_k^\neq(k - 4)$ that can be tested on two extra data points:

$$\Delta_k^\neq(k - 4) = (-1)^{k+1} \left(\frac{1}{6}k^3 - 10k^2 + \frac{821}{6}k - 487 \right) \quad \text{for } k \geq 7. \quad (4.25)$$

Next, assuming the correctness also of (4.25), we get one additional data point to test the fit to C_{13} (not surprisingly, it checks) and we can infer C_{14} if we don't demand any extra data points to test it. In turn, knowing the polynomial C_{13} , we can guess one further correction term $\Delta_k^\neq(k - \ell)$:

$$\Delta_k^\neq(k - 5) = (-1)^{k+1} \left(\frac{1}{24}k^4 - \frac{53}{12}k^3 + \frac{3107}{24}k^2 - \frac{15817}{12}k + 4253 \right) \quad \text{for } k \geq 9, \quad (4.26)$$

where here there are *no* additional data points to test the fit if we use only C_{13} , but there is one additional data point if we trust also the inferred C_{14} . Finally, assuming the correctness of (4.26), we can infer C_{15} (but without any extra data points to test the fit). All the polynomials C_k for $k \leq 15$ are shown in Table 4.

We can extend slightly our results by noticing the following two empirical results from the formulae for $\Delta_k^\neq(k-\ell)$ in (4.23)–(4.26): (a) the leading coefficient in $\Delta_k^\neq(k-\ell)$ is $1/(\ell-1)!$, and (b) the next-to-leading coefficient is $-1/(\ell-1)! \times [0, 7, 27, 60, 106]$, which is fitted by $\frac{1}{2}(\ell-1)(13\ell-12)$. If these patterns persist, then we need only 4 coefficients (rather than 6) to get $\Delta_k^\neq(k-6)$, i.e. $k = 11, 12, 13, 14$, so we can then get C_{15} with one extra data point, or C_{16} without. The result of the fit is

$$\Delta_k^\neq(k-6) = (-1)^{k+1} \left(\frac{1}{120}k^5 - \frac{11}{8}k^4 + \frac{1693}{24}k^3 - \frac{11565}{8}k^2 + \frac{248889}{20}k - 378651 \right) \quad \text{for } k \geq 11, \quad (4.27)$$

where here there is one additional data point if we trust also the inferred C_{14} and C_{15} .

Remark. In Section 5.5 we will infer also C_{17} by exploiting the known large- q series for the bulk free energy [1, 54], which gives us the coefficients α_k ; we then need only *one* additional data point to infer β_k and hence C_k . All the polynomials C_k for $k \leq 17$ are shown in Table 4.

4.3 Results for $S_{m,n}^\equiv$

We carried out a completely analogous analysis for the case of $=$ boundary conditions; we shall therefore be brief in describing it, stressing only the differences from the preceding analysis and the final results.

We were able to compute $\lambda_{*,=}(m)$ for $1 \leq m \leq 12$ (one term more than for \neq boundary conditions). The resulting coefficients $b_k^\equiv(m)$ and $c_k^\equiv(m)$ for $0 \leq k \leq 15$ are displayed in Tables 6 and 7, respectively.¹⁹ We observe *empirically* that, for each fixed k , the coefficients $b_k^\equiv(m)$ [resp. $c_k^\equiv(m)$] are the restriction to integers m of a polynomial $B_k(m)$ [resp. $C_k(m)$] of degree k (resp. degree 1) in m , *provided that we restrict attention to $m \geq m_{\min}^\equiv(k)$* with

$$m_{\min}^\equiv(k) = k + 1. \quad (4.28)$$

Furthermore, the polynomials $B_k(m)$ and $C_k(m)$ are empirically found to be the *same* as those for \neq boundary conditions. Using our available data together with the tricks shown in the preceding subsection, we are able to confirm this equality for $k \leq 17$. Let us sketch quickly the logic of this computation and the relevant intermediate results.

As before, we can extract the desired information most efficiently by fitting the coefficients $c_k^\equiv(m)$ to a polynomial $C_k(m)$ of degree 1, for $m \geq m_{\min}^\equiv(k) = k + 1$. As we need only two coefficients for such a polynomial, we can obtain these polynomials up to $k = 9$ (if we want at least one extra data point to test the fit) or $k = 10$ (if we don't). The results are equal to those of \neq boundary conditions.

Next we try to improve these results, as before, by defining the difference $\Delta_k^\equiv(m) = c_k^\equiv(m) - C_k(m)$ and attempting to guess an analytic form for some of the coefficients

¹⁹The complete data set for $0 \leq k \leq 40$ is contained in the MATHEMATICA file `data.Eq.m` that is included in the on-line version of this paper at arXiv.org.

$\Delta_k^-(m)$: see Table 8, where we initially know only $k \leq 10$. As in the case of \neq boundary conditions, we find empirically that the coefficients $\Delta_k^-(m)$ closest to the boundary $m_{\min}^-(k)$ are the restriction to integers m of certain polynomials. Because $m_{\min}^-(k) = k + 1$, we are concerned this time with $\Delta_k^-(k - \ell)$ for $\ell \geq 0$ (rather than $\ell \geq 1$ as before). We obtain:

$$\Delta_k^-(k) = (-1)^{k+1} \quad \text{for } k \geq 1 \quad (4.29a)$$

$$\Delta_k^-(k-1) = (-1)^{k+1} (k-5) \quad \text{for } k \geq 3 \quad (4.29b)$$

$$\Delta_k^-(k-2) = (-1)^{k+1} \left(\frac{1}{2}k^2 - \frac{23}{2}k + 37 \right) \quad \text{for } k \geq 5 \quad (4.29c)$$

$$\Delta_k^-(k-3) = (-1)^{k+1} \left(\frac{1}{6}k^3 - 9k^2 + \frac{623}{6}k - 303 \right) \quad \text{for } k \geq 7 \quad (4.29d)$$

We are able to test each fit on at least one additional data point.²⁰ The pattern is slightly different from that for \neq boundary conditions: here $\Delta_k^-(k - \ell)$ is $(-1)^{k+1}$ times a polynomial of degree ℓ in k , valid for $k \geq 2\ell + 1$. By this method, we can obtain the polynomials C_k up to $k = 13$ (if we demand at least one extra data point to test the fit) or $k = 14$ (if we don't).

We can then guess one further correction term $\Delta_k^-(k - \ell)$:

$$\Delta_k^-(k-4) = (-1)^{k+1} \left(\frac{1}{24}k^4 - \frac{49}{12}k^3 + \frac{2555}{24}k^2 - \frac{11225}{12}k + 2573 \right) \quad \text{for } k \geq 9. \quad (4.30)$$

where there are no additional data points to test the fit if we use only C_{13} , but there is one additional data point if we trust also the inferred C_{14} . Finally, assuming the correctness of (4.30), we can infer C_{15} (but without any extra data points to test the fit).

As for \neq boundary conditions, we can extend slightly our results by looking at the patterns for the first two terms in $\Delta_k^-(k - \ell)$ (4.29d)/(4.30): The leading coefficient in $\Delta_k^-(k - \ell)$ is $1/\ell!$, and the next-to-leading coefficient is $-1/\ell! \times [0, 5, 23, 54, 98]$, which is fitted by $\frac{1}{2}\ell(13\ell - 3)$. If these patterns persist, then we need only 4 coefficients (rather than 6) to get $\Delta_k^-(k-5)$, so we can then get C_{15} with one extra data point, or C_{16} without. The result of the fit is

$$\Delta_k^-(k-5) = (-1)^{k-4} \left(-\frac{1}{120}k^5 + \frac{31}{24}k^4 - \frac{1457}{24}k^3 + \frac{26705}{24}k^2 - \frac{506477}{60}k + 22330 \right) \quad \text{for } k \geq 11, \quad (4.31)$$

where here there is one additional data point if we trust also the inferred C_{14} and C_{15} . We find, in all cases, the *same* polynomials C_k as for \neq boundary conditions.

Remark. In Section 5.5 we will infer also C_{17} for $=$ boundary conditions by exploiting the known large- q series for the bulk free energy [1, 54].

4.4 Comparing $S_{m,n}^{\neq}$ with $S_{m,n}^-=$

We were able to compute the difference $(-1)^{m+1}[\lambda_{*,=}(m) - \lambda_{*,\neq}(m)]$ for $1 \leq m \leq 11$, and we have extracted the coefficients $d_\ell(m)$ [cf. (4.11)] for $1 \leq m \leq 11$ and $1 \leq \ell \leq 20$.

²⁰For $\ell = 3$ we do not *immediately* have such an extra data point, but we can obtain it after using $\ell = 0, 1, 2$ to infer C_{11} and C_{12} . The reasoning is completely analogous to what was explained in detail for the case of \neq boundary conditions.

The resulting coefficients are displayed in Table 9 for $1 \leq \ell \leq 13$. (The complete data set for $1 \leq \ell \leq 20$ is included in the MATHEMATICA file `data_Diff.m` that is included in the on-line version of this paper at arXiv.org.) We observe *empirically* that, for each fixed ℓ , the coefficients $d_\ell(m)$ are the restriction to integers m of a polynomial $D_\ell(m)$ of degree ℓ in m , *provided that we restrict attention to $m \geq m_{\min}(\ell) = \ell + 1$* [cf. (4.28)]. We start by trying to perform such fit: As we need $\ell + 1$ coefficients for the polynomial $D_\ell(m)$, we are able to obtain these polynomials for $\ell \leq 4$ (if we allow for at least one extra data point to test the fit) or $\ell \leq 5$ (if we don't). Our results are:

$$D_1(m) = 3m - 4 \quad (4.32a)$$

$$D_2(m) = \frac{9}{2}m^2 - \frac{37}{2}m + 14 \quad (4.32b)$$

$$D_3(m) = \frac{9}{2}m^3 - \frac{75}{2}m^2 + 84m - 55 \quad (4.32c)$$

$$D_4(m) = \frac{27}{8}m^4 - \frac{189}{4}m^3 + \frac{1681}{8}m^2 - \frac{1461}{4}m + 224 \quad (4.32d)$$

$$D_5(m) = \frac{81}{40}m^5 - \frac{171}{4}m^4 + \frac{2523}{8}m^3 - \frac{4147}{4}m^2 + \frac{15661}{10}m - 880 \quad (4.32e)$$

As in the preceding sections, we can extract more information by considering the coefficients $e_\ell(m)$ arising in the *logarithm* of the difference of eigenvalues [cf. (4.13)]. These coefficients are displayed in Table 10 for $1 \leq \ell \leq 13$, and the complete set is included in the file `data_Diff.m`. We again observe *empirically* that, for each fixed ℓ , the coefficients $e_\ell(m)$ are the restriction to integers m of a polynomial $E_\ell(m)$ of degree 1 in m , *provided that we restrict attention to $m \geq m_{\min}(\ell) = \ell + 1$* . As we need two coefficients for such a polynomial, we can obtain these polynomials up to $\ell = 8$ (if we want at least one extra data point to test the fit) or $\ell = 9$ (if we don't). The first polynomials are given by

$$E_1(m) = -3m + 4 \quad (4.33a)$$

$$E_2(m) = -\frac{13}{2}m + 6 \quad (4.33b)$$

$$E_3(m) = -16m + \frac{61}{3} \quad (4.33c)$$

$$E_4(m) = -\frac{181}{4}m + 66 \quad (4.33d)$$

$$E_5(m) = -\frac{658}{5}m + \frac{934}{5} \quad (4.33e)$$

and the results for $6 \leq \ell \leq 9$ are shown in Table 4. The polynomials D_ℓ for $\ell \leq 9$ can then be determined from the E_ℓ using (4.11)/(4.13).

Next we try to improve these results, as before, by defining the difference

$$\Delta_\ell^{(e)}(m) = e_\ell(m) - E_\ell(m) \quad (4.34)$$

and attempting to guess an analytic form for some of the coefficients $\Delta_\ell^{(e)}(k)$: see Table 11, where we initially know only $\ell \leq 9$. As in the previous cases, we find empirically that the coefficients $\Delta_\ell^{(e)}(k)$ closest to the boundary $k_{\min}(\ell) = \ell + 1$ are the restriction to integers ℓ

of certain polynomials. We obtain:

$$\Delta_\ell^{(e)}(\ell) = (-1)^\ell \quad \text{for } \ell \geq 1 \quad (4.35a)$$

$$\Delta_\ell^{(e)}(\ell - 1) = (-1)^\ell (4\ell - 9) \quad \text{for } \ell \geq 3 \quad (4.35b)$$

$$\Delta_\ell^{(e)}(\ell - 2) = (-1)^\ell (-\ell^2 - 8\ell + 39) \quad \text{for } \ell \geq 5 \quad (4.35c)$$

$$\Delta_\ell^{(e)}(\ell - 3) = (-1)^\ell \left(\frac{14}{3}\ell^3 - 65\ell^2 + \frac{985}{3}\ell - 613 \right) \quad \text{for } \ell \geq 7 \quad (4.35d)$$

We are able to test each fit on at least one additional data point. By this method, we are able to extract the polynomials E_ℓ up to $\ell = 12$ (if we demand at least one extra data point to test the fit) or $\ell = 13$ (if we don't).

The same game can be played with the coefficients $f_\ell(m)$ [cf. (4.14)]. These coefficients are displayed in Table 12 for $1 \leq \ell \leq 12$, and the complete set is included in the file `data_Diff.m`. From this table we see that the coefficients $\ell f_\ell(m)$ are not integers, in contrast to the observed behavior for the coefficients $\ell e_\ell(m)$ (see Table 10). We observe *empirically* that, for each fixed ℓ , the coefficients $f_\ell(m)$ are the restriction to integers m of a polynomial $F_\ell(m)$ of degree 1 in m , *provided that we restrict attention to $m \geq m_{\min}(\ell) = \ell + 1$* . Again, we can obtain these polynomials up to $\ell = 8$ (if we want at least one extra data point to test the fit) or $\ell = 9$ (if we don't). The first polynomials are given by

$$F_1(m) = m - 5 \quad (4.36a)$$

$$F_2(m) = \frac{11}{2}m - \frac{17}{2} \quad (4.36b)$$

$$F_3(m) = \frac{49}{3}m - \frac{77}{3} \quad (4.36c)$$

$$F_4(m) = \frac{191}{4}m - \frac{305}{4} \quad (4.36d)$$

$$F_5(m) = \frac{686}{5}m - 203 \quad (4.36e)$$

and the ones for $6 \leq \ell \leq 9$ are shown in Table 4. (In Section 5.4 we *prove* that $f_1(m) = m - 5$ for $m \geq 2$.)

We now try to improve these results by defining the difference

$$\Delta_\ell^{(f)}(m) = f_\ell(m) - F_\ell(m) \quad (4.37)$$

and attempting to guess an analytic form for some of the coefficients $\Delta_\ell^{(f)}(m)$: see Table 13, where we initially know only $\ell \leq 9$. As in the previous cases, we find empirically that the coefficients $\Delta_\ell^{(f)}(m)$ closest to the boundary $m_{\min}(\ell) = \ell + 1$ are the restriction to integers ℓ of certain polynomials. We obtain:

$$\Delta_\ell^{(f)}(\ell) = (-1)^{\ell+1} \frac{3}{2} \quad \text{for } \ell \geq 1 \quad (4.38a)$$

$$\Delta_\ell^{(f)}(\ell - 1) = (-1)^{\ell+1} \left(\frac{9}{2}\ell - 11 \right) \quad \text{for } \ell \geq 3 \quad (4.38b)$$

$$\Delta_\ell^{(f)}(\ell - 2) = (-1)^\ell \left(\frac{3}{2}\ell^2 + \frac{53}{4}\ell - 54 \right) \quad \text{for } \ell \geq 5 \quad (4.38c)$$

$$\Delta_\ell^{(f)}(\ell - 3) = (-1)^\ell \left(\frac{19}{4}\ell^3 - \frac{277}{4}\ell^2 + \frac{747}{2}\ell - 736 \right) \quad \text{for } \ell \geq 7 \quad (4.38d)$$

We are able to test each fit on at least one additional data point. By this method, we are able to extract the polynomials F_ℓ up to $\ell = 12$ (if we demand at least one extra data point to test the fit) or $\ell = 13$ (if we don't).

If we look carefully at Table 4, we realize that the polynomials C_ℓ , E_ℓ and F_ℓ are not independent, but they satisfy (at least for $1 \leq \ell \leq 13$) the relation

$$C_\ell(m) = E_\ell(m) + F_\ell(m). \quad (4.39)$$

The same relation of course holds for the corresponding coefficients $c_\ell^\neq(m)$, $e_\ell(m)$ and $f_\ell(m)$ for $m \geq \ell + 1$:

$$c_\ell^\neq(m) = e_\ell(m) + f_\ell(m) \quad \text{for } m \geq \ell + 1. \quad (4.40)$$

We can understand this latter relation by using (4.3)/(4.13)/(4.14) and defining

$$G(m) = \sum_{\ell=1}^{\infty} \left[e_\ell(m) + f_\ell(m) - c_\ell^\neq(m) \right] q^{-\ell} = \log \left(\frac{\frac{\lambda_{*,=}(m)}{\lambda_{*,\neq}(m)} - 1}{\log \frac{\lambda_{*,=}(m)}{\lambda_{*,\neq}(m)}} \right). \quad (4.41)$$

Since $\lambda_{*,=}(m)/\lambda_{*,\neq}(m) = 1 + O(q^{-m})$ from (3.43)/(4.5a)/(4.7), it follows that $G(m) = O(q^{-m})$, i.e. $[q^{-\ell}]G(m) = 0$ for $\ell < m$, which is precisely (4.40).

4.5 Summary of conjectured behavior

Let us conclude this section by summarizing our empirical findings concerning the eigenvalues $\lambda_{*,=}(m)$ and $\lambda_{*,\neq}(m)$ and their difference. First recall that in Proposition 3.10 we *prove* that

$$\lambda_{*,=}(m) - \lambda_{*,\neq}(m) = (-1)^{m+1} + O(q^{-1}). \quad (4.42)$$

We have found *empirically* that stronger results hold. Our first finding concerns the behavior of the free energies for \neq and $=$ boundary conditions:

Conjecture 4.1 *There exist polynomials C_1, C_2, \dots with rational coefficients, of degree 1, such that*

$$\log \frac{\lambda_{*,\neq}(m)}{q^m} = \sum_{k=1}^m C_k(m) q^{-k} + O(q^{-(m+1)}) \quad (4.43a)$$

$$\log \frac{\lambda_{*,=}(m)}{q^m} = \sum_{k=1}^m C_k(m) q^{-k} + (-1)^{m+1} q^{-m} + O(q^{-(m+1)}) \quad (4.43b)$$

We have verified this conjecture for $m \leq 10$, using the polynomials C_1, \dots, C_{10} shown in Table 4. A special case of Conjecture 4.1 is Proposition 3.10 concerning the *difference* of eigenvalues.

Secondly, the empirical observation that the coefficients $d_\ell(m)$ defined in (4.11) are the restriction to integers $m \geq \ell + 1$ of a polynomial of degree ℓ in the variable m can be formalized as a conjecture as follows:

Conjecture 4.2 *There exist polynomials D_1, D_2, \dots with rational coefficients, with $\deg D_\ell = \ell$, such that*

$$\lambda_{*,=(m)} - \lambda_{*,\neq(m)} = (-1)^{m+1} \left[1 + \sum_{\ell=1}^{m-1} (-1)^\ell D_\ell(m) q^{-\ell} \right] + O(q^{-m}). \quad (4.44)$$

We have verified this conjecture for $m \leq 6$, using the polynomials D_1, \dots, D_5 given in (4.32). Moreover, the same polynomials D_1, \dots, D_5 give correctly the expansion through order q^{-5} for all $m \leq 11$.

Finally, the empirical observation that the coefficients $e_\ell(m)$ and $f_\ell(m)$ defined in (4.13)/(4.14) are the restriction to integers $m \geq \ell + 1$ of a polynomial of degree 1 in the variable m can be formalized as a conjecture as follows:

Conjecture 4.3 *There exist polynomials E_1, E_2, \dots and F_1, F_2, \dots with rational coefficients, of degree 1, such that*

$$\log [(-1)^{m+1} (\lambda_{*,=(m)} - \lambda_{*,\neq(m)})] = \sum_{\ell=1}^{m-1} E_\ell(m) q^{-\ell} + O(q^{-m}) \quad (4.45)$$

$$-\log \left[(-1)^{m+1} q^m \log \left(\frac{\lambda_{*,=(m)}}{\lambda_{*,\neq(m)}} \right) \right] = \sum_{\ell=1}^{m-1} F_\ell(m) q^{-\ell} + O(q^{-m}) \quad (4.46)$$

We have verified this conjecture for $m \leq 10$, using the polynomials E_1, \dots, E_9 and F_1, \dots, F_9 shown in Table 4.

5 Thermodynamic limit $m \rightarrow \infty$ of the free energies

In the previous section we studied the large- q expansion of the leading eigenvalues $\lambda_{*,=(m)}$ and $\lambda_{*,\neq(m)}$ — or what is essentially equivalent, the strip free energies f_m^- and f_m^\neq to be defined in (5.2)/(5.4) below — for strips of fixed width m with $=$ or \neq boundary conditions. In this section we will study the thermodynamic limit $m \rightarrow \infty$ of these free energies.

The plan of this section is as follows: In Section 5.1 we introduce some preliminary definitions and discuss the expected behavior of the strip free energies per unit length, $f_m^-(q)$ and $f_m^\neq(q)$, as a function of the strip width m . We then give, in Section 5.2, an overview of the computations we have performed and the results we have obtained. In Section 5.3 we present a hand computation of the first four terms in the large- q expansion of the bulk, surface and corner free energies for $=$ and \neq boundary conditions. In Section 5.4 we prove some exact results, valid to all orders in $1/q$, for the difference between the free energies with $=$ and \neq boundary conditions. Finally, in Section 5.5 we explain one of the empirical observations from Sections 4.2 and 4.3, and we extract additional information on the vertical-surface free energies from our transfer matrices.

5.1 Generalities and finite-size-scaling theory

Corollary 3.4 shows that, for each width m and each boundary condition ($=$ or \neq), the transfer matrix has, for sufficiently large $|q|$, a *single* dominant eigenvalue $\lambda_\star(q)$ that moreover is an analytic function of q (in fact, it is q^m times an analytic function of q^{-1}). Theorem 3.9 actually proves that $\lambda_{\star,\sharp}(q)$ is q^m times an analytic function of q^{-1} whenever $|q| > 33.855628$, uniformly in m .

Let us now introduce the free energy per site²¹ for a finite strip with $=$ or \neq boundary conditions,

$$f_{m,n}^\sharp(q) = \frac{1}{mn} \log P_{S_{m,n}^\sharp}(q) \quad (5.1)$$

where \sharp denotes $=$ or \neq , and its limiting value for a semi-infinite strip,

$$f_m^\sharp(q) = \lim_{n \rightarrow \infty} \frac{1}{mn} \log P_{S_{m,n}^\sharp}(q) . \quad (5.2)$$

Finally, let us introduce the free energy per site for the infinite lattice,

$$f^\sharp(q) = \lim_{m,n \rightarrow \infty} \frac{1}{mn} \log P_{S_{m,n}^\sharp}(q) . \quad (5.3)$$

Here we are assuming that the indicated limits exist and that in (5.3) the limit is independent of the way that m and n tend to infinity. Furthermore, it is natural to expect that in (5.3) the limiting free energy is independent of boundary conditions, in which case we can omit the superscripts $=$ or \neq and write simply $f(q)$.

In fact, some of these assumptions can be proven. Indeed, the above discussion guarantees that, at least for $|q| > 33.855628$, the limiting strip free energy $f_m(q)$ exists for all m and is given by

$$f_m^\sharp(q) = \frac{1}{m} \log \lambda_{\star,\sharp}(q) , \quad (5.4)$$

which is moreover an analytic function of q in the indicated domain. Moreover, Procacci *et al.* [49, Theorem 2] have proven that, when $|q|$ is large enough (namely, $|q| > 8e^3 \approx 160.684295$), the infinite-volume limiting free energy $f(q)$ exists and is analytic in $1/q$ and is the same for all sequences of graphs $G_{m \times n}$ with free boundary conditions; in particular, it is independent of the way that m and n tend to infinity.²² We *expect* that the same result holds for $=$ or \neq boundary conditions and gives rise to the *same* infinite-volume limiting free energy $f(q)$ as for free boundary conditions (indeed, we expect that this can

²¹Actually *minus* the free energy per site in the usual thermodynamic convention — but we prefer not to encumber our formulae with unnecessary minus signs, or to encumber our text with constant repetition of the word “minus”.

²²In fact, Procacci *et al.* prove that this limit is the same for all Følner–van Hove sequences of finite subvolumes of the infinite lattice, not just rectangles; and they prove this result for a wide variety of lattices (namely, locally-finite connected quasi-transitive amenable infinite graphs), not just the square lattice. On the other hand, we mistakenly asserted in [54, Section 5.1] that Procacci *et al.* had proven this result also for cylindrical, cyclic and toroidal boundary conditions. We suspect that such a result can indeed be obtained by a suitable modification of their proof, but we were wrong to assert that it is contained in their paper.

be proven by a modification of the Procacci *et al.* argument). In this paper we will take $n \rightarrow \infty$ first and then take $m \rightarrow \infty$, so that

$$f(q) = \lim_{m \rightarrow \infty} f_m^\sharp(q). \quad (5.5)$$

Finite-size-scaling theory [48, Section 2.5] gives a rather precise prediction for the form of the free energy (5.1)/(5.2) for a finite or semi-infinite system away from a critical point (and in the absence of soft modes). In particular, for an $m \times n$ strip with $=$ or \neq boundary conditions and bulk correlation length $\xi_{\text{bulk}} \ll m, n$, the predicted behavior is

$$f_{m,n}^\sharp = f_{\text{bulk}} + \frac{n f_{\text{surf,vert}}^\sharp + m f_{\text{surf,horiz}}^\sharp}{mn} + \frac{1}{mn} f_{\text{corner}}^\sharp + O(e^{-\min(m,n)/\xi_{\text{bulk}}}), \quad (5.6)$$

where \sharp denotes $=$ or \neq , and $f_{\text{bulk}} = f$, $f_{\text{surf,vert}}^\sharp$, $f_{\text{surf,horiz}}^\sharp$ and f_{corner}^\sharp are, respectively, the free energies for the bulk, the two vertical surfaces (at left and right), the two horizontal surfaces (at top and bottom), and the four corners plus the extra sites. For a semi-infinite strip $m \times \infty$ with $=$ or \neq boundary conditions, we have

$$f_m^\sharp = f_{\text{bulk}} + \frac{1}{m} f_{\text{surf,vert}}^\sharp + O(e^{-m/\xi_{\text{bulk}}}). \quad (5.7)$$

Since the families $S_{m,n}^\sharp$ are not invariant under 90° rotation, we expect the vertical and horizontal free energies to be different. Finally, we cannot take for granted that the surface and corner free energies are the same for $=$ and \neq boundary conditions.

In this section we *assume* that the behaviors (5.6)/(5.7) hold and that expansion in $1/m$ and $1/n$ can be commuted freely with expansion in $1/q$. (We expect that this may be provable by an extension of the Procacci *et al.* argument.) This assumption justifies the manipulations to be made in the following subsections.

The relation (5.7) of course holds for the chromatic polynomials at *fixed* large q . But we can also argue heuristically what it should imply for the series expansion in powers of $1/q$. It is not difficult to see that, for large q , we have

$$e^{-1/\xi_{\text{bulk}}(q)} = \frac{1}{q} + O\left(\frac{1}{q^2}\right) \quad (5.8)$$

(just as for a *one-dimensional* Potts antiferromagnet at zero temperature). As explained in detail in [54], we can therefore interpret $O(e^{-m/\xi_{\text{bulk}}(q)})$ as meaning $O(q^{-m})$. Therefore, we expect that

$$f_m^\sharp(q) = f_{\text{bulk}}(q) + \frac{1}{m} f_{\text{surf,vert}}^\sharp(q) + O(q^{-m}), \quad (5.9)$$

or in other words we predict $m_{\min}^\sharp(k) = k + 1$. Of course, we should not take too seriously the “+1” here, since the *amplitude* of the correction term in (5.7) could be proportional to a positive or negative power of q . But we do predict that $m_{\min}^\sharp(k) \approx k$ in the sense that $\lim_{k \rightarrow \infty} m_{\min}^\sharp(k)/k = 1$. This is indeed what we found for $=$ and \neq boundary conditions.

5.2 Overview of computations and results

Before beginning the detailed computations, it is useful to give an overview of the methods to be used and the results obtained, taking into account both the computations reported below for $=$ and \neq boundary conditions and those reported in a previous paper [54, Sections 5.2–5.4] for free (F) and cylindrical (P) boundary conditions.

The computations we are able to carry out are as follows:

- For the *bulk* free energy (which is of course the same for all four boundary conditions), we obtained in [54] long series (through order q^{-47}) using the finite-lattice method for free boundary conditions. We are also able to check these series up to moderate order (namely, order q^{-33} , q^{-16} , q^{-15} , q^{-15} respectively for F, P, $=$ and \neq boundary conditions) by transfer-matrix calculations of the leading eigenvalue.
- For the *vertical surface* free energy with $=$ or \neq boundary conditions, we have a hand calculation through order q^{-4} , which we can extend to order q^{-16} or q^{-17} by transfer-matrix calculations of the leading eigenvalue.
- For the *horizontal surface* free energy with $=$ or \neq boundary conditions, we have only a hand calculation through order q^{-4} . [The horizontal surface free energy does not appear in the strip eigenvalue (5.4)/(5.7).]
- For the *corner* free energy with $=$ or \neq boundary conditions, we have likewise only a hand calculation through order q^{-4} .

Our conclusions (from the available orders) are as follows:

- The *bulk* free energy agrees for all four boundary conditions (no surprise).
- The *horizontal surface* free energy agrees for $=$ and \neq boundary conditions. This is again no surprise, as the horizontal surfaces are the same for the two boundary conditions.
- The *vertical surface* free energy agrees for $=$ and \neq boundary conditions. *A priori* this might be somewhat of a surprise, as it is far from obvious whether the effect of the edge connecting the two extra sites (which is $v = \infty$ or -1 according as the boundary conditions are $=$ or \neq) is of order 1 (it is, after all, only a single edge) or is of order n (its endpoints are directly connected to the whole vertical sides). It turns out that the former is the case. But on closer examination this is no surprise at all: the equality $f_{\text{surf,vert}}^= = f_{\text{surf,vert}}^{\neq}$ follows immediately from (5.4)/(5.9) together with Proposition 3.10, since $\log[\lambda_{*,=}(m)/\lambda_{*,\neq}(m)] = (-1)^{m+1}q^{-m} + O(q^{-m-1})$ vanishes to all orders in q^{-1} as $m \rightarrow \infty$.
- The horizontal and vertical surface free energies are different from each other, and different from the surface free energy for free (F) boundary conditions.
- The *corner* free energies are different for $=$, \neq and free boundary conditions. However, the *difference* between the corner free energies for $=$ and \neq boundary conditions is simple: $f_{\text{corner}}^=(q) - f_{\text{corner}}^{\neq}(q) = -\log(1 - q^{-1})$.

Let us conclude this subsection by recalling the large- q series for the bulk free energy that was obtained in [54] through order q^{-47} (extending previous series by Bakaev and Kabanovich [1]) by using the finite-lattice method [22–25, 43, 46] for free boundary conditions.²³ As $|q| \rightarrow \infty$, the exponential of the free energy per site for an infinite square lattice is given by the series expansion

$$e^{f(q)} = \frac{(q-1)^2}{q} \left[1 + z^3 + z^7 + 3z^8 + 4z^9 + 3z^{10} + 3z^{11} + 11z^{12} + 24z^{13} + 8z^{14} - 91z^{15} - 261z^{16} - 290z^{17} + \dots - 598931311074z^{47} + O(z^{48}) \right], \quad (5.10)$$

where z is defined as

$$z = \frac{1}{q-1}. \quad (5.11)$$

We have here copied the first few terms and the last one; the remaining terms are reported in [54, Table 9]. In terms of the variable $1/q$, we obtain

$$e^{f(q)} = q \left[1 - 2q^{-1} + q^{-2} + q^{-3} + q^{-4} + q^{-5} + q^{-6} + 2q^{-7} + 9q^{-8} + 38q^{-9} + 130q^{-10} + 378q^{-11} + 987q^{-12} + \dots + 1311159363081366872q^{-47} + O(q^{-48}) \right]. \quad (5.12)$$

Finally, for the bulk free energy $f(q)$ itself (rather than its exponential) in terms of the variable $1/q$, we obtain

$$f(q) = \log q - \frac{2}{q} - \frac{1}{q^2} + \frac{1}{3q^3} + \frac{5}{2q^4} + \frac{28}{5q^5} + \frac{55}{6q^6} + \frac{89}{7q^7} + \frac{81}{4q^8} + \frac{505}{9q^9} + \frac{1029}{5q^{10}} + \frac{7742}{11q^{11}} + \frac{25291}{12q^{12}} + \frac{73552}{13q^{13}} + \frac{197755}{14q^{14}} + \dots + \frac{190018276619486037135}{47q^{47}} + O(q^{-48}). \quad (5.13)$$

Clearly, $e^{f(q)}$ has a much simpler expansion than $f(q)$; in particular, its coefficients are integers (at least through the order calculated thus far).²⁴ A further simplification is obtained by using the variable $z = 1/(q-1)$ in place of $1/q$: the integer coefficients become much smaller. Finally, a slight extra simplification arises from extracting the prefactor $(q-1)^2/q$ in (5.10).

Unfortunately, the finite-lattice method — which is an extraordinarily efficient method for calculating series expansions — does not appear to be applicable to $=$ and \neq boundary conditions. We therefore resorted to a hand calculation, to be reported in the next subsection, which we carried through order q^{-4} .

5.3 Hand calculation of large- q expansion for the bulk, surface and corner free energies

First of all, as we are interested in the large- q limit, it is convenient to explicitly remove the leading term $\log q$ in the free energy by considering the modified chromatic

²³After the completion of this work, we learned that Jacobsen [32] had extended the series expansions for the bulk, surface and corner free energies to orders $O(q^{-79})$, $O(q^{-79})$ and $O(q^{-78})$, respectively.

²⁴The coefficients of $f(q)$ are not integers, but $k[q^{-k}]f(q)$ is an integer (at least through the order calculated thus far). Indeed, it is not hard to show that if $F(z)$ is a power series with integer coefficients and constant term 1, then $k[z^k] \log F(z)$ is always an integer.

polynomial \tilde{P}_G for a loopless graph $G = (V, E)$:

$$\tilde{P}_G(q) = q^{-|V|} P_G(q) . \quad (5.14)$$

Using the Fortuin–Kasteleyn representation (2.4) we get

$$\tilde{P}_G(q) = \sum_{A \subseteq E} (-1)^{|A|} q^{k(A) - |V|} \quad (5.15a)$$

$$= \sum_{A \subseteq E} (-1)^{|A|} (1/q)^{|A| - c(A)} , \quad (5.15b)$$

where $c(A) = |A| - |V| + k(A)$ is the cyclomatic number of the subgraph (V, A) .

It is instructive to begin by computing “by hand” the first few terms of the large- q expansion for the bulk, surface and corner free energies. To do this, let us first consider an $m \times n$ square lattice with \neq boundary conditions: it has $|V| = mn + 2$ sites, $|E| = 2mn - m + n + 1$ edges, $|F_{\text{sq}}| = (m-1)(n-1)$ square faces, and $|F_{\text{tri}}| = 2(n-1)$ triangular faces. There are also two extra faces, each bounded by a cycle of length $m+2$, cf. the inner and outer faces in Figure 7b; but these faces will play no role in the calculation if m is large enough (see below). We can compute the first few first terms in the large- q expansion for the modified chromatic polynomial $\tilde{P}_{S_{m,n}}(q)$ by using (5.15b) and explicitly identifying the subsets A having a given small value of $|A| - c(A)$:

$|A| - c(A) = 0$: Only $A = \emptyset$.

$|A| - c(A) = 1$: $A =$ any single edge.

$|A| - c(A) = 2$: $A =$ two distinct edges *or* three edges forming a triangular face.

$|A| - c(A) = 3$: $A =$ three distinct edges not forming a triangular face, *or* four edges forming a cycle of length four (i.e. a square face or the boundary cycle of two adjacent triangular faces), *or* five edges consisting of all the edges of two adjacent triangular faces.

We have also identified the contributions of the subsets with $|A| - c(A) = 4$ and will include them in our calculation, but we refrain from writing them down as their description is rather lengthy. For small m we also have to worry about terms A that wind horizontally around the lattice using the two extra sites; the smallest of these are cycles of length $m+2$. But since all such terms have $|A| - c(A) \geq m+1$, we can avoid them simply by assuming that m is large enough, i.e. $m \geq k$ if we want an expansion valid through order q^{-k} . In particular, we can obtain the expansion through order q^{-4} by assuming that

$m \geq 4$ and ignoring “winding” subsets A . We therefore have

$$\begin{aligned}
\tilde{P}_{S_{m,n}^\neq}(q) = & 1 - \frac{|E|}{q} + \left[\frac{|E|(|E| - 1)}{2} - F_{\text{tri}} \right] \frac{1}{q^2} \\
& - \left[\frac{|E|(|E| - 1)(|E| - 2)}{6} - |F_{\text{sq}}| - |F_{\text{tri}}|(|E| - 2) \right] \frac{1}{q^3} \\
& + \left[\frac{|E|(|E| - 1)(|E| - 2)(|E| - 3)}{24} - (|F_{\text{tri}}| + |F_{\text{sq}}|)(|E| - 3) \right. \\
& \quad \left. - |F_{\text{tri}}| \frac{(|E| - 3)(|E| - 4)}{2} + \frac{|F_{\text{tri}}|(|F_{\text{tri}}| - 1)}{2} \right] \frac{1}{q^4} \\
& + O(q^{-5})
\end{aligned} \tag{5.16}$$

and hence

$$\begin{aligned}
\log \tilde{P}_{S_{m,n}^\neq}(q) = & -\frac{|E|}{q} - \frac{1}{2q^2}(|E| - 2|F_{\text{tri}}|) - \frac{1}{3q^3}(|E| - 3|F_{\text{sq}}| + 6|F_{\text{tri}}|) \\
& - \frac{1}{4q^4}(|E| - 12|F_{\text{sq}}| + 14|F_{\text{tri}}|) + O(q^{-5}).
\end{aligned} \tag{5.17}$$

Note that in the expression for $\log \tilde{P}_{S_{m,n}^\neq}(q)$, all geometrical quantities occur *linearly* (as they should). Inserting the values of $|E|$, $|F_{\text{sq}}|$ and $|F_{\text{tri}}|$, dividing by mn , expanding in $1/n$ and $1/m$, and putting back the leading term $\log q$, one finds the large- q expansion for the free energy

$$\begin{aligned}
f_{m,n}^\neq(q) = & \log q - \frac{2}{q} - \frac{1}{q^2} + \frac{1}{3q^3} + \frac{5}{2q^4} + \left[-\frac{1}{q} - \frac{5}{2q^2} - \frac{16}{3q^3} - \frac{41}{4q^4} \right] \frac{1}{m} \\
& + \left[\frac{1}{q} + \frac{1}{2q^2} - \frac{2}{3q^3} - \frac{11}{4q^4} \right] \frac{1}{n} + \left[-\frac{1}{q} + \frac{3}{2q^2} + \frac{14}{3q^3} + \frac{39}{4q^4} \right] \frac{1}{mn} \\
& + O(q^{-5}).
\end{aligned} \tag{5.18}$$

Comparing to the finite-size-scaling Ansatz (5.6), we obtain

$$f_{\text{bulk}}(q) = \log q - \frac{2}{q} - \frac{1}{q^2} + \frac{1}{3q^3} + \frac{5}{2q^4} + O(q^{-5}) \tag{5.19a}$$

$$f_{\text{surf,vert}}^\neq(q) = -\frac{1}{q} - \frac{5}{2q^2} - \frac{16}{3q^3} - \frac{41}{4q^4} + O(q^{-5}) \tag{5.19b}$$

$$f_{\text{surf,horiz}}^\neq(q) = \frac{1}{q} + \frac{1}{2q^2} - \frac{2}{3q^3} - \frac{11}{4q^4} + O(q^{-5}) \tag{5.19c}$$

$$f_{\text{corner}}^\neq(q) = -\frac{1}{q} + \frac{3}{2q^2} + \frac{14}{3q^3} + \frac{39}{4q^4} + O(q^{-5}) \tag{5.19d}$$

We can do the same computation for the family $S_{m,n}^\equiv$: it has $|V| = mn + 1$ sites, $|E| = 2mn - m + n$ edges, $|F_{\text{sq}}| = (m - 1)(n - 1)$ square faces, and $|F_{\text{tri}}| = 2(n - 1)$ triangular faces. There are also two extra faces, each bounded by a cycle of length $m+1$, cf. the inner and outer faces in Figure 6b; but these faces will play no role in the computation

if m is large enough. The subsets A contributing through order $O(q^{-4})$ are exactly the same as for the family $S_{m,n}^\neq$. The only difference is that the “winding” terms now start with cycles of length $m+1$ rather than $m+2$, and they have $|A| - c(A) \geq m$ instead of $m+1$. Therefore, we must take $m \geq k+1$ if we want an expansion valid through order q^{-k} . In particular, we can obtain the expansion through order q^{-4} by assuming that $m \geq 5$. The large- q expansion for $\log \tilde{P}_{S_{m,n}^\neq}(q)$ is given by the *same* formula (5.17) but with the new value of $|E|$ inserted (note that $|F_{\text{sq}}|$ and $|F_{\text{tri}}|$ remain the same). Dividing by mn , expanding in $1/n$ and $1/m$, and putting back the leading term $\log q$, one finds the large- q expansion for the free energy

$$\begin{aligned} f_{m,n}^\neq(q) = & \log q - \frac{2}{q} - \frac{1}{q^2} + \frac{1}{3q^3} + \frac{5}{2q^4} + \left[-\frac{1}{q} - \frac{5}{2q^2} - \frac{16}{3q^3} - \frac{41}{4q^4} \right] \frac{1}{m} \\ & + \left[\frac{1}{q} + \frac{1}{2q^2} - \frac{2}{3q^3} - \frac{11}{4q^4} \right] \frac{1}{n} + \left[\frac{2}{q^2} + \frac{5}{q^3} + \frac{10}{q^4} \right] \frac{1}{mn} \\ & + O(q^{-5}). \end{aligned} \quad (5.20)$$

Comparing to the finite-size-scaling Ansatz (5.6), we obtain

$$f_{\text{bulk}}(q) = \log q - \frac{2}{q} - \frac{1}{q^2} + \frac{1}{3q^3} + \frac{5}{2q^4} + O(q^{-5}) \quad (5.21a)$$

$$f_{\text{surf,vert}}^\neq(q) = -\frac{1}{q} - \frac{5}{2q^2} - \frac{16}{3q^3} - \frac{41}{4q^4} + O(q^{-5}) \quad (5.21b)$$

$$f_{\text{surf,horiz}}^\neq(q) = \frac{1}{q} + \frac{1}{2q^2} - \frac{2}{3q^3} - \frac{11}{4q^4} + O(q^{-5}) \quad (5.21c)$$

$$f_{\text{corner}}^\neq(q) = \frac{2}{q^2} + \frac{5}{q^3} + \frac{10}{q^4} + O(q^{-5}) \quad (5.21d)$$

If we compare the series (5.19) with (5.21), we conclude that:

1) The bulk contributions are the same for \neq and $=$ boundary conditions, and they agree also with the result for free and cylindrical boundary conditions [54, Eq. (5.14a)].

2) The surface contributions are the same for both boundary conditions, and they depend on the orientation of the “surface” (i.e. vertical or horizontal). Moreover, $f_{\text{surf,horiz}}^\neq = f_{\text{surf,horiz}}^\neq$ agrees with the surface free energy for free boundary conditions [54, Eq. (5.14b)]. This is not unexpected, as the top and bottom rows are identical for all these boundary conditions.

3) The corner free energies do depend on the boundary conditions (i.e. $f_{\text{corner}}^\neq \neq f_{\text{corner}}^\neq$) and they also differ from the corner free energy for free boundary conditions [54, Eq. (5.14c)]. We observe the curious fact

$$f_{\text{corner}}^\neq(q) - f_{\text{corner}}^\neq(q) = \frac{1}{q} + \frac{1}{2q^2} + \frac{1}{3q^3} + \frac{1}{4q^4} + O(q^{-5}). \quad (5.22)$$

In the next subsection we will establish this equality to all orders in $1/q$.

5.4 Exact results for the bulk, surface and corner free energies

We can obtain some exact results concerning the *difference* between the free energies $f_{m,n}^\neq(q)$ and $f_{m,n}^\neq(q)$ — and hence between the bulk, surface and corner free energies for

$=$ and \neq boundary conditions — by using the results of Section 3.5. Let us write the modified chromatic polynomials $\tilde{P}_{S_{m,n}^\#}(q)$ [cf. (5.14)] in terms of the partial chromatic polynomials of the two-terminal graphs $(S_{m,n}, s, t)$ introduced in Section 3.5; we obtain

$$\tilde{P}_{S_{m,n}^\#}(q) = q^{-mn-1} \left[P_{S_{m,n}}^{(s \leftrightarrow t)}(q) + q^{-1} P_{S_{m,n}}^{(s \not\leftrightarrow t)}(q) \right] \quad (5.23a)$$

$$\tilde{P}_{S_{m,n}^\neq}(q) = q^{-mn-2} (1 - q^{-1}) P_{S_{m,n}}^{(s \not\leftrightarrow t)}(q) \quad (5.23b)$$

Therefore, the difference between the finite-size free energies for the two boundary conditions can be written as

$$f_{m,n}^\#(q) - f_{m,n}^\neq(q) = \frac{1}{mn} \left[\log \tilde{P}_{S_{m,n}^\#}(q) - \log \tilde{P}_{S_{m,n}^\neq}(q) \right] \quad (5.24a)$$

$$= -\frac{1}{mn} \log \left(1 - \frac{1}{q} \right) + \frac{1}{mn} \log \left[1 + q \frac{\tilde{P}_{S_{m,n}}^{(s \leftrightarrow t)}(q)}{\tilde{P}_{S_{m,n}}^{(s \not\leftrightarrow t)}(q)} \right] \quad (5.24b)$$

where $\tilde{P}_{S_{m,n}}^{(s \leftrightarrow t)}$ and $\tilde{P}_{S_{m,n}}^{(s \not\leftrightarrow t)}$ are the corresponding modified chromatic polynomials. From (3.49) and (3.52) we see immediately that

$$\tilde{P}_{S_{m,n}}^{(s \not\leftrightarrow t)}(q) = 1 + O(q^{-1}) \quad (5.25a)$$

$$\tilde{P}_{S_{m,n}}^{(s \leftrightarrow t)}(q) = n(-1)^{m+1} q^{-(m+1)} [1 + O(q^{-1})] \quad (5.25b)$$

and hence

$$f_{m,n}^\#(q) - f_{m,n}^\neq(q) = -\frac{1}{mn} \log \left(1 - \frac{1}{q} \right) + \frac{(-1)^{m+1}}{m} q^{-m} + O(q^{-(m+1)}). \quad (5.26)$$

The term proportional to q^{-m} disappears to all orders in $1/q$ as $m \rightarrow \infty$, hence we have

$$f_{\text{surf,horiz}}^\#(q) = f_{\text{surf,horiz}}^\neq(q) \quad (5.27a)$$

$$f_{\text{surf,vert}}^\#(q) = f_{\text{surf,vert}}^\neq(q) \quad (5.27b)$$

$$f_{\text{corner}}^\#(q) = f_{\text{corner}}^\neq(q) - \log \left(1 - \frac{1}{q} \right) \quad (5.27c)$$

to all orders in $1/q$.²⁵ In particular, this proves (5.22) to all orders in $1/q$.

We can actually push the expansions (5.25a,b) to higher order in $1/q$ by methods similar to those used in the preceding subsection. Indeed, $\tilde{P}_{S_{m,n}}^{(s \not\leftrightarrow t)}$ is exactly equal to $\tilde{P}_{S_{m,n}}^\neq$ whenever m is large enough (compared to the order in $1/q$ being considered) so that winding subsets A (i.e. sets connecting the two terminals s, t) are absent. In particular, $\tilde{P}_{S_{m,n}}^{(s \not\leftrightarrow t)}$ is given through order q^{-k} ($k \leq 4$) by (5.16) whenever $m \geq k$. On the other hand, a straightforward hand computation yields

$$\tilde{P}_{S_{m,n}}^{(s \leftrightarrow t)}(q) = \frac{(-1)^{m+1}}{q^{m+1}} \left[n - \frac{n|E| + mn - 5n - m + 4}{q} + O(q^{-2}) \right] \quad (5.28)$$

²⁵We can interpret the correction term $O(q^{-m})$ as $O(e^{-m/\xi_{\text{bulk}}})$ [cf. (5.8)].

whenever $m \geq 2$. It follows that

$$\log \lambda_{*,=}(m) - \log \lambda_{*,\neq}(m) = \lim_{n \rightarrow \infty} \frac{1}{n} \log \left(1 + q \frac{\tilde{P}_{S_{m,n}}^{(s \leftrightarrow t)}(q)}{\tilde{P}_{S_{m,n}}^{(s \nleftrightarrow t)}(q)} \right) \quad (5.29a)$$

$$= \frac{(-1)^{m+1}}{q^m} \left[1 - \frac{m-5}{q} + O(q^{-2}) \right]. \quad (5.29b)$$

In terms of the quantities $f_\ell(m)$ defined in (4.14), this says that $f_1(m) = m - 5$ for $m \geq 2$, which agrees with Table 12.

5.5 Families $S_{m,n}^\neq$ and $S_{m,n}^-$ via strip free energies

Using finite-size-scaling theory, we can understand (non-rigorously) a fact observed empirically in Sections 4.2 and 4.3: namely, that the coefficients $c_k^\sharp(m)$ arising in the large- $|q|$ expansion of the free energy (4.3) are represented for $m \geq m_{\min}^\sharp(k)$ by a polynomial of degree 1 in the strip width m , i.e.

$$c_k^-(m) = c_k^\neq(m) = C_k(m) = \alpha_k m + \beta_k \quad \text{for } m \geq m_{\min}(k). \quad (5.30)$$

To see this, it suffices to compare the large- $|q|$ expansion of the limiting free energy for a semi-infinite strip,

$$\begin{aligned} f_m^\sharp(q) &= \frac{1}{m} \log \lambda_{*,\sharp}(q) \\ &= \log q + \frac{1}{m} \log \left[\sum_{k=0}^{\infty} (-1)^k b_k^\sharp(m) q^{-k} \right] \\ &= \log q + \frac{1}{m} \sum_{k=1}^{\infty} (-1)^k c_k^\sharp(m) q^{-k}, \end{aligned} \quad (5.31)$$

with the finite-size-scaling Ansatz (5.7)/(5.9). The behavior (5.30) is an immediate consequence, where α_k (resp. β_k) is the coefficient of q^{-k} in the bulk (resp. vertical surface) free energy. As discussed after (5.9), we expect $m_{\min}^\sharp(k) \approx k$.

We can also use our transfer matrices to check in part the result (5.13) for the bulk free energy and to notably extend the results (5.19b)/(5.21b) for the vertical surface free energy. Indeed, the coefficients in both these expansions can be immediately read off from the coefficients α_k and β_k in Table 4. We thus obtain an independent check of the first 15 terms of the series (5.13). We also obtain the first 15 terms in the large- q expansion of the vertical surface free energy $f_{\text{surf,vert}}^\neq = f_{\text{surf,vert}}^-$:

$$\begin{aligned} f_{\text{surf,vert}}^\sharp(q) &= -\frac{1}{q} - \frac{5}{2q^2} - \frac{16}{3q^3} - \frac{41}{4q^4} - \frac{81}{5q^5} - \frac{49}{3q^6} + \frac{55}{7q^7} + \frac{719}{8q^8} + \frac{2459}{9q^9} \\ &\quad + \frac{1239}{2q^{10}} + \frac{15168}{11q^{11}} + \frac{23051}{6q^{12}} + \frac{171677}{13q^{13}} + \frac{647719}{14q^{14}} + \frac{744743}{5q^{15}} \\ &\quad + \frac{6898415}{16q^{16}} + O(q^{-17}) \end{aligned} \quad (5.32)$$

We can slightly extend this latter series by using the series (5.13) for f_{bulk} as an *input*: in this case, each polynomial C_k contains a single unknown coefficient to be determined (rather than two unknown coefficients). We then obtain the coefficient of the term q^{-17} in $f_{\text{surf,vert}}^\sharp$,

$$[q^{-17}] f_{\text{surf,vert}}^\sharp = \frac{19118828}{17}, \quad (5.33)$$

and thus the polynomial C_{17} shown in Table 4.

Finally, the simplest expression for the surface free energy is given by its exponential in terms of the variable $z = 1/(q - 1)$:

$$\begin{aligned} e^{f_{\text{surf,vert}}^\sharp(q)} = & 1 - z - z^2 + z^4 + 3z^5 + 2z^6 - 5z^7 - 11z^8 + 3z^9 + 43z^{10} + 57z^{11} - 34z^{12} \\ & - 178z^{13} - 122z^{14} + 220z^{15} + 200z^{16} - 1170z^{17} + O(z^{18}). \end{aligned} \quad (5.34)$$

6 Numerical results II: Limiting curves \mathcal{B}_m

For each $1 \leq m \leq 10$, we have computed the *symbolic* transfer matrix $T''(m)$, as well as the vectors \mathbf{f}_{id} and $\boldsymbol{\omega}^T$. In this computation we exploited the fact that $T''(m)$ is block-diagonal [cf. (3.31)/(3.33)], which allows us to obtain *separately* the two diagonal blocks $T''_{\text{=}}(m)$ and $T''_{\text{\neq}}(m)$ and, for each block, the corresponding left and right vectors $\boldsymbol{\omega}^T$ and \mathbf{f}_{id} .

The symbolic computations were done by means of a MATHEMATICA program for $1 \leq m \leq 5$ and by a perl script for $1 \leq m \leq 10$. The perl script runs faster and uses a smaller amount of memory than the MATHEMATICA program for the same width m . We have checked that both programs give the same answer for $1 \leq m \leq 5$. We also performed several checks on our symbolic results using the identity

$$P_{S_{m,n}}(q) = P_{\widehat{S}_{n,m}}(q), \quad (6.1)$$

where $\widehat{S}_{m,n}$ is the graph that is just like $S_{m,n}$ except that the two extra sites lie at top and bottom rather than left and right (see Figure 8). Of course $S_{m,n}$ and $\widehat{S}_{n,m}$ are isomorphic, so that the identity (6.1) holds trivially, but the transfer-matrix approaches to calculating their chromatic polynomials are rather different, because of a reversal in which direction is considered “longitudinal” and which “transverse” (see Appendix C). The identity (6.1) thus constitutes a nontrivial check on the correctness of our computations. We checked it for $1 \leq m \leq 8$ and $1 \leq n \leq 6$.

For each $1 \leq m \leq 6$, we computed the zeros of the chromatic polynomials $P_{S_{m,\rho m}}(q)$ for strips of aspect ratio $\rho = 10, 20$, and we also computed the accumulation set \mathcal{B}_m of chromatic roots in the limit $\rho \rightarrow \infty$. For $m \leq 4$, we used the resultant method [53, Section 4.1.1] to compute the limiting curve \mathcal{B}_m , together with the direct-search method [53, Section 4.1.2] to refine some details. For $m = 5$, we used the resultant method to compute the endpoints of the limiting curve, while the rest of the curve was obtained via the direct-search method. For $m = 6$, the full limiting curve was obtained using the direct-search method. We took advantage of a few slight improvements to these methods as described in detail in Ref. [38, Section 2]. In principle we could have determined the limiting curve \mathcal{B}_m also for $7 \leq m \leq 10$; but it is extremely laborious (in both human and CPU time)

to determine accurately the small details in \mathcal{B}_m using the direct-search method, so we decided to stop at $m = 6$.

Since \mathbf{H} is a projection, the basis elements in our transfer-matrix calculation are given by $\mathbf{f}_{\mathcal{P}} = \mathbf{H}\mathbf{e}_{\mathcal{P}}$, and *not* by $\mathbf{e}_{\mathcal{P}}$, as explained in Section 2.2. However, to lighten the notation, we will represent the basis for a given strip as a collection of vectors $\mathbf{e}_{\mathcal{P}}$; but it should be understood that the basis vectors are actually $\mathbf{f}_{\mathcal{P}}$. We shall use the delta-function shorthand (2.13) to write the vectors $\mathbf{e}_{\mathcal{P}}$.

6.1 $m = 1$

The transfer matrix $\mathbf{T}_{=}(1)$ is one-dimensional, and a basis is given by $\mathbf{B}_{=} = \{\mathbf{1}\}$. This matrix and the corresponding left and right vectors are, in this basis,

$$\mathbf{T}_{=}(1) = q - 2 \quad (6.2a)$$

$$\boldsymbol{\omega}^{\text{T}} = q(q - 1) \quad (6.2b)$$

$$\mathbf{f}_{\text{id}}^{\text{T}} = 1 \quad (6.2c)$$

The transfer matrix $\mathbf{T}_{\neq}(1)$ is also one-dimensional, and a basis is given by $\mathbf{B}_{\neq} = \{\mathbf{1}\}$. In this basis, the transfer matrix and the corresponding vectors are given by

$$\mathbf{T}_{\neq}(1) = q - 3 \quad (6.3a)$$

$$\boldsymbol{\omega}^{\text{T}} = q(q - 1)(q - 2) \quad (6.3b)$$

$$\mathbf{f}_{\text{id}}^{\text{T}} = 1 \quad (6.3c)$$

The two eigenvalues are evidently $\lambda_{=} = q - 2$ and $\lambda_{\neq} = q - 3$, which become equimodular along the line

$$\text{Re } q = \frac{5}{2}. \quad (6.4)$$

Thus, this is the limiting curve for this strip. The amplitudes can be easily read off from (6.2)/(6.3): i.e., $\alpha_{=} = q(q - 1)$ and $\alpha_{\neq} = q(q - 1)(q - 2)$, in agreement with the exact result (2.28).

The dominant eigenvalue in the half-plane $\text{Re } q < 5/2$ is $\lambda_{\neq} = q - 3$, while the dominant eigenvalue in the half-plane $\text{Re } q > 5/2$ is $\lambda_{=} = q - 2$. The amplitude of the dominant eigenvalue vanishes at $q = 0, 1, 2$ (and only there); hence, these three points are the only isolated limiting points for this strip. The limiting curve \mathcal{B}_1 and the chromatic roots for $n = 10, 20$ are depicted in Figure 9.

6.2 $m = 2$

The transfer matrix $\mathbf{T}_{\neq}(2)$ is one-dimensional. In the basis $\mathbf{B}_{=} = \{\mathbf{1}\}$, this matrix and the corresponding vectors take the form

$$\mathbf{T}_{=}(2) = q^2 - 5q + 7 \quad (6.5a)$$

$$\boldsymbol{\omega}^{\text{T}} = q(q - 1)(q - 2) \quad (6.5b)$$

$$\mathbf{f}_{\text{id}}^{\text{T}} = 1 \quad (6.5c)$$

The transfer matrix $\mathbf{T}''_{\neq}(2)$ is two-dimensional. Let us choose the basis as $\mathbf{B}_{\neq} = \{\delta_{0,2} + \delta_{1,3}, \mathbf{1}\}$. The transfer matrix and the left and right vectors for this strip are then

$$\mathbf{T}''_{\neq}(2) = \begin{pmatrix} 2-q & -1 \\ 2(q-2) & q^2-5q+8 \end{pmatrix} \quad (6.6a)$$

$$\boldsymbol{\omega}^T = q(q-1) (2(q-1), q^2-3q+3) \quad (6.6b)$$

$$\mathbf{f}_{\text{id}}^T = (0, 1) \quad (6.6c)$$

The eigenvalues are given by

$$\lambda_{=} = q^2 - 5q + 7 \quad (6.7a)$$

$$\lambda_{\neq,1} = \frac{1}{2} \left(10 - 6q + q^2 - \sqrt{Q_2} \right) \quad (6.7b)$$

$$\lambda_{\neq,2} = \frac{1}{2} \left(10 - 6q + q^2 + \sqrt{Q_2} \right) \quad (6.7c)$$

where we have used the shorthand notation

$$Q_2(q) = q^4 - 8q^3 + 28q^2 - 56q + 52. \quad (6.8)$$

The eigenvalues $\lambda_{\neq,1}$ and $\lambda_{\neq,2}$ are the solutions of the quadratic equation

$$x^2 - x(q^2 - 6q + 10) - q^3 + 7q^2 - 16q + 12 = 0. \quad (6.9)$$

The amplitudes are given by

$$\alpha_{=} = q(q-1)(q-2) \quad (6.10a)$$

$$\alpha_{\neq,1} = \frac{q(q-1)}{2} \frac{(3-3q+q^2)\sqrt{Q_2} - (22-34q+21q^2-7q^3+q^4)}{\sqrt{Q_2}} \quad (6.10b)$$

$$\alpha_{\neq,2} = \frac{q(q-1)}{2} \frac{(3-3q+q^2)\sqrt{Q_2} + (22-34q+21q^2-7q^3+q^4)}{\sqrt{Q_2}} \quad (6.10c)$$

We have computed the limiting curve \mathcal{B}_2 by using the resultant method. This curve crosses the real q -axis at $q = 3$, which is a quadruple point. There are two pairs of complex-conjugate T points, namely $q \approx 2.6099757836 \pm 1.8423725343i$ and $q \approx 2.8900242164 \pm 0.5194968788i$.

In the two regions having nonempty intersection with the real q -axis, the dominant eigenvalue comes from $\mathbf{T}''_{\neq}(2)$; in the other four regions, the dominant eigenvalue is $\lambda_{=}$. On the complex-conjugate curves connecting the T points $q \approx 2.6099757836 \pm 1.8423725343i$ and $q \approx 2.8900242164 \pm 0.5194968788i$, $\lambda_{\neq,1}$ and $\lambda_{\neq,2}$ are equimodular. Hence, at the four T points the three eigenvalues become equimodular. Finally, at the quadruple point $\lambda_{=} = \lambda_{\neq,2} = 1$ and $\lambda_{\neq,1} = 0$.²⁶

²⁶The eigenvalues $\lambda_{\neq,1}$ and $\lambda_{\neq,2}$ are analytic functions of q except at the branch cuts of the function $\sqrt{Q_2(q)}$. The polynomial Q_2 has zeros at $q = 2 \pm i + \sqrt{-1 \mp 2i} \approx 2.78615 \mp 0.27202i$ and at $q = 2 \mp i - \sqrt{-1 \pm 2i} \approx 1.21305 \mp 2.27202i$. These four zeros belong to regions where $\lambda_{=}$ is dominant: namely, the first pair of zeros belong to the two oval-like closed regions protruding from the quadruple point $q = 3$, while the later pair belong to the other two regions not intersecting the real q -axis. We have chosen the branch cuts to be horizontal lines starting at each zero and going to $q \rightarrow -\infty$: i.e., for each zero q_i with $i = 1, \dots, 4$, we define $q = q_i + r_i e^{i\theta_i}$ with $r_i \geq 0$ and $-\pi < \theta_i \leq \pi$. With this definition of branch cuts, $\lambda_{\neq,2}$ is dominant in the two regions having nonempty intersection with the real q -axis, except whenever $2.27202 \gtrsim |\text{Im } q| \gtrsim 0.27202$ and $\text{Re } q$ lies to the left of the lines joining two T points.

There are four isolated limiting points at $q = 0, 1, 2, B_5$. At these values the dominant amplitude $\alpha_{\neq,2}$ vanishes. The limiting curve \mathcal{B}_2 and the chromatic roots for $n = 20, 40$ are depicted in Figure 10.

6.3 $m = 3$

The transfer matrix $\mathsf{T}''_{=}(3)$ has dimension 3. The basis is chosen as $\mathbf{B}_{=} = \{\delta_{0,2}, \delta_{1,3}, \mathbf{1}\}$. In this basis, the transfer matrix and the left and right vectors for this strip are

$$\mathsf{T}''_{=}(3) = \begin{pmatrix} -L_{4,4} & -1 & 5-2q \\ 0 & q-2 & 1 \\ L_{4,4} & L_{5,7} & T_1 \end{pmatrix} \quad (6.11a)$$

$$\boldsymbol{\omega}^T = q(q-1)(q-1, q-1, L_{3,3}) \quad (6.11b)$$

$$\mathbf{f}_{\text{id}}^T = (0, 0, 1) \quad (6.11c)$$

where we have used the shorthand notation

$$T_1(q) = q^3 - 7q^2 + 19q - 20 \quad (6.12a)$$

$$L_{m,n}(q) = q^2 - mq + n \quad (6.12b)$$

The transfer matrix $\mathsf{T}''_{\neq}(3)$ has dimension 4. The basis is chosen as $\mathbf{B}_{\neq} = \{\delta_{0,2} + \delta_{4,2}, \delta_{0,3} + \delta_{1,4}, \delta_{1,3}, \mathbf{1}\}$. In this basis, the transfer matrix and the left and right vectors for this strip are

$$\mathsf{T}''_{\neq}(3) = \begin{pmatrix} -L_{5,6} & q-3 & -1 & 3-q \\ q-2 & -L_{5,7} & q-2 & 1 \\ 0 & 0 & q-2 & 1 \\ 2L_{5,6} & 2L_{5,7} & L_{6,9} & T_1-1 \end{pmatrix} \quad (6.13a)$$

$$\boldsymbol{\omega}^T = q(q-1)(q-2)(2(q-1), 2(q-1), q-1, L_{2,2}) \quad (6.13b)$$

$$\mathbf{f}_{\text{id}}^T = (0, 0, 0, 1) \quad (6.13c)$$

where we have used (6.12).

The three eigenvalues of $\mathsf{T}''_{=}(3)$ come from the third-order polynomial

$$\begin{aligned} x^3 &- x^2(q^3 - 8q^2 + 24q - 26) - x(q^5 - 12q^4 + 59q^3 - 149q^2 + 193q - 101) \\ &+ q^6 - 13q^5 + 70q^4 - 200q^3 + 320q^2 - 272q + 96 \end{aligned} \quad (6.14)$$

while the four eigenvalues of $\mathsf{T}''_{\neq}(3)$ come from the fourth-order polynomial

$$\begin{aligned} x^4 &- x^3(q^3 - 9q^2 + 30q - 36) - x^2(2q^5 - 26q^4 + 140q^3 - 388q^2 + 551q - 318) \\ &- x(q^7 - 19q^6 + 153q^5 - 681q^4 + 1815q^3 - 2901q^2 + 2577q - 981) \\ &+ q^8 - 19q^7 + 157q^6 - 738q^5 + 2161q^4 - 4039q^3 \\ &+ 4707q^2 - 3128q + 908. \end{aligned} \quad (6.15)$$

We have computed the limiting curve by using the resultant method, and fine-tuned the results using the direct-search method. The limiting curve \mathcal{B} crosses the real q -axis at $q \approx 2.8177131118$. There is one pair of complex-conjugate endpoints at $q \approx$

$2.7852013976 \pm 0.7798713630i$. There are seven pairs of complex-conjugate T points at $q \approx 1.0229779807 \pm 2.4615628248i$, $q \approx 2.3154363287 \pm 1.9575822608i$, $q \approx 2.4538824566 \pm 1.8334262878i$, $q \approx 2.5862741033 \pm 1.5583461255i$, $q \approx 2.8988477958 \pm 0.4358504561i$, $q \approx 2.9168615472 \pm 0.6195940190i$, and $q \approx 3.0476880109 \pm 0.4560842031i$. There are four isolated limiting points at $q = 0, 1, 2, B_5$.

The dominant eigenvalue comes from $T''_{\neq}(3)$ in the region containing the interval $q \in (-\infty, 2.8177131118)$, and in the two large regions bounded asymptotically by $|\arg q| \in (\pi/6, \pi/2)$ as $|q| \rightarrow \infty$. The dominant eigenvalue comes from $T''_{=}(3)$ in the other three large regions: the one that contains the interval $q \in (2.8177131118, \infty)$ and the other two asymptotically bounded by $|\arg q| \in (\pi/2, 5\pi/6)$ as $|q| \rightarrow \infty$.

There are four isolated limiting points at $q = 0, 1, 2, B_5$. The limiting curve \mathcal{B}_3 and the chromatic roots for $n = 30, 60$ are depicted in Figure 11.

6.4 $m = 4$

The transfer matrix $T''_{=}(4)$ has dimension 5, and $T''_{\neq}(4)$ has dimension 9. They are too lengthy to be reported here, but they can be found in the MATHEMATICA file `square_extra_sites.m` (1.9 MB) that is available on request from the authors.

We have computed the limiting curve by using the resultant method, and fine-tuned the results using the direct-search method. The limiting curve \mathcal{B} crosses the real q -axis at $q \approx 2.9060325277$ and $q \approx 3.9030119682$. There are two pairs of complex-conjugate endpoints at $q \approx 2.6169563471 \pm 1.4357301392i$, and $q \approx 2.8849105593 \pm 0.7356893954i$.

There are ten pairs of complex-conjugate T points at $q \approx 0.3411402631 \pm 2.3118521368i$, $q \approx 1.1260056618 \pm 2.5364550333i$, $q \approx 1.3027336503 \pm 2.5447465991i$, $q \approx 2.2640047808 \pm 1.9520686076i$, $q \approx 2.4920548627 \pm 1.7925248200i$, $q \approx 2.7002452362 \pm 1.5923412229i$, $q \approx 2.8652031850 \pm 1.1531618171i$, $q \approx 2.9601783483 \pm 0.5518584736i$, $q \approx 2.9623803372 \pm 0.5807622346i$, and $q \approx 3.0624715624 \pm 0.6434188421i$. There is a pair of bulb-like regions protruding from T points $q \approx 2.7002452362 \pm 1.5923412229i$.

The dominant eigenvalue comes from $T''_{\neq}(4)$ in the region containing the interval $q \in (-\infty, 2.9060325277) \cup (3.9030119682, \infty)$, and in the two large regions bounded asymptotically by $|\arg q| \in (3\pi/8, 5\pi/8)$ as $|q| \rightarrow \infty$. The dominant eigenvalue comes from $T''_{=}(4)$ in the other four large regions: i.e., those asymptotically bounded by $|\arg q| \in (\pi/8, 3\pi/8)$ and $|\arg q| \in (5\pi/8, 7\pi/8)$ as $|q| \rightarrow \infty$. The dominant eigenvalue comes from this block also in the region containing the interval $q \in (2.9060325277, 3.9030119682)$, and the other two closed regions pointing to the right in Figure 12.

There are four real isolated limiting points at $q = 0, 1, 2, B_5$, and a pair of complex-conjugate isolated limiting points at $q \approx 2.8555521103 \pm 0.9018551071i$. The limiting curve \mathcal{B}_4 and the chromatic roots for $n = 40, 80$ are depicted in Figure 12.

6.5 $m = 5$

The transfer matrix $T''_{=}(5)$ has dimension 11, and the matrix $T''_{\neq}(5)$ has dimension 21.

This is the first case where we have computed the limiting curve using the direct-search method, except for the endpoints that were computed using the resultant method. The limiting curve \mathcal{B} crosses the real q -axis at $q \approx 2.9268787368$.

There are 14 pairs of complex-conjugate T points at $q \approx 0.0265421747 \pm 2.1428032766 i$, $q \approx 0.2211937394 \pm 2.2964381892 i$, $q \approx 0.5678532323 \pm 2.4981722822 i$, $q \approx 1.5459127222 \pm 2.4751057958 i$, $q \approx 1.5503506823 \pm 2.4742675615 i$, $q \approx 2.2165122888 \pm 2.0475480936 i$, $q \approx 2.3467238502 \pm 1.9855375152 i$, $q \approx 2.5384138871 \pm 1.7717517039 i$, $q \approx 2.8417052689 \pm 1.2459939540 i$, $q \approx 2.9278218101 \pm 0.9693176128 i$, $q \approx 2.9651600535 \pm 0.7574018277 i$, $q \approx 3.0055390406 \pm 0.9222249388 i$, $q \approx 3.1196012894 \pm 0.2666719871 i$, and $q \approx 3.1587639645 \pm 0.5586982282 i$. There are two pairs of complex-conjugate endpoints at $q \approx 2.0144392334 \pm 2.0277231065 i$, and $q \approx 2.3246979483 \pm 1.9016376971 i$. Finally, there is a pair of complex-conjugate bulk-like regions protruding from the T points $q \approx 2.3467238502 \pm 1.9855375152 i$.

There are four real isolated limiting points at $q = 0, 1, 2, B_5$, and two pairs of complex-conjugate isolated limiting points at $q \approx 2.7190757419 \pm 1.4455587779 i$, and $q \approx 2.8265910048 \pm 0.9420673312 i$. The limiting curve \mathcal{B}_5 and the chromatic roots for $n = 50, 100$ are depicted in Figure 13.

6.6 $m = 6$

The transfer matrix $T''(6)$ has dimension 21, and the matrix $T''_{\neq}(6)$ has dimension 49.

The limiting curve has been completely determined by using the direct-search method. This curve \mathcal{B} crosses the real q -axis at $q \approx 2.9477131589$, and $q \approx 4.2138764783$.

There are 16 pairs of complex-conjugate T points at $q \approx 0.1195227877 \pm 2.2972440367 i$, $q \approx 0.8945659676 \pm 2.5558662562 i$, $q \approx 1.0187320850 \pm 2.5519732169 i$, $q \approx 1.7361257994 \pm 2.4200684634 i$, $q \approx 2.0496846729 \pm 2.2109675624 i$, $q \approx 2.0659399006 \pm 2.1928587989 i$, $q \approx 2.1816875305 \pm 2.1274251306 i$, $q \approx 2.5037573375 \pm 1.8512451004 i$, $q \approx 2.7553322546 \pm 1.4607519460 i$, $q \approx 2.9072366988 \pm 1.0781535615 i$, $q \approx 2.9302627055 \pm 1.0265712687 i$, $q \approx 2.9319763271 \pm 1.0161098821 i$, $q \approx 2.9600871035 \pm 0.8562446926 i$, $q \approx 3.0829802406 \pm 0.7932348764 i$, $q \approx 3.0859998597 \pm 0.4641385413 i$, and $q \approx 3.0934600966 \pm 0.4747067803 i$. There are two pairs of complex-conjugate endpoints at $q \approx 1.8355583156 \pm 2.1088360158 i$, and $q \approx 2.8978250409 \pm 1.0665199267 i$.

In this case we have been able to find four isolated limiting points at $q = 0, 1, 2, B_5$; but we cannot rule out the existence of other isolated limiting points (especially complex ones). The limiting curve \mathcal{B}_6 and the chromatic roots for $n = 60, 120$ are depicted in Figure 14.

6.7 Comparison of $1 \leq m \leq 6$

In Figure 15 we show the limiting curves \mathcal{B}_m for $1 \leq m \leq 6$, plotted together. We see clearly that:

- (a) There is an oval-shaped region at small q , extending roughly from $q = 0$ to $q = 3$ in the real direction and between $q \approx 1.1 \pm 2.6 i$ in the imaginary direction, where the limiting curves \mathcal{B}_m do not enter, or at least from which they retreat as $m \rightarrow \infty$.
- (b) Outside of this region, the curves \mathcal{B}_m appear to become *dense* as $m \rightarrow \infty$, except possibly near the real axis.

- (c) The curve \mathcal{B}_m also exhibits, for each $m \geq 3$, $m-1$ small “fingers” extending outside the oval-shaped region towards the right (these “fingers” are more easily seen on Figures 11–14).

In Figure 15 we have also superposed, in dark gray, the limiting curve $\mathcal{B}_{11}^{\text{cyl}}$ for a square-lattice strip of width $m = 11$ and *cylindrical* boundary conditions [34]. This curve can be taken as a rough approximation of the expected *infinite-volume* limiting curve $\mathcal{B}_\infty(\text{sq}) = \lim_{m \rightarrow \infty} \mathcal{B}_m^{\text{cyl}}$ for the square-lattice model with cylindrical boundary conditions, with the exception that we expect the curves $\mathcal{B}_m^{\text{cyl}}$ to move slightly outward as m grows and to close up at $q = 0$; in particular we expect $\mathcal{B}_\infty(\text{sq})$ to be a *closed* curve that crosses the real q -axis at $q = 0$ and $q_0 = q_c = 3$ [34, 53]. We expect, furthermore, that the same limiting curve will be obtained for free boundary conditions [34, 53].

Figure 15 clearly suggests that the oval-shaped curve to which the curves \mathcal{B}_m are retreating as $m \rightarrow \infty$ is the *same* as the curve $\mathcal{B}_\infty(\text{sq})$ obtained for cylindrical (or free) boundary conditions. The region where the curves \mathcal{B}_m are apparently becoming dense is precisely the exterior of $\mathcal{B}_\infty(\text{sq})$.

7 Conjectures on the limiting curves \mathcal{B}_m as $m \rightarrow \infty$

In this section we discuss in more detail the behavior at large $|q|$ of the limiting curves \mathcal{B}_m ; in particular, we formulate conjectures concerning the behavior of these limiting curves as $m \rightarrow \infty$.

7.1 Behavior at large $|q|$ for each m

Figures 9–14 show the limiting curves \mathcal{B}_m for $1 \leq m \leq 6$: in each case we give both a “close-up” view that shows the details of the small- $|q|$ behavior and a “distance” view that makes clear the large- $|q|$ asymptotics. We notice, first of all, that the curve \mathcal{B}_m has $2m$ outward branches tending to $q = \infty$, with asymptotic (as $|q| \rightarrow \infty$) angles that are equally spaced around the circle. These empirical findings for $1 \leq m \leq 6$ motivate the following result:

Proposition 7.1 *Fix $m \geq 1$. Then the limiting curve \mathcal{B}_m for chromatic roots of the square-lattice strips $S_{m,n}$ ($n \rightarrow \infty$) has exactly $2m$ outward branches extending to infinity, with asymptotic angles $\arg q = \theta_{k,m}$ where*

$$\theta_{k,m} = \left(k - \frac{1}{2}\right) \frac{\pi}{m} \quad \text{for } k = 1, \dots, 2m. \quad (7.1)$$

Moreover, the dominant eigenvalue comes from $\mathbb{T}_\pm''(m)$ in the asymptotic regions

$$\theta_{k,m} < \arg q < \theta_{k+1,m} \quad \text{for} \quad \begin{cases} k = 1, 3, \dots, 2m-1 & \text{if } m \text{ is even} \\ k = 2, 4, \dots, 2m & \text{if } m \text{ is odd} \end{cases} \quad (7.2)$$

while in the other asymptotic sectors the dominant eigenvalue comes from $\mathbb{T}_\neq''(m)$.

PROOF. By the Beraha–Kahane–Weiss theorem (Theorem 2.2), the limiting curve \mathcal{B}_m consists of those q for which

$$\left| \frac{\lambda_{*,=(m)}}{\lambda_{*,\neq(m)}} \right| = 1, \quad (7.3)$$

or equivalently

$$\log \left(\frac{\lambda_{*,=(m)}}{\lambda_{*,\neq(m)}} \right) = i\theta \quad \text{with } \theta \text{ real}, \quad (7.4)$$

or equivalently

$$\log \left[(-1)^{m+1} \log \left(\frac{\lambda_{*,=(m)}}{\lambda_{*,\neq(m)}} \right) \right] = -(2k-1) \frac{\pi}{2} \quad \text{with } k \text{ integer} \quad (7.5)$$

[the factor $(-1)^{m+1}$ is included here solely for future convenience]. If we now define

$$\mathcal{F}_m(q) = -\log \left[(-1)^{m+1} q^m \log \left(\frac{\lambda_{*,=(m)}}{\lambda_{*,\neq(m)}} \right) \right] \quad (7.6)$$

[compare (4.14)], then (7.5) can be rewritten as

$$\arg q = (2k-1) \frac{\pi}{2m} - \operatorname{Im} \frac{\mathcal{F}_m(q)}{m}. \quad (7.7)$$

On the other hand, Proposition 3.10 together with (4.5a) tells us that

$$\mathcal{F}_m(q) = O(q^{-1}), \quad (7.8)$$

so that the curve \mathcal{B}_m is given by

$$\arg q = (2k-1) \frac{\pi}{2m} + O(|q|^{-1}). \quad (7.9)$$

This proves the first statement of Proposition 7.1.

The second statement of Proposition 7.1 follows easily from

$$\frac{\lambda_{*,=(m)}}{\lambda_{*,\neq(m)}} = 1 + (-1)^{m+1} q^{-m} + O(q^{-(m+1)}), \quad (7.10)$$

which implies

$$\left| \frac{\lambda_{*,=(m)}}{\lambda_{*,\neq(m)}} \right| = 1 + (-1)^{m+1} \operatorname{Re}(q^{-m}) + O(q^{-(m+1)}). \quad (7.11)$$

□

Remark. This proof of Proposition 7.1 actually uses a bit less than the full strength of Proposition 3.10. More specifically, the first statement of Proposition 7.1 follows from

$$\lambda_{*,=(m)} - \lambda_{*,\neq(m)} = c_m + o(1) \quad \text{with } c_m \text{ real } \neq 0, \quad (7.12)$$

while the second statement uses $\operatorname{sgn}(c_m) = (-1)^{m+1}$. In neither case do we need the exact value $c_m = (-1)^{m+1}$, nor do we need to know that the error $o(1)$ is actually $O(q^{-1})$. □

Using Proposition 3.10 we can actually go farther, and compute the corrections to $\arg q = \theta_{k,m}$ as a series in inverse powers of $|q|$. It suffices to use the fundamental relation (7.7) and insert the expansion

$$\mathcal{F}_m(q) = \sum_{\ell=1}^{\infty} f_{\ell}(m) q^{-\ell} \quad (7.13)$$

[cf. (4.14)], which is guaranteed by Corollary 3.4 together with Proposition 3.10 to be convergent for all sufficiently large $|q|$ (how large may depend on m). It is then straightforward to determine iteratively $\arg q$ as a power series in $|q|^{-1}$. For instance, the series through order $|q|^{-3}$ is given by

$$\begin{aligned} \arg q &= \theta_{k,m} + \left(\frac{f_1(m)}{m} \sin \theta_{k,m} \right) |q|^{-1} + \left[\left(\frac{f_1(m)^2}{2m^2} + \frac{f_2(m)}{m} \right) \sin 2\theta_{k,m} \right] |q|^{-2} \\ &+ \left[\left(\frac{f_1(m)^3}{8m^3} + \frac{f_1(m)f_2(m)}{2m^2} \right) (3 \sin 3\theta_{k,m} - \sin \theta_{k,m}) + \frac{f_3(m)}{m} \sin 3\theta_{k,m} \right] |q|^{-3} \\ &+ O(|q|^{-4}). \end{aligned} \quad (7.14)$$

In particular, for $m \leq 11$ we know explicitly the coefficients $f_{\ell}(m)$.

If we assume Conjecture 4.3, then we can replace $f_{\ell}(m)$ by the polynomial $F_{\ell}(m)$ whenever $m \geq \ell + 1$, and we can moreover use the specific forms of $F_{\ell}(m)$ shown in Table 4 at least for $\ell \leq 9$.

In Figures 9–14 we compare the exact limiting curves \mathcal{B}_m with the approximations (7.14) through orders q^0 , q^{-1} , q^{-2} and q^{-3} . We have checked numerically the correctness of the asymptotic expansions (7.14), by plotting the deviations of $\arg q$ from (7.14) truncated at order $|q|^{-\ell}$, multiplied by $|q|^{\ell+1}$, versus $|q|$, and verifying that they are tending to constants (or at least bounded) as $|q| \rightarrow \infty$.

7.2 Uniformity in m and density of chromatic roots

Since the asymptotic rays $\arg q = \theta_{k,m}$ arising in Proposition 7.1 become *dense* as $m \rightarrow \infty$, it is natural to expect that the chromatic roots of the graphs $S_{m,n}$ become dense as $m, n \rightarrow \infty$ in the whole complex plane outside of a bounded set (analogously to what happens for the generalized theta graphs [63]). We can formalize this conjecture as follows:

Conjecture 7.2 *There exists a constant $Q < \infty$ such that the chromatic roots of the graphs $S_{m,n}$ become dense in the region $|q| > Q$ when $m, n \rightarrow \infty$.*

We stress that Conjecture 7.2 does *not* follow from Proposition 7.1 alone — or from the more fundamental Proposition 3.10 and Conjectures 4.2–4.3 — because these results apply to each value of m separately, and there is no guarantee that the error bounds in these asymptotic expansions are uniform in m ; in particular, there is no guarantee that they can be made to apply to a region $|q| > Q$ where Q is *independent of m* . In this subsection we would like to discuss a refinement of Proposition 3.10 from which Conjecture 7.2 can indeed be deduced.

We know rigorously that there exists $Q_0 < \infty$, independent of m , such that $\lambda_{*,=}(m)$ and $\lambda_{*,\neq}(m)$ are analytic and nonvanishing in $|q| > Q_0$ for all $m \geq 1$ (see Theorem 3.9 and the discussion following it, where it is shown that $Q_0 = 33.855628$ suffices). If we now use Proposition 3.10, we can conclude that the functions $\mathcal{F}_m(q)$ defined in (7.6) are likewise analytic in $|q| > Q_0$ for all $m \geq 1$ and moreover vanishing at $q = \infty$, so that they are given for $|q| > Q_0$ by a convergent expansion (7.13). Let us now make the following hypothesis:

Conjecture 7.3 *There exist $Q_1 \in (Q_0, \infty)$ and $C < \infty$ such that*

$$\sup_{|q|=Q_1} |\mathcal{F}_m(q)| \leq Cm \quad \text{for all } m. \quad (7.15)$$

Note that here Q_1 and C are independent of m .

This hypothesis is natural in view of Conjecture 4.3, which says that the coefficients $f_\ell(m)$ in (7.13) are given for $m \geq \ell + 1$ by polynomials $F_\ell(m) = \epsilon_\ell m + \phi_\ell$ of degree 1 in m ; so it is natural to expect that $\mathcal{F}_m(q)$ will likewise satisfy a bound that is linear in m . The trouble is that the coefficients $f_\ell(m)$ for $\ell \geq m$ are completely uncontrolled, so we cannot deduce Conjecture 7.3 from Conjecture 4.3. It is, nevertheless, a natural extension of Conjecture 4.3.

Let us now prove that Conjecture 7.3 implies Conjecture 7.2:

PROOF OF CONJECTURE 7.2, GIVEN CONJECTURE 7.3. Using the hypothesis (7.15) together with the Cauchy integral formula in the variable $z = 1/q$, we conclude that

$$|\mathcal{F}'_m(q)| \leq 4Cm \frac{Q_1}{|q|^2} \quad \text{whenever } |q| \geq 2Q_1. \quad (7.16)$$

We now use the fundamental formula (7.7) determining the curve \mathcal{B}_m , and we consider $\text{Im } \mathcal{F}_m(q)/m$ as a function of $\arg q$ for each fixed $|q|$:

$$f_m(\arg q; |q|) = \text{Im } \frac{\mathcal{F}_m(q)}{m}. \quad (7.17)$$

It follows from (7.16) that

$$\left| f'_m(\arg q; |q|) \right| \leq 4C \frac{Q_1}{|q|} \quad \text{whenever } |q| \geq 2Q_1 \quad (7.18)$$

and hence that

$$\left| f'_m(\arg q; |q|) \right| \leq \frac{1}{2} \quad \text{whenever } |q| \geq Q_2 \equiv \max(8CQ_1, 2Q_1). \quad (7.19)$$

Now (7.7) amounts to solving the equation

$$h_m(\arg q) = y \quad (7.20)$$

for a set of values of y spaced by π/m , where

$$h_m(x) = x + f_m(x; |q|) \quad (7.21)$$

is a continuously differentiable (in fact infinitely differentiable) function satisfying $h'_m(x) \geq 1/2$ (and also $h'_m(x) \leq 3/2$, but we do not need this) whenever $|q| \geq Q_2$. It follows that the spacing between consecutive solutions of (7.20) cannot exceed $2\pi/m$. Taking $m \rightarrow \infty$, we conclude that the union of the curves \mathcal{B}_m is dense in the region $|q| \geq Q_2$. It easily follows from this and the Beraha–Kahane–Weiss theorem that the union of the chromatic roots of $S_{m,n}$ as $m, n \rightarrow \infty$ is dense in the region $|q| \geq Q_2$ as well. \square

7.3 Size of the discontinuity in the derivative of the free energy

It is curious that the branches at large $|q|$ of the curves \mathcal{B}_m are caused by *very small* differences between the two eigenvalues — namely, $|\lambda_{*,=} - \lambda_{*,\neq}| \approx 1$ compared to $|\lambda_{*,=}| \approx |\lambda_{*,\neq}| \approx |q|^m$ — which moreover become *irrelevant* in the limit $m \rightarrow \infty$.

In Figure 16 we plot the real part of the free energy

$$f_m(q) = \max[f_m^=(q), f_m^{\neq}(q)] = \frac{1}{m} \max[\log \lambda_{*,=}(q), \log \lambda_{*,\neq}(q)] \quad (7.22)$$

for a semi-infinite strip of width m ($1 \leq m \leq 6$) as a function of $\operatorname{Re} q$ for fixed $\operatorname{Im} q = 3$ or 4. The solid dots show the points of discontinuity in the derivative of the free energy, which arise from the transition between the dominance of $\lambda_{*,=}$ and $\lambda_{*,\neq}$. The discontinuity is small already for $m = 1$ and $\operatorname{Im} q = 3$, and it decreases as m and $\operatorname{Im} q$ grow; indeed, it is essentially invisible for all $m \geq 2$.

This should be contrasted with the behavior at the phase transition between the “disordered” phase (at large $|q|$) and the “ordered phase” (at small $|q|$), which are separated by a curve lying close to $\mathcal{B}_\infty(\text{sq}) = \lim_{m \rightarrow \infty} \mathcal{B}_m^{\text{cyl}}$ (see Section 6.7). At this transition — which occurs also for cylindrical and free boundary conditions, and which is the fundamental phase transition for this model — the discontinuities in the derivative of the free energy do *not* disappear as $m \rightarrow \infty$. This can be seen clearly in Figure 17, which is analogous to Figure 16 but for smaller values of $\operatorname{Im} q$ (namely, 0, 0.25, 0.5 and 1).

We conclude that the outward branches (tending to $q = \infty$) of the curves \mathcal{B}_m do *not* correspond to phase transitions of the infinite-volume free energy. This is no surprise, because no such phase transitions are observed for free or cylindrical boundary conditions, and we believe that the infinite-volume free energy $f(q)$ is the *same* for $=$, \neq , free and cylindrical boundary conditions (at least in the “disordered” phase, where we have checked it in the large- q expansion through order q^{-15} , cf. Section 5.2).

7.4 Largest magnitude of a chromatic root

By Proposition 7.1 we know that, for each $m \geq 1$, the chromatic roots of $S_{m,n}$ become dense as $n \rightarrow \infty$ on a curve \mathcal{B}_m that contains $2m$ outward branches extending to infinity. It is natural to ask: At what rate does this curve get filled out as $n \rightarrow \infty$? In particular, what is the largest magnitude of a chromatic root of $S_{m,n}$?

For the generalized theta graphs $\Theta^{(s,p)}$, Brown, Hickman, Sokal and Wagner [12, Theorem 1.3] proved that the chromatic roots are bounded in modulus by $[1 + o(1)]p/\log p$, uniformly in s and p , where $o(1)$ denotes a constant $C(p)$ that tends to zero as $p \rightarrow \infty$.

They furthermore showed [12, Corollary 5.2] that this bound is sharp when $s = 2$. However, when $s > 2$ we expect that this bound is far from sharp; in particular, we expect that the root of largest modulus grows as $p \rightarrow \infty$ only like $(p/\log p)^{1/(s-1)}$.

For our graphs $S_{m,n}$, the only thing we know rigorously is that the chromatic roots are bounded in modulus by $C \max(n, 4)$, where

$$C = \frac{W(e/2)}{[1 - W(e/2)]^2} \approx 6.907652 \quad (7.23)$$

and W is the Lambert W function [17], i.e. the inverse function to $x \mapsto xe^x$; this follows from a result of Fernández and Procacci [26] bounding the chromatic roots of arbitrary graphs in terms of the graph's maximum degree (i.e., the maximum number of neighbors of any vertex).²⁷ However, by analogy with the generalized theta graphs it is natural to expect that the chromatic roots of the graphs $S_{m,n}$ in fact obey an upper bound that is *sublinear* in n , e.g. $n/\log n$ or even $(n/\log n)^{1/m}$ [since s corresponds to $m + 1$].

It is an interesting open problem to verify (or refute) these conjectures, first for the generalized theta graphs and then for the family $S_{m,n}$.

8 Discussion

In this section we make some final comments and some suggestions for future research.

8.1 Comparison with the work of Jacobsen, Saleur and Dubail

In a series of recent papers [20, 39–41], Jacobsen, Saleur and Dubail have studied models of densely packed self-avoiding loops on the annulus in which loops touching one or both rims of the annulus receive different weights from “bulk” loops. By a generalization of the Baxter–Kelland–Wu [4] mapping, such models can be mapped onto Potts models in which spins lying on the rims of the annulus lie in specified subsets of $\{1, \dots, q\}$, or equivalently Fortuin–Kasteleyn models in which clusters touching one or both rims of the annulus receive different weights from “bulk” clusters.

These latter models can be defined in a very general way as follows [20]: Let $G = (V, E)$ be a finite graph, and let $V_1, V_2 \subseteq V$ be *disjoint* subsets of V . Fix subsets $S_1, S_2 \subseteq \{1, \dots, q\}$, and let us define a Potts model in which spins at a site in V_i are required to lie in S_i ($i = 1, 2$):

$$Z_G^{\text{Potts}}(q, S_1, S_2, \mathbf{v}) = \sum_{\substack{\sigma: V \rightarrow \{1, 2, \dots, q\} \\ \sigma[V_1] \subseteq S_1 \\ \sigma[V_2] \subseteq S_2}} \prod_{e=ij \in E} [1 + v_e \delta(\sigma_i, \sigma_j)] . \quad (8.1)$$

²⁷Earlier, Sokal [62] had obtained the same result with the weaker constant 7.963907. The identification of the Fernández–Procacci constant in terms of the Lambert W function is due to Jackson, Procacci and Sokal [31].

Likewise, let us define a Fortuin–Kasteleyn model in which clusters touching V_1 or V_2 or both receive different weights from “bulk” clusters:

$$Z_G(q, q_1, q_2, q_{12}, \mathbf{v}) = \sum_{A \subseteq E} q^{k_0(A)} q_1^{k_1(A)} q_2^{k_2(A)} q_{12}^{k_{12}(A)} \prod_{e \in A} v_e, \quad (8.2)$$

where $k_0(A), k_1(A), k_2(A), k_{12}(A)$ denote, respectively, the number of connected components in the subgraph (V, A) that intersect neither V_1 nor V_2 , V_1 but not V_2 , V_2 but not V_1 , or both V_1 and V_2 . It is then easy to see that

$$Z_G^{\text{Potts}}(q, S_1, S_2, \mathbf{v}) = Z_G(q, q_1, q_2, q_{12}, \mathbf{v}) \quad (8.3)$$

provided that we identify

$$q_1 = |S_1|, \quad q_2 = |S_2|, \quad q_{12} = |S_1 \cap S_2|. \quad (8.4)$$

Our partition functions $Z_{S_{m,n}^=}(q, \mathbf{v})$ and $Z_{S_{m,n}^{\neq}}(q, \mathbf{v})$ are, up to trivial prefactors, special cases of this construction. Indeed, let G be the usual $m \times n$ square lattice with free boundary conditions ($m \geq 2$), and let V_1 (resp. V_2) consist of the sites in the leftmost (resp. rightmost) column. Then it is easy to see that

$$Z_{S_{m,n}^=}(q, \mathbf{v}) = q Z_G(q, q-1, q-1, q-1, \mathbf{v}) \quad (8.5a)$$

$$Z_{S_{m,n}^{\neq}}(q, \mathbf{v}) = q(q-1) Z_G(q, q-1, q-1, q-2, \mathbf{v}) \quad (8.5b)$$

Dubail, Jacobsen and Saleur (DJS) have used the loop-model representation associated to the Fortuin–Kasteleyn model (8.2) to obtain the conformal properties (central charge, critical exponents, exact continuum-limit partition functions, etc.) both for the usual critical point $n = \sqrt{q}$ [20] and for the Berker–Kadanoff phase $n = -\sqrt{q}$ [41], where n is the bulk loop weight.²⁸ This analysis is relevant for values of q lying *inside* the limiting curve $\mathcal{B}_\infty(\text{sq})$. By contrast, in the present paper we have focused on the behavior at large $|q|$, i.e. on the disordered (and non-critical) phase lying *outside* the limiting curve $\mathcal{B}_\infty(\text{sq})$.

There are, however, some points of contact between our work and that of DJS. In particular, our transfer-matrix eigenvalues should correspond to the sector with no non-contractible clusters in the work of DJS (who used periodic longitudinal boundary conditions).

8.2 Density of zeros

Let us go back to the question raised at the beginning of this paper: When does the accumulation of partition-function zeros at some parameter value (or on some curve in the complex plane of some parameter) signal a nonanalyticity of the infinite-volume free energy? The answer is straightforward: when the zeros have a *nonzero density per unit volume* in the infinite-volume limit. Thus, in the trivial example $Z_n(x) = x$ for a system in

²⁸The analysis of the Berker–Kadanoff phase in [41] is actually restricted to the one-boundary case $q_2 = q, q_{12} = q_1$, but it could presumably be generalized.

volume n , the zero at $x = 0$ has multiplicity 1, so the density of zeros is $1/n$, which tends to zero as $n \rightarrow \infty$; hence the infinite-volume free energy does *not* exhibit nonanalyticity at $x = 0$. Similarly for an isolated limiting point in the Beraha–Kahane–Weiss theorem: it has fixed multiplicity, independent of the system length n , so that the density of zeros again tends to zero as $n \rightarrow \infty$.

It would therefore be very interesting to try to understand analytically the density of zeros in the various graph families considered in this paper: starting with the bi-fans $P_n + \bar{K}_2$ and bipyramids $C_n + \bar{K}_2$ (Section 2.4), continuing with the generalized theta graphs $\Theta^{(s,p)}$ (Section 2.5), and finishing with the graphs $S_{m,n}$. For the first three families one might hope to find exact expressions for the density of zeros as n or p tends to infinity; furthermore, for the generalized theta graphs one might be able to study the subsequent limit $s \rightarrow \infty$. For $S_{m,n}$ it seems unlikely that one could obtain exact expressions (except for very small m); but one might hope at least to obtain expansions in powers of q^{-1} .

8.3 Some concluding remarks

In this paper we have studied the graphs $S_{m,n}$ that are obtained from an $m \times n$ square grid (m columns, n rows, free boundary conditions in both directions) by adjoining one new vertex adjacent to all the sites in the leftmost column and a second new vertex adjacent to all the sites in the rightmost column. By similar transfer-matrix methods one can study the graphs $T_{m,n}$ that are obtained analogously from a $m \times n$ grid of the *triangular* lattice. (The triangular lattice is most easily viewed as a square lattice with a SW–NE diagonal edge added to each face.) All of these graphs are 3-connected and planar, and we expect the square and triangular families to have a similar qualitative behavior, though the details of the limiting curves will differ [34, 38, 53]. The triangular lattice has the advantage that there exists a precise conjecture for at least the outer boundary of the limiting curve \mathcal{B}_∞ for ordinary (e.g., free or cylindrical) boundary conditions: see Baxter [2, 3] for this conjecture and the remarkable Bethe-Ansatz computation supporting it, and see [38, especially Section 6] for further discussion.

More interestingly, one can also study the graphs $S_{m,n}^{\text{per}}$ (resp. $T_{m,n}^{\text{per}}$) that are obtained by this construction starting from an $m \times n$ grid with *periodic* boundary conditions in the longitudinal (n) direction. These are 4-connected planar graphs (resp. 4-connected plane triangulations), and for $m = 1$ they reduce to the bipyramids $C_n + \bar{K}_2$. Their chromatic polynomials can once again be analyzed by transfer-matrix methods [35, 36]. The transfer matrices are larger than in the free-longitudinal-boundary-condition case, since they have to keep track of the connections among the sites of the top *and bottom* rows. On the other hand, the transfer matrix is block-triangular: firstly in terms of the number ℓ of disjoint paths connecting the top and bottom rows, and secondly in terms of the connectivity of the bottom row. Moreover, the amplitudes $\alpha_k(q)$ are explicitly determinable polynomials in q . For this reason the computation is more involved than for free longitudinal boundary conditions, but not vastly computationally more demanding. See [35–37] for more details.

Let us conclude with a vague idea. It may be possible to prove Conjecture 7.3 by using the polymer expansion [49] and exploiting the uniform (in m) convergence of the polymer expansion for sufficiently large $|q|$.

Acknowledgments

We wish to thank Bill Jackson, Jesper Jacobsen and Steve Noble for helpful conversations. We also wish to thank two referees for incisive comments on the first version of this paper.

J.S. is grateful for the kind hospitality of the Physics Department of New York University and the Mathematics Department of University College London, where part of this work was done. Likewise, A.D.S. is grateful for the kind hospitality of the M.S.M.I. group of the Universidad Carlos III de Madrid. Both authors also thank the Isaac Newton Institute for Mathematical Sciences, University of Cambridge, for hospitality during the programme on Combinatorics and Statistical Mechanics (January–June 2008); LPTHE-Jussieu and the École Normale Supérieure for hospitality in June 2009; and the École Normale Supérieure for hospitality in May–June 2011. Finally, A.D.S. thanks the Institut Henri Poincaré – Centre Emile Borel for hospitality during the programmes on Interacting Particle Systems, Statistical Mechanics and Probability Theory (September–December 2008) and Statistical Physics, Combinatorics and Probability (September–December 2009).

The authors’ research was supported in part by U.S. National Science Foundation grant PHY-0424082 (A.D.S.) and by Spanish MEC grants FPA2009-08785 and MTM2008-03020 (J.S.).

A Proof of Proposition 3.5

In this appendix we prove Proposition 3.5 concerning the dominant diagonal entries in the transfer matrix.

In Ref. [54, Section 3.2], we showed that the dominant diagonal entry $t_F(m)$ of the transfer matrix for a square-lattice strip of width m and *free* boundary conditions is equal to the partition function for a certain one-dimensional m -site polymer gas (with free boundary conditions). In this polymer model, each polymer of length $\ell \geq 1$ gets a fugacity $\mu_\ell = v^{\ell-1}(q + \ell v')$, where v (resp. v') is the weight of all horizontal (resp. vertical) edges in the corresponding Potts model. We solved this problem by using the generating function (“grand partition function”)

$$\Phi_F(z) = \sum_{m=1}^{\infty} z^m t_F(m) = \frac{\Psi(z)}{1 - \Psi(z)}, \quad (\text{A.1})$$

where

$$\Psi(z) = \sum_{\ell=1}^{\infty} z^\ell v^{\ell-1}(q + \ell v') = z \left[\frac{q}{1 - zv} + \frac{v'}{(1 - zv)^2} \right] \quad (\text{A.2})$$

is the total weight for a single polymer of arbitrary size. It follows from (A.1)/(A.2) that

$$\Phi_F(z) = \frac{(q - 1)z + qz^2}{1 - (q + 2v + v')z + v(q + v)z^2}. \quad (\text{A.3})$$

We then expanded (A.3) in powers of z to extract the coefficients $t_F(m)$. A similar analysis [54, Section 3.3] handled the case of cylindrical boundary conditions.

In this appendix we shall perform the analogous computations for the transfer matrices associated to the graph families $S_{m,n}^=$ and $S_{m,n}^\neq$, culminating in a proof of Proposition 3.5.

Let us start with the family $S_{m,n}^=$. As explained in Section 3.3 above, the boundary conditions for this family can be handled by considering $m+1$ sites on a circle, where the site labelled 0 is special. Consider first the action of \mathbf{H} on the start vector \mathbf{e}_{id} . It generates 2^{m+1} terms, each of which corresponds to a partition \mathcal{P} in which all the blocks are sequential sets of vertices on the $(m+1)$ -cycle (we shall call these sets “polymers”). Each polymer of size $\ell < m+1$ picks up a factor $v^{\ell-1}$, while a polymer of size $m+1$ picks up a factor $v^{m+1} + (m+1)v^m$ (the v^{m+1} comes from the case in which all edges are occupied, while the $(m+1)v^m$ comes from the $m+1$ cases in which all edges but one are occupied).

Consider next the action of \mathbf{V} on a basis vector $\mathbf{e}_{\mathcal{P}}$ corresponding to an arbitrary partition $\mathcal{P} = \{P_1, \dots, P_k\}$. If we are to end up with the partition \mathbf{e}_{id} , then for each block P_j we must either choose the detach operator \mathbf{D}_i for all $i \in P_j$ (the last deletion gives a factor of q) or else choose the detach operator for all but one $i \in P_j$ and choose $v'I$ for the last site (this can be done in $|P_j|$ ways). This means that the fugacity for any polymer of size $1 \leq \ell \leq m$ *not containing* the special site 0, the fugacity is given by

$$\mu_\ell = v^{\ell-1}(q + \ell v'). \quad (\text{A.4})$$

However, the fugacity for a polymer of length $1 \leq \ell \leq m+1$ containing the special site 0 is given by the formula²⁹

$$\nu_\ell^{(m)} = \begin{cases} v^{\ell-1} & \text{for } 1 \leq \ell \leq m \\ v^m(v + m + 1) & \text{for } \ell = m + 1 \end{cases} \quad (\text{A.5})$$

because the vertical operator \mathbf{V} does not include \mathbf{D}_0 (therefore, for any block P_j containing the site 0, we are forced to choose the detach operator \mathbf{D}_i for all $i \in P_j$ other than the special site $0 \in P_j$).

As we did for cylindrical boundary conditions in [54, Section 3.3], we can compute $t_=(m)$ by using a simple recursion relating our case to that of free boundary conditions:

$$t_=(m) = \sum_{k=1}^m k \nu_k^{(m)} t_{\text{F}}(m+1-k) + \nu_{m+1}^{(m)}. \quad (\text{A.6})$$

To prove (A.6), let $k \geq 1$ the size of the polymer containing site 0. If $k \leq m$, there are k ways of placing this polymer such that the site 0 belongs to it, with fugacity $\nu_k^{(m)} = v^{k-1}$ for each placement; and for the rest of ring, the total weight of all admissible polymer configurations is $t_{\text{F}}(m+1-k)$. Finally, if $k = m+1$, there is only one way of placing the polymer, and it receives a weight $\nu_{m+1}^{(m)}$. This proves (A.6).

²⁹Let us remark that the analogous definition [54, eq. (3.51)] suffers from an unfortunate notational ambiguity: $\hat{\mu}_\ell$ should have been written as $\hat{\mu}_\ell^{(m)}$, because the weight in question depends on m as well as ℓ . The same superscript $^{(m)}$ should appear also in [54, eqs. (3.52) and (3.53)]. This notational clarity is important because, although at this stage we are considering one fixed value of m , we will soon be summing over m .

In order to compute explicitly the $t_=(m)$, we introduce the generating function

$$\Phi_=(z) = \sum_{m=1}^{\infty} z^m t_=(m) . \quad (\text{A.7})$$

The upper limit on the sum in (A.6) can be replaced by ∞ , provided that we define $t_F(\ell) = 0$ for $\ell \leq 0$ [which is anyway implicit in the definition (A.3)]. Multiplying both sides of (A.6) by z^m and summing over m , we arrive at the equation

$$\Phi_=(z) = \frac{\Phi_F(z)}{(1-vz)^2} + \frac{v^2 z}{1-vz} + \frac{vz(2-vz)}{(1-vz)^2} . \quad (\text{A.8})$$

When $v = v' = -1$, we obtain the final formula

$$\Phi_=(z) = -\frac{1}{1+z} + \frac{1}{1-(q-3)z-(q-1)z^2} . \quad (\text{A.9})$$

By expanding this function in powers of z , we have checked that it agrees with the dominant diagonal elements $t_=(m)$ for $m \leq 15$.

Let us next consider the family $S_{m,n}^\neq$. Defining the generating function

$$\Phi_\neq(z) = \sum_{m=1}^{\infty} z^m t_\neq(m) , \quad (\text{A.10})$$

it follows easily from (A.7) and (3.13) that

$$\Phi_\neq(z) = \Phi_=(z) - \frac{v^2 z}{1-vz} . \quad (\text{A.11})$$

When $v = v' = -1$, we obtain the final formula

$$\Phi_\neq(z) = -1 + \frac{1}{1-(q-3)z-(q-1)z^2} . \quad (\text{A.12})$$

By expanding this function in powers of z , we have checked that it agrees with the dominant diagonal elements $t_\neq(m)$ for $m \leq 15$.

It is now straightforward to extract from (A.7)/(A.9) and (A.10)/(A.12) the coefficients $t_=(m)$ and $t_\neq(m)$. In view of (3.13)/(3.14), it suffices to study one of the two; and it turns out that $t_\neq(m)$ takes a slightly simpler form [compare (3.24a) with (3.24b)]. Let us use the notation $[z^m]P(z)$ to denote the coefficient of z^m in a polynomial or formal power series. Using the identity [54, eq. (3.21a)]

$$[z^m] \frac{1}{1-az-bz^2} = \sum_{j=0}^{\lfloor m/2 \rfloor} \binom{m-j}{j} a^{m-2j} b^j , \quad (\text{A.13})$$

we get for $m \geq 1$

$$t_\neq(m) = [z^m] \Phi_\neq(z) = \sum_{j=0}^{\lfloor m/2 \rfloor} \binom{m-j}{j} (q-3)^{m-2j} (q-1)^j , \quad (\text{A.14})$$

which is manifestly a polynomial in q of degree m , as claimed in (3.24).

The next goal is to compute the coefficients $a_k(m)$ arising in (3.24), where $m \geq 1$ and $0 \leq k \leq m$. Expanding the binomials in (A.14), we have

$$a_k(m) = \sum_{j=0}^{\lfloor m/2 \rfloor} \sum_{\ell=0}^{\infty} \binom{m-j}{j} \binom{m-2j}{k+\ell-2j} \binom{j}{\ell} 3^{k+\ell-2j} (-1)^j. \quad (\text{A.15})$$

We now want to substitute the m -dependent upper index in the sum over j by something independent of m , e.g. by k .

There are two nontrivial cases: a) If $k < \lfloor m/2 \rfloor$, then the second binomial vanishes whenever $k + \ell - 2j < 0$, and the third binomial is non-vanishing only if $j \geq \ell$. Therefore for $j > k$ and $j \geq \ell$ we have that $k + \ell - 2j < k + \ell - k - \ell = 0$. So all these terms vanish. b) If $k > \lfloor m/2 \rfloor$, then the first binomial does not vanish only when $0 \leq j \leq \lfloor m/2 \rfloor$ or when $j \geq m + 1$. As we are adding terms with $\lfloor m/2 \rfloor + 1 \leq j \leq k - 1 \leq m - 1$, none of them give rise to a non-vanishing contribution. Therefore, we can re-write (A.15) as

$$a_k(m) = \sum_{j=0}^k \sum_{\ell=0}^{\infty} \binom{m-j}{j} \binom{m-2j}{k+\ell-2j} \binom{j}{\ell} 3^{k+\ell-2j} (-1)^j. \quad (\text{A.16})$$

where the independent variable m does not appear in the summation limits. After some straightforward but lengthy algebra we can rewrite the above formula in a more compact form:

$$a_k(m) = \sum_{p=0}^k \binom{m-p}{p} (-1)^p \sum_{q=0}^{k-p} 3^q \binom{m-2p}{q} \binom{p}{k-p-q}. \quad (\text{A.17})$$

It is clear from (A.17) that $a_k(m)$ is for fixed $k \geq 0$, the restriction to integers $m \geq \max(1, k)$ of a polynomial in m of degree at most k , as m appears only in the upper index of the binomials and

$$\binom{m}{j} = \frac{m^{\underline{j}}}{j!} = \frac{m(m-1)(m-2) \cdots (m-j+1)}{j!} \quad (\text{A.18})$$

is a polynomial in m of degree j . [Here we use Knuth's [30] notation for falling powers: $x^{\underline{j}} = x(x-1) \cdots (x-j+1)$.]

To see that the degree of $a_k(m)$ is exactly k , let us extract the term of order m^k :

$$[m^k]a_k(m) = \sum_{p=0}^k \frac{(-1)^p 3^{k-p}}{p!(k-p)!} = \frac{2^k}{k!} \neq 0. \quad (\text{A.19})$$

This equation also implies that the coefficient $a_{k,0} = 1$ [cf. (3.30a)] for all $k \geq 0$.

This completes the proof of Proposition 3.5.

Just to be safe, we have checked for $0 \leq k \leq m \leq 30$ that (A.17) agrees with the expansion of (A.12).

B Dimension of the transfer matrices

In this appendix we compute the dimensionalities $N_=(m)$ and $N_\neq(m)$ of the transfer matrices for $=$ and \neq boundary conditions, proving the formulae stated in Theorems 3.6 and 3.7. As a corollary we obtain the dimensionality $\dim \mathbb{T}''(m) = \text{SqFree}(m+2) = N_\neq(m) + N_=(m)$ of the full symmetry-reduced transfer matrix, confirming the formula (2.17) and proving the alternative formulae (3.40a,b,c).

B.1 Catalan, Motzkin and Riordan numbers

The number of non-crossing partitions of $\{1, \dots, m\}$ is given by the Catalan number [66]

$$C_m = \frac{(2m)!}{m!(m+1)!} = \frac{1}{m+1} \binom{2m}{m}. \quad (\text{B.1})$$

The generating function for the Catalan numbers is

$$C(z) = \sum_{m=0}^{\infty} C_m z^m = \frac{1 - \sqrt{1 - 4z}}{2z}. \quad (\text{B.2})$$

The number of non-crossing non-nearest-neighbor partitions of the set $\{1, 2, \dots, m\}$ is given by the Motzkin number M_{m-1} , where [9]³⁰

$$M_m = \sum_{k=0}^{\lfloor m/2 \rfloor} \binom{m}{2k} C_k. \quad (\text{B.3})$$

If we consider the same vertex set *on a circle*, then the number of non-crossing non-nearest-neighbor partitions is given by the numbers [53]

$$d_m = \begin{cases} 1 & \text{for } m = 1 \\ R_m & \text{for } m \geq 2 \end{cases} \quad (\text{B.4})$$

where the R_m are the Riordan numbers (or Motzkin alternating sums) defined by [9]³¹

$$R_m = \begin{cases} 1 & \text{for } m = 0 \\ \sum_{k=1}^{m-1} (-1)^{m-k-1} M_k & \text{for } m \geq 1 \end{cases} \quad (\text{B.5})$$

In the following we will need the linear recursion for the Riordan numbers

$$R_m = -R_{m-1} + M_{m-1} + \delta_{m,0} \quad (\text{B.6})$$

³⁰ *Warning:* Several references use the notation m_n to denote what we call M_n ; and one reference [19] writes M_n to denote a *different* sequence.

³¹Equation (3.59) of [53] erroneously runs the sum down to $k = 0$.

and the generating functions for M_m , R_m and d_m :

$$M(z) = \sum_{m=0}^{\infty} M_m z^m = \frac{1 - z - \sqrt{(1+z)(1-3z)}}{2z^2} \quad (\text{B.7})$$

$$R(z) = \sum_{m=0}^{\infty} R_m z^m = \frac{1 + z - \sqrt{(1+z)(1-3z)}}{2z(1+z)} \quad (\text{B.8})$$

$$D(z) = \sum_{m=1}^{\infty} d_m z^m = R(z) - 1 + z = \frac{1 - z + 2z^3 - \sqrt{(1+z)(1-3z)}}{2z(1+z)} \quad (\text{B.9})$$

The numbers d_m for $1 \leq m \leq 16$ are displayed in Table 14.

B.2 Partitions on a circle modulo reflection

Our goal is to compute the number of equivalence classes modulo reflection of non-crossing non-nearest-neighbor (or “ncnnn” for short) partitions of the set $\{1, 2, \dots, m\}$ on a circle. However, on a circle there are two distinct types of reflection:

- Reflection \mathcal{R}_2 with respect to an axis going halfway between a pair of neighboring sites (which we shall fix to be 1 and m)
- Reflection \mathcal{R}_3 with respect to an axis going through a site (which we shall fix to be the site 1)

Therefore, we define $N_2(m)$ [resp. $N_3(m)$] to be the number of equivalence classes modulo a reflection of type \mathcal{R}_2 (resp. \mathcal{R}_3) of ncnnn partitions of the set $\{1, 2, \dots, m\}$ on a circle. Of course, the two types of reflection coincide when m is odd, so that

$$N_2(2\ell + 1) = N_3(2\ell + 1) \quad \text{for } \ell = 0, 1, 2, \dots \quad (\text{B.10})$$

For m even we have to solve the two problems separately.

The first step is to define

$$X(m) = \begin{array}{l} \text{\#ncnnn partitions of } \{1, \dots, m\} \text{ on a circle} \\ \text{that are invariant under a reflection of type } \mathcal{R}_2. \end{array} \quad (\text{B.11})$$

The values of $X(m)$ for $1 \leq m \leq 16$ are displayed in Table 14. We furthermore denote by $\mathbf{X}(m)$ the set of all \mathcal{R}_2 -invariant ncnnn partitions of $\{1, \dots, m\}$ on a circle. The first sets $\mathbf{X}(m)$ are easy to write down. Using the delta-function shorthand (2.13) for partitions, we find that $\mathbf{X}(m) = \{\mathbf{1}\}$ for $m = 1, 2, 3, 4$, $\mathbf{X}(5) = \{\mathbf{1}, \delta_{24}\}$, $\mathbf{X}(6) = \{\mathbf{1}, \delta_{25}, \delta_{13}\delta_{46}\}$, $\mathbf{X}(7) = \{\mathbf{1}, \delta_{26}, \delta_{35}, \delta_{26}\delta_{35}, \delta_{13}\delta_{57}, \delta_{246}\}$, and $\mathbf{X}(8) = \{\mathbf{1}, \delta_{27}, \delta_{36}, \delta_{27}\delta_{36}, \delta_{13}\delta_{68}, \delta_{14}\delta_{58}, \delta_{24}\delta_{57}\}$.

Because each equivalence class modulo reflection contains either one or two elements, according as those elements are or are not invariant under reflection, we have

$$N_2(m) = \frac{1}{2} [X(m) + d_m] \quad (\text{B.12})$$

It turns out that the numbers $X(m)$ give us not only N_2 but also N_3 :

Lemma B.1 *The number $N_3(m)$ of equivalence classes modulo a reflection of type \mathcal{R}_3 of ncnnn partitions of the set $\{1, 2, \dots, m\}$ on a circle is given by*

$$N_3(m) = \begin{cases} N_2(m) = \frac{1}{2} [X(m) + d_m] & \text{for } m \text{ odd} \\ \frac{1}{2} [X(m+2) + d_m] & \text{for } m \text{ even} \end{cases} \quad (\text{B.13})$$

PROOF. The equality for odd m is trivial from (B.10)/(B.12). For even m we start by defining the quantity

$$Y(m) = 2N_3(m) - d_m, \quad (\text{B.14})$$

which is equal to the number of ncnnn partitions that are invariant under a reflection of type \mathcal{R}_3 . Let us now show that $Y(2\ell) = X(2\ell+2)$ for all $\ell \geq 1$. In this proof we shall denote by $\mathbf{Y}(m)$ the set of all \mathcal{R}_3 -invariant ncnnn partitions of $\{1, \dots, m\}$ on a circle.

The idea is to show that there is a bijection between the set $\mathbf{Y}(2\ell)$ of \mathcal{R}_3 -invariant ncnnn partitions of $\{1, 2, \dots, \ell, \ell+1, \dots, 2\ell\}$ on a circle and the set $\mathbf{X}(2\ell+2)$ of \mathcal{R}_2 -invariant ncnnn partitions of $\{1, 2, \dots, \ell, \ell+1, (\ell+1)', \ell+2, \dots, 2\ell, 1'\}$ on a circle. The trick is to split the vertices 1 and $\ell+1$ into two pairs of nearest-neighbor vertices $1, 1'$ and $\ell+1, (\ell+1)'$, respectively.

This bijection is clear between the subset of $\mathbf{Y}(2\ell)$ with 1 and $\ell+1$ singletons, and the subset of $\mathbf{X}(2\ell+2)$ for which $1, 1', (\ell+1), (\ell+1)'$ are all singletons. Using the delta-function shorthand (2.13), those partitions belonging to the above subsets have exactly the same expression (e.g., for $\ell = 3$, the ncnnn partitions $\delta_{2,6}$ and $\delta_{3,5}$ belong to these subsets).

There is also a bijection between the subset of $\mathbf{Y}(2\ell)$ with $\ell+1$ a singleton and 1 joined to some \mathcal{R}_3 -symmetric block $B \cup B'$ with $B \subseteq \{3, 4, \dots, \ell\}$ and $B' = \mathcal{R}_3 B$, and the subset of $\mathbf{X}(2\ell+2)$ with both $(\ell+1)$ and $(\ell+1)'$ singletons, and the sites 1 and $1'$ joined to the blocks B and B' , respectively. This property is due to the facts that 1 and $1'$ [resp. $\ell+1$ and $(\ell+1)'$] are nearest-neighbor vertices, and the partitions are non-crossing. For instance, if $\ell = 3$, the partition $\delta_{1,3,5}$ in $\mathbf{Y}(6)$ corresponds uniquely to the partition $\delta_{1,3}\delta_{1',5}$ in $\mathbf{X}(8)$, and vice versa. A similar bijection can be shown when 1 is a singleton, but $\ell+1$ is joined to some \mathcal{R}_3 -symmetric block.

Finally, there is a bijection between the subset of $\mathbf{Y}(2\ell)$ with both 1 and $\ell+1$ joined to some \mathcal{R}_3 -symmetric blocks $B_1 \cup B'_1$ and $B_2 \cup B'_2$ (that might be the same), and the subset of $\mathbf{X}(2\ell+2)$ characterized by the blocks $\{1\} \cup B_1$, $\{1'\} \cup B'_1$, $\{\ell+1\} \cup B_2$, and $\{(\ell+1)'\} \cup B'_2$. (If 1 and $\ell+1$ belong to the same block, the modifications are obvious.)

As the above subsets are non-intersecting and contain all partitions of both $\mathbf{Y}(2\ell)$ and $\mathbf{X}(2\ell+2)$, we conclude that such bijection exists, and therefore, that $Y(2\ell) = X(2\ell+2)$, as claimed. \square

Henceforth we consider only reflections of type \mathcal{R}_2 . Our goal is to obtain a closed formula for the quantity $X(m)$. Our results can be summarized in the following proposition:

Proposition B.2 *The quantity $X(m)$ is given by*

$$X(m) = \begin{cases} 1 & \text{if } m = 1 \\ \sum_{k \geq 0} \binom{\lfloor \frac{m-1}{2} \rfloor}{k} \binom{\lfloor \frac{m-1}{2} \rfloor - k}{k + I[m \text{ is odd}]} & \text{if } m \geq 2 \end{cases} \quad (\text{B.15})$$

The generating function for this sequence is

$$G(z) = \sum_{m=1}^{\infty} X(m)z^m = \frac{1}{2z} \left[\frac{2z^3 - z^2 + 1}{\sqrt{(1+z^2)(1-3z^2)}} + 2z^2 - 1 \right]. \quad (\text{B.16})$$

In what follows, it is convenient to change the notation for the vertices: When $m = 2\ell$ is even, we renumber the vertices $1, \dots, \ell, \ell+1, \dots, 2\ell$ as $1, \dots, \ell, \ell', \dots, 1'$, so that the vertices j and j' ($1 \leq j \leq \ell$) are transformed into each other under a reflection \mathcal{R}_2 . When $m = 2\ell + 1$ is odd, we renumber the vertices $1, \dots, \ell, \ell+1, \ell+2, \dots, 2\ell+1$ as $1, \dots, \ell, \ell+1, \ell', \dots, 1'$, so that the vertices j and j' ($1 \leq j \leq \ell$) are again related by reflection, while the vertex $\ell+1$ is invariant under reflection. See Figure 18 for a few examples.

PROOF OF PROPOSITION B.2. The idea is to obtain a recursion for the $X(m)$, and then solve this recursion. First, we want to obtain $X(2m+1)$ from $X(2m)$. We use the notation $i \leftrightarrow j$ to denote that i and j belong to the same block of the partition being discussed. We observe that for a partition in $\mathbf{X}(2m)$, we have $1 \leftrightarrow m$ if and only if $1' \leftrightarrow m'$ (since the partition is \mathcal{R}_2 -invariant). We then split the set $\mathbf{X}(2m)$ into three subsets, as follows:

- a) $\mathbf{X}_a(2m)$ is the set of partitions in $\mathbf{X}(2m)$ such that there is no block containing both unprimed and primed vertices and such that $1 \not\leftrightarrow m$;
- b) $\mathbf{X}_b(2m)$ is the set of partitions in $\mathbf{X}(2m)$ such that there is no block containing both unprimed and primed vertices and such that $1 \leftrightarrow m$;
- c) $\mathbf{X}_c(2m)$ is the set of partitions in $\mathbf{X}(2m)$ such that there is at least one block containing both unprimed and primed vertices. [Note that any such block B is necessarily \mathcal{R}_2 -invariant, for otherwise B would cross $\mathcal{R}_2 B$.]

We denote by $X_a(2m)$, $X_b(2m)$ and $X_c(2m)$ the number of elements within the corresponding subset. For instance, for $\mathbf{X}(8)$ we have the decomposition $\mathbf{X}_a(8) = \{1, \delta_{13}\delta_{1'3'}, \delta_{24}\delta_{2'4'}\}$, $\mathbf{X}_b(8) = \{\delta_{14}, \delta_{1'4'}\}$ and $\mathbf{X}_c(8) = \{\delta_{22'}, \delta_{33'}, \delta_{22'}\delta_{33'}\}$.

Let us suppose that $m \geq 3$. Going from $\mathbf{X}(2m)$ to $\mathbf{X}(2m+1)$ means that we have to add a new vertex labeled $m+1$ between m and m' . Indeed, if $\mathcal{P} \in \mathbf{X}(2m)$, then it also belongs to $\mathbf{X}(2m+1)$ [with the new vertex $m+1$ becoming a singleton]. Furthermore, to any partition $\mathcal{P} \in \mathbf{X}_a(2m) \cup \mathbf{X}_c(2m)$ we can adjoin a factor $\delta_{mm'}$ [i.e. contract the blocks containing m and m' into a single block] and get a partition in $\mathbf{X}(2m+1)$ [with the new vertex $m+1$ again becoming a singleton]; please note that this is not possible if $\mathcal{P} \in \mathbf{X}_b(2m)$ since the new partition would include a nearest-neighbor connection $1 \leftrightarrow 1'$. Finally, if $\mathcal{P} \in \mathbf{X}_c(2m)$, we can generate a new partition in $\mathbf{X}(2m+1)$ by joining the new vertex $m+1$ to the closest block containing both primed and unprimed vertices. It is not hard to see that in this way we generate *all* the elements of $\mathbf{X}(2m+1)$, and that we generate each one exactly once; therefore,

$$X(2m+1) = X(2m) + X_a(2m) + 2X_c(2m). \quad (\text{B.17})$$

Now, $X_a(2m) + X_b(2m)$ is just the total number of partitions in $\mathbf{X}(2m)$ with no block containing both unprimed and primed vertices. But this number is obviously equal to the number of ncnnn partitions of the set $\{1, 2, \dots, m\}$ with free boundary conditions, i.e. the Motzkin number M_{m-1} :

$$X_a(2m) + X_b(2m) = M_{m-1} . \quad (\text{B.18})$$

On the other hand, $X_b(2m)$ can be interpreted as the number of ncnnn partitions of $\{1, 2, \dots, m\}$ with free boundary conditions, such that m and 1 always belong to the same block. But this is equivalent to the number of ncnnn partitions of $\{1, 2, \dots, m-1\}$ on a circle, so we have

$$X_b(2m) = d_{m-1} = R_{m-1} \quad (\text{B.19})$$

since $m \geq 3$. Putting everything together we obtain the recursion

$$X(2m+1) = 3X(2m) - (M_{m-1} + R_{m-1}) \quad \text{for } m \geq 3 \quad (\text{B.20})$$

together with the initial conditions $X(1) = 1$, $X(3) = 1$, $X(5) = 2$. It is interesting to note that the same recursion holds also for $m = 1, 2$, as can be checked from Tables 14 and 1. Thus, our final result is

$$X(2m+1) = 3X(2m) - (M_{m-1} + R_{m-1}) \quad \text{for } m \geq 1 \quad (\text{B.21})$$

with the initial condition $X(1) = 1$.

The second half of the recursion can be obtained by considering how to obtain the partitions in $\mathbf{X}(2m+2)$ by starting from those in $\mathbf{X}(2m+1)$. In this case, the vertex $m+1$ is split into a pair of nearest-neighbors $m+1$ and $(m+1)'$. Let us assume that $m \geq 2$.

Consider a partition $\mathcal{P} \in \mathbf{X}(2m+1)$ in which the block containing the vertex $m+1$ is $\{m+1\} \cup B \cup B'$, where B contains only unprimed vertices and $B' = \mathcal{R}_2 B$ contains only primed vertices (note that B could be the empty set). We can then create a partition $\tilde{\mathcal{P}} \in \mathbf{X}(2m+2)$ by creating blocks $\{m+1\} \cup B$ and $\{(m+1)'\} \cup B'$ and leaving all other blocks of \mathcal{P} as is. The partition $\tilde{\mathcal{P}}$ has the property that, if one contracts the blocks containing $m+1$ and $(m+1)'$ into a single block, one obtains \mathcal{P} ; moreover, $\tilde{\mathcal{P}}$ is the *unique* partition in $\mathbf{X}(2m+2)$ with this property (it is not hard to see that all other \mathcal{R}_2 -invariant partitions with this property would contain either a nearest-neighbor connection or a crossing). Moreover, every partition in $\mathbf{X}(2m+2)$ is obtained in this way *except* those in which $1 \leftrightarrow m+1$ [and hence also $1' \leftrightarrow (m+1)'$]; these latter partitions cannot be obtained because contracting $m+1$ to $(m+1)'$ would create a nearest-neighbor connection $1 \leftrightarrow 1'$. Now, the number of these extra partitions is equal to the number of ncnnn partitions of $\{1, 2, \dots, m\}$ on a circle, which is d_m ; and since $m \geq 2$, this also equals R_m [cf. (B.4)]. We therefore conclude that

$$X(2m+2) = X(2m+1) + R_m \quad \text{for } m \geq 2 \quad (\text{B.22})$$

together with the initial conditions $X(2) = X(4) = 1$. It is interesting to note that the same recursion holds also for $m = 1$, as can be checked from Table 14. Thus, our final result is

$$X(2m+2) = X(2m+1) + R_m \quad \text{for } m \geq 1 \quad (\text{B.23})$$

with the initial condition $X(2) = 1$.

By combining (B.21)/(B.23) and (B.6), we can obtain the following recurrences for $X(m)$:

$$X(2m) = 3X(2m-2) - 2R_{m-2} \quad \text{for } m \geq 2 \quad (\text{B.24a})$$

$$X(2m+1) = 3X(2m-1) - R_m + R_{m-1} \quad \text{for } m \geq 2 \quad (\text{B.24b})$$

with the initial conditions $X(m) = 1$ for $m = 1, 2, 3$.

A solution of (B.24a) can be obtained by defining $\bar{X}(m) = X(2m+2)$ for $m \geq 0$. The recurrence (B.24a) can then be written in terms of the \bar{X} as

$$\bar{X}(m) = 3\bar{X}(m-1) - 2R_{m-1} \quad \text{for } m \geq 1 \quad (\text{B.25})$$

with the initial condition $\bar{X}(0) = 1$. From this equation we obtain the corresponding generating function

$$\bar{G}(z) = \sum_{k=0}^{\infty} \bar{X}(k) z^k = \frac{1 - 2zR(z)}{1 - 3z} = \frac{1}{\sqrt{(1+z)(1-3z)}}, \quad (\text{B.26})$$

where $R(z)$ is the generating function (B.8) for the Riordan numbers.

Let us now observe that (B.26) coincides with the generating function of the central trinomial coefficients [16, p. 163] [61, sequence A002426], so we have

$$\bar{X}(m) = [t^m](1+t+t^2)^m \quad \text{for } m \geq 0. \quad (\text{B.27})$$

By a double application of the binomial theorem we arrive at the expressions

$$\bar{X}(m) = \sum_{k=0}^m \binom{m}{k} \binom{m-k}{k} \quad \text{for } m \geq 0. \quad (\text{B.28})$$

Note that many terms on the right-hand side of (B.28) vanish, as $\binom{m-k}{k} = 0$ whenever $k > m/2$. In order to lighten the notation, we will use the generic summation over nonnegative k , and only at the end we will make the upper bound explicit.

The formula for $X(2m)$ and its generating function $G_2(z)$ can be obtained from (B.28)/(B.26):

$$X(2m) = \sum_{k \geq 0} \binom{m-1}{k} \binom{m-1-k}{k} \quad (\text{B.29a})$$

$$G_2(z) = \sum_{m=1}^{\infty} X(2m) z^{2m} = z^2 \bar{G}(z^2) = \frac{z^2}{\sqrt{(1+z^2)(1-3z^2)}} \quad (\text{B.29b})$$

A solution of (B.24b) can be obtained in a similar way by defining $\hat{X}(m) = X(2m+1)$ for $m \geq 1$ (we will treat $X(1) = 1$ separately). The recursion (B.24b) can then be written as

$$\hat{X}(m) = 3\hat{X}(m-1) - R_m + R_{m-1} \quad \text{for } m \geq 2 \quad (\text{B.30})$$

with the initial condition $\widehat{X}(1) = 1$. From this equation we obtain the corresponding generating function

$$\begin{aligned}\widehat{G}(z) &= \sum_{k=1}^{\infty} \widehat{X}(m) z^m = \frac{R(z)(z-1) + 1}{1-3z} \\ &= \frac{2z}{(1+z)(1-3z) + (1-z)\sqrt{(1+z)(1-3z)}} .\end{aligned}\quad (\text{B.31})$$

We now observe that (B.31) coincides with the generating function of the next-to-central trinomial coefficients [61, sequence A005717], so we have

$$\widehat{X}(m) = [t^{m+1}](1+t+t^2)^m = [t^{m-1}](1+t+t^2)^m \quad \text{for } m \geq 1 . \quad (\text{B.32})$$

By a double application of the binomial theorem we arrive at the expressions

$$\widehat{X}(m) = \sum_{k=0}^m \binom{m}{k} \binom{m-k}{k+1} = \sum_{k=0}^m \binom{m}{k} \binom{m-k}{k-1} \quad \text{for } m \geq 1 . \quad (\text{B.33})$$

The formula for $X(2m+1)$ and its generating function $G_1(z)$ can be obtained from (B.33)/(B.31):

$$X(2m+1) = \begin{cases} 1 & \text{for } m = 0 \\ \sum_{k \geq 0} \binom{m}{k} \binom{m-k}{k+1} & \text{for } m \geq 1 \end{cases} \quad (\text{B.34a})$$

$$\begin{aligned}G_1(z) &= \sum_{m=0}^{\infty} X(2m+1) z^{2m+1} = z + z\widehat{G}(z^2) \\ &= z + \frac{2z^3}{(1+z^2)(1-3z^2) + (1-z^2)\sqrt{(1+z^2)(1-3z^2)}}\end{aligned}\quad (\text{B.34b})$$

From (B.29a)/(B.34a) it is easy to obtain (B.15). From (B.29b)/(B.34b) it is easy to obtain the formula (B.16) for the generating function $G(z) = G_1(z) + G_2(z)$. \square

By Proposition B.2 together with (B.12)/(B.13), it is easy to compute closed expressions for $N_2(m)$ and $N_3(m)$ as well as for their generating functions. We have

$$N_2(m) = \begin{cases} 1 & \text{for } m = 1 \\ \frac{1}{2}R_m + \frac{1}{2} \sum_{k \geq 0} \binom{\lfloor \frac{m-1}{2} \rfloor}{k} \binom{\lfloor \frac{m-1}{2} \rfloor - k}{k + I[m \text{ is odd}]} & \text{for } m \geq 2 \end{cases} \quad (\text{B.35})$$

and

$$N_3(m) = \begin{cases} 1 & \text{for } m = 1 \\ \frac{1}{2}R_m + \frac{1}{2} \sum_{k \geq 0} \binom{\lfloor \frac{m}{2} \rfloor}{k} \binom{\lfloor \frac{m}{2} \rfloor - k}{k + I[m \text{ is odd}]} & \text{for } m \geq 2 \end{cases} \quad (\text{B.36})$$

The corresponding generating functions are

$$\begin{aligned}
F_2(z) &= \sum_{m=1}^{\infty} N_2(m) z^m = \frac{1}{2} [G(z) + D(z)] \\
&= \frac{1}{4z} \left[\frac{2z^3 - z^2 + 1}{\sqrt{(1+z^2)(1-3z^2)}} - \sqrt{\frac{1-3z}{1+z}} + 2z(2z-1) \right]
\end{aligned} \tag{B.37}$$

$$\begin{aligned}
F_3(z) &= \sum_{m=1}^{\infty} N_3(m) z^m = \frac{1}{2} \left[G_1(z) + \frac{G_2(z)}{z^2} - 1 + D(z) \right] \\
&= z - 1 - \frac{1}{4z} \sqrt{\frac{1-3z}{1+z}} + \frac{1+2z-z^2}{4z\sqrt{(1+z^2)(1-3z^2)}}
\end{aligned} \tag{B.38}$$

Note that

$$F_3(z) - F_2(z) = z^2 \widehat{G}(z^2), \tag{B.39}$$

so that

$$N_3(2\ell+2) - N_2(2\ell+2) = [t^{\ell-1}](1+t+t^2)^\ell \quad \text{for } \ell \geq 0. \tag{B.40}$$

B.3 The dimensions $N_{\neq}(m)$ and $N_{=}(m)$

We can now prove the theorems stated in Section 3.3.

PROOF OF THEOREMS 3.6 AND 3.7. As explained in Section 3.3, we have

$$N_{=}(m) = N_3(m+1) \tag{B.41a}$$

$$N_{\neq}(m) = N_2(m+2) \tag{B.41b}$$

The formulae (3.34)/(3.37) for $N_{=}(m)$ and $N_{\neq}(m)$ then follow trivially from the formulae (B.35)/(B.36) for $N_2(m)$ and $N_3(m)$. The results for the generating functions follow likewise from the identities

$$G_{=}(z) = \frac{1}{z} [F_3(z) - z] \tag{B.42a}$$

$$G_{\neq}(z) = \frac{1}{z^2} [F_2(z) - z - z^2] \tag{B.42b}$$

□

Remark. We see from (B.10) and (B.41) that

$$N_{\neq}(m) = N_{=}(m+1) \quad \text{for } m \text{ odd} \tag{B.43}$$

(cf. Table 1).

PROOF OF COROLLARY 3.8. From Theorems 3.6 and 3.7 we have

$$\begin{aligned}
\dim \mathbb{T}''(m) &= N_=(m) + N_{\neq}(m) \\
&= \frac{1}{2}(R_{m+1} + R_{m+2}) + \frac{1}{2} \sum_{k \geq 0} \binom{m'}{k} \left\{ \binom{m'-k}{k+1} + \binom{m'-k}{k} \right\} \\
&= \frac{1}{2} M_{m+1} + \frac{1}{2} \sum_{k \geq 0} \binom{m'}{k} \binom{m'-k+1}{k+1}
\end{aligned} \tag{B.44}$$

where we have used the relation (B.6) and the elementary recursion relation for the binomials; this proves (3.40a).

To prove (3.40b), we start from (B.33) and add $\binom{m}{k} \binom{m-k}{k}$ to the summand on both sides; using the elementary recursion for binomials, we get

$$\sum_{k \geq 0} \binom{m}{k} \binom{m-k+1}{k+1} = \sum_{k \geq 0} \binom{m}{k} \binom{m-k+1}{k}. \tag{B.45}$$

Applying this with m replaced by m' shows the equivalence of (3.40b) with (3.40a).

Finally, by adding (3.40a) and (3.40b), dividing by 2, and using once again the recursion relation for binomials, we prove (3.40c). \square

PROOF OF (2.17). We replace $m+2$ by m in (3.40b), which entails replacing m' by $m'-1$. Expanding the binomials into factorials yields (2.17). \square

C Chromatic polynomials for the family $\widehat{S}_{m,n}$

We denote by $\widehat{S}_{m,n}$ the graph obtained from the square-lattice strip of width m , length n and free boundary conditions in both directions by attaching one extra site to all the sites on the *top* row and another extra site to all the sites on the *bottom* row (see Figure 8). This graph is obviously isomorphic to the graph $S_{n,m}$; we have merely rotated the picture by 90 degrees. In particular, the chromatic polynomials of $\widehat{S}_{m,n}$ and $S_{n,m}$ must coincide, i.e.

$$P_{\widehat{S}_{m,n}}(q) = P_{S_{n,m}}(q), \tag{C.1}$$

and we can use this as a check on the correctness of our computations.

Here we shall develop the transfer-matrix formalism for the family $\widehat{S}_{m,n}$, where m is fixed (and small) and n is arbitrary; this is complementary to the formalism developed in Section 3, which treats $S_{n,m}$ for n fixed (and small) and m arbitrary.

The graph $\widehat{S}_{1,n}$ is simply the path P_{n+2} , so its chromatic polynomial is

$$P_{\widehat{S}_{1,n}}(q) = P_{P_{n+2}}(q) = q(q-1)^{n+1}. \tag{C.2}$$

The chromatic polynomial of the graph $\widehat{S}_{2,n}$ can be computed by noting that this graph is obtained by gluing together $n - 1$ squares C_4 and two triangles C_3 along edges. Its chromatic polynomial is therefore

$$P_{\widehat{S}_{2,n}}(q) = \frac{P_{C_4}(q)^{n-1} P_{C_3}(q)^2}{[q(q-1)]^n} = q(q-1)(q-2)^2(q^2-3q+3)^{n-1}. \quad (\text{C.3})$$

To handle the graphs $\widehat{S}_{m,n}$ with $m \geq 3$ we need a different technique. The idea is to use the standard transfer matrices $\mathsf{T}''(m_{\text{F}})$ for square-lattice strips with free boundary conditions³² but with different initial and final vectors to take account of the extra sites attached to the top and bottom rows. More specifically, we have

$$P_{\widehat{S}_{m,n}} = \boldsymbol{\omega}_+^{\text{T}} \mathsf{T}''(m_{\text{F}})^{n-1} \mathbf{f}_+, \quad (\text{C.4})$$

where the initial vector \mathbf{f}_+ is given by

$$\mathbf{f}_+ = \mathsf{H} \mathsf{V} \mathbf{e}_{\text{contr}} \quad (\text{C.5})$$

where $\mathbf{e}_{\text{contr}}$ is the basis vector for the partition with all sites in the same block, while the final vector $\boldsymbol{\omega}_+$ is defined by [compare to (2.11)]

$$\boldsymbol{\omega}_+^{\text{T}} \mathbf{e}_{\mathcal{P}} = q(q-1)^{|\mathcal{P}|}. \quad (\text{C.6})$$

The reason for this last formula is clear: the factor q comes from the extra vertex on top, and we obtain a factor of $q-1$ for each block of the partition \mathcal{P} (instead of a factor of q) because each site on the top row is attached to the extra site, so that there are only $q-1$ allowed colors for those sites (rather than q).

For instance, for $m = 3$ the chromatic polynomial of the graph $\widehat{S}_{3,n}$ is given in the basis $\mathbf{B} = \{\mathbf{1}, \delta_{13}\}$ by³³

$$P_{\widehat{S}_{3,n}} = q(q-1)(q-2) \begin{pmatrix} q-2 \\ 1 \end{pmatrix}^{\text{T}} \cdot \mathsf{T}''(3_{\text{F}})^{n-1} \cdot \begin{pmatrix} q-3 \\ q \end{pmatrix} \quad (\text{C.7})$$

with

$$\mathsf{T}''(3_{\text{F}}) = \begin{pmatrix} q^3 - 5q^2 + 10q - 8 & q^2 - 4q + 5 \\ 1 & q - 2 \end{pmatrix}. \quad (\text{C.8})$$

For $m = 4$, the corresponding chromatic polynomial is given in the basis $\mathbf{B} = \{\mathbf{1}, \delta_{13} + \delta_{24}, \delta_{14}\}$ by

$$P_{\widehat{S}_{4,n}} = q(q-1)(q-2) \begin{pmatrix} (q-2)^2 \\ 2(q-2) \\ q-3 \end{pmatrix}^{\text{T}} \cdot \mathsf{T}''(4_{\text{F}})^{n-1} \cdot \begin{pmatrix} q-4 \\ 1 \\ 1 \end{pmatrix} \quad (\text{C.9})$$

³²See Section 2.2 above, and see [53] for more details. Since $v = -1$, the horizontal transfer matrix H is a projection, so we can use the modified transfer matrix $\mathsf{T}' = \mathsf{H} \mathsf{V} \mathsf{H}$ and the modified basis vectors $\mathbf{f}_{\mathcal{P}} = \mathsf{H} \mathbf{e}_{\mathcal{P}}$. Moreover, since the graphs $\widehat{S}_{m,n}$ are invariant under reflection in the central vertical axis, we can use the symmetry-reduced transfer matrix T'' . These transfer matrices are precisely the ones that can be found in [53, Section 5] (but denoted there T rather than T'').

³³Please recall from Section 6 that we are using a shorthand notation for basis elements: we write the basis as a collection of vectors $\mathbf{e}_{\mathcal{P}}$, but it should be understood that the basis vectors are actually $\mathbf{f}_{\mathcal{P}} = \mathsf{H} \mathbf{e}_{\mathcal{P}}$. This convention applies throughout this Appendix.

with

$$\mathsf{T}''(4_{\text{F}}) = \begin{pmatrix} q^4 - 7q^3 + 21q^2 - 32q + 21 & 2(q^3 - 6q^2 + 14q - 12) & q^3 - 7q^2 + 19q - 20 \\ q - 2 & q^2 - 4q + 5 & 3 - q \\ -1 & -2(q - 2) & q^2 - 5q + 7 \end{pmatrix}. \quad (\text{C.10})$$

We have performed the corresponding computation also for widths $m = 5$ and 6 , and we have checked that the identity (C.1) holds for $1 \leq m \leq 6$ and $1 \leq n \leq 8$.

We can alternatively obtain the chromatic polynomial of the strip graph $\widehat{S}_{m,n}$ by using a different technique, which is useful when dealing with more complicated endgraphs. Our starting graph consists of a strip together with attached endgraphs at top and bottom; each of these endgraphs consists of one or more extra vertices and several extra edges. The idea is to use the deletion-contraction identity on the extra edges of the endgraphs to get rid of the extra vertices. At the end, the chromatic polynomial $P_{\widehat{S}_{m,n}}$ can be written as a linear combination of chromatic polynomials $P_{S_{m,n,j}}$ associated to different strip graphs $S_{m,n,j}$, each of which is obtained from the $m_{\text{F}} \times n_{\text{F}}$ grid by adding only extra *edges* to the top and/or bottom rows. (This approach is closely related to a method developed by Roček, Shrock and Tsai [52].) These extra edges can be handled by inserting the appropriate operators $\mathbf{Q}_{ij} = I + v_{ij}\mathbf{J}_{ij}$ at left and/or right in the standard expression (2.10) for the chromatic polynomial in terms of transfer matrices. There is, however, one complication: for $m \geq 4$, these extra edges can give rise to *crossing* partitions (for instance, if in a grid of width $m = 4$ we add an extra edge 13 on the bottom row *and* an extra edge 24 on the top row).³⁴ We must therefore work in a basis that includes also (non-nearest-neighbor) *crossing* partitions.

For $m = 3$ we have

$$P_{\widehat{S}_{3,n}}(q) = (q - 2)^2 P_{3_{\text{F}} \times n_{\text{F}}}(q) - 2(q - 2) P_{S_{3,n,a}}(q) + P_{S_{3,n,b}}(q) \quad (\text{C.11})$$

where $3_{\text{F}} \times n_{\text{F}}$ is a square-lattice strip of width $m = 3$, length n and free boundary conditions; $S_{3,n,a}$ is the chromatic polynomial of the graph obtained by adding to $3_{\text{F}} \times n_{\text{F}}$ an extra edge joining the sites 1 and 3 on the bottom row; and $S_{3,n,b}$ is the graph obtained by adding to $S_{3,n,a}$ one further edge joining sites 1 and 3 on the top row. The chromatic polynomials of these three graphs can then be obtained by a transfer-matrix formalism. For the graph $3_{\text{F}} \times n_{\text{F}}$, we can use the standard method discussed in Section 2.2. For the other two graphs, we obtain the corresponding chromatic polynomial by inserting the operators \mathbf{Q}_{13} appropriately. Thus, the chromatic polynomial for $\widehat{S}_{3,n}$ can be written as

$$\begin{aligned} P_{\widehat{S}_{3,n}}(q) &= (q - 2)^2 P_{3_{\text{F}} \times n_{\text{F}}}(q) - 2(q - 2) \boldsymbol{\omega}^{\text{T}} \cdot \mathsf{T}''(3_{\text{F}})^{n-1} \cdot \mathbf{Q}_{13} \cdot \mathbf{f}_{\text{id}} \\ &\quad + \boldsymbol{\omega}^{\text{T}} \cdot \mathbf{Q}_{13} \cdot \mathsf{T}''(3_{\text{F}})^{n-1} \cdot \mathbf{Q}_{13} \cdot \mathbf{f}_{\text{id}} \end{aligned} \quad (\text{C.12})$$

³⁴Notice that this can happen even though the graph with the extra edges is planar (as it is in the just-mentioned example). To avoid crossing partitions we need to be able to draw the graph in a planar fashion *within the $m \times n$ box*.

where $\mathsf{T}''(3_F)$ is given by (C.8). After some algebra we find

$$P_{\widehat{S}_{3,n}}(q) = q(q-1)(q-2) \left\{ (q-2) \begin{pmatrix} q-1 \\ 1 \end{pmatrix}^T \cdot \mathsf{T}''(3_F)^{n-1} \cdot \begin{pmatrix} 1 \\ 0 \end{pmatrix} + \begin{pmatrix} 3-2q \\ -2 \end{pmatrix}^T \cdot \mathsf{T}''(3_F)^{n-1} \cdot \begin{pmatrix} 1 \\ -1 \end{pmatrix} \right\}. \quad (\text{C.13})$$

For $m = 4$ the situation is similar but more involved algebraically. We shall work in the basis $\mathbf{B} = \{\mathbf{1}, \delta_{13} + \delta_{24}, \delta_{14}, \delta_{13}\delta_{24}\}$, where the last basis element corresponds to the crossing partition. After application of the deletion-contraction identity, and some algebra, we find

$$\begin{aligned} P_{\widehat{S}_{4,n}}(q) &= (q-2)^2 P_{4_F \times n_F}(q) - 2(q-1) \boldsymbol{\omega}^T \widetilde{\mathsf{T}}''(4_F)^{n-1} \mathbf{Q}_{14} \mathbf{f}_{\text{id}} \\ &\quad - 2(q-1) \boldsymbol{\omega}^T \widetilde{\mathsf{T}}''(4_F)^{n-1} (\mathbf{Q}_{13} + \mathbf{Q}_{24}) \mathbf{f}_{\text{id}} + \boldsymbol{\omega}^T \mathbf{Q}_{14} \widetilde{\mathsf{T}}''(4_F)^{n-1} \mathbf{Q}_{14} \mathbf{f}_{\text{id}} \\ &\quad + 2\boldsymbol{\omega}^T \mathbf{Q}_{14} \widetilde{\mathsf{T}}''(4_F)^{n-1} (\mathbf{Q}_{13} + \mathbf{Q}_{24}) \mathbf{f}_{\text{id}} \\ &\quad + \boldsymbol{\omega}^T (\mathbf{Q}_{13} + \mathbf{Q}_{24}) \widetilde{\mathsf{T}}''(4_F)^{n-1} (\mathbf{Q}_{13} + \mathbf{Q}_{24}) \mathbf{f}_{\text{id}} \end{aligned} \quad (\text{C.14})$$

with the transfer matrix

$$\widetilde{\mathsf{T}}''(4_F) = \left(\begin{array}{ccc|c} & & & q^2 - 5q + 8 \\ & \mathsf{T}''(4_F) & & q - 3 \\ & & & -1 \\ \hline 0 & 0 & 0 & 1 \end{array} \right) \quad (\text{C.15})$$

where the upper-left 3×3 submatrix is given by (C.10). Notice that we have symmetrized the operators \mathbf{Q}_{13} and \mathbf{Q}_{24} in order to use the symmetrized connectivity basis \mathbf{B} as above (i.e., classes of non-nearest-neighbor connectivities that are invariant under reflections with respect to the center of the strip). The definition (2.11) of the left vector $\boldsymbol{\omega}$ continues to be valid even in the presence of crossing partitions. After some algebra we find

$$\begin{aligned} P_{\widehat{S}_{4,n}}(q) &= q(q-1) \left\{ (q-1) \begin{pmatrix} (q-1)^2 \\ 2(q-1) \\ q-2 \\ 1 \end{pmatrix}^T \cdot \widetilde{\mathsf{T}}''(4_F)^{n-1} \cdot \begin{pmatrix} q-7 \\ 2 \\ 2 \\ 0 \end{pmatrix} \right. \\ &\quad + \begin{pmatrix} q^2 - 3q + 3 \\ 2(q-1) \\ 0 \\ 1 \end{pmatrix}^T \cdot \widetilde{\mathsf{T}}''(4_F)^{n-1} \cdot \begin{pmatrix} 5 \\ -2 \\ -1 \\ 0 \end{pmatrix} \\ &\quad \left. + 2(q-2) \begin{pmatrix} q-1 \\ 1 \\ 1 \\ 0 \end{pmatrix}^T \cdot \widetilde{\mathsf{T}}''(4_F)^{n-1} \cdot \begin{pmatrix} 2 \\ -1 \\ 0 \\ 0 \end{pmatrix} \right\}. \end{aligned} \quad (\text{C.16})$$

Note that in this final expression the crossing partitions play no role, because all three right vectors have zero in the last entry, and the transfer matrix (C.15) has zeros in

the last row in all columns other than the last. So we could have restricted attention to non-crossing partitions, after all! We suspect that a cancellation of this type occurs whenever the graph is planar, and that a transfer-matrix description using only non-crossing partitions can be obtained by adding extra layers at top and bottom together with suitable $v = \infty$ vertical and/or horizontal edges.

With this method we have checked the identity (C.1) for $1 \leq m \leq 4$ and $1 \leq n \leq 8$.

References

- [1] A.V. Bakaev and V.I. Kabanovich, Series expansions for the q -colour problem on the square and cubic lattices, *J. Phys. A: Math. Gen.* **27**, 6731–6739 (1994).
- [2] R.J. Baxter, q colourings of the triangular lattice, *J. Phys. A: Math. Gen.* **19**, 2821–2839 (1986).
- [3] R.J. Baxter, Chromatic polynomials of large triangular lattices, *J. Phys. A: Math. Gen.* **20**, 5241–5261 (1987).
- [4] R.J. Baxter, S.B. Kelland and F.Y. Wu, Equivalence of the Potts model or Whitney polynomial with an ice-type model, *J. Phys. A: Math. Gen.* **9**, 397–406 (1976).
- [5] S. Beraha and J. Kahane, Is the four-color conjecture almost false?, *J. Combin. Theory B* **27**, 1–12 (1979).
- [6] S. Beraha, J. Kahane and N.J. Weiss, Limits of zeroes of recursively defined polynomials, *Proc. Nat. Acad. Sci. USA* **72**, 4209 (1975).
- [7] S. Beraha, J. Kahane and N.J. Weiss, Limits of zeroes of recursively defined families of polynomials, in *Studies in Foundations and Combinatorics* (Advances in Mathematics Supplementary Studies, Vol. 1), ed. G.-C. Rota, pp. 213–232 (Academic Press, New York, 1978).
- [8] S. Beraha, J. Kahane and N.J. Weiss, Limits of chromatic zeros of some families of maps, *J. Combin. Theory B* **28**, 52–65 (1980).
- [9] F.R. Bernhart, Catalan, Motzkin, and Riordan numbers, *Discrete Math.* **204**, 73–112 (1999).
- [10] G.D. Birkhoff, A determinant formula for the number of ways of coloring a map, *Ann. Math.* **14**, 42–46 (1912).
- [11] H.W.J. Blöte and M.P. Nightingale, Critical behaviour of the two-dimensional Potts model with a continuous number of states: A finite size scaling analysis, *Physica A* **112**, 405–465 (1982).
- [12] J.I. Brown, C.A. Hickman, A.D. Sokal and D.G. Wagner, On the chromatic roots of generalized theta graphs, *J. Combin. Theory B* **83**, 272–297 (2001), math.CO/0012033 at arXiv.org.

- [13] S.-C. Chang, J. Salas and R. Shrock, Exact Potts model partition functions for strips of the square lattice, *J. Stat. Phys.* **107**, 1207–1253 (2002), cond-mat/0108144 at arXiv.org.
- [14] S.-C. Chang and R. Shrock, Exact Potts model partition function on strips of the triangular lattice, *Physica A* **286**, 189–238 (2000), cond-mat/0004181 at arXiv.org.
- [15] S.-C. Chang and R. Shrock, Exact Potts model partition functions on wider arbitrary-length strips of the square lattice, *Physica A* **296**, 234–288 (2001), cond-mat/0011503 at arXiv.org.
- [16] L. Comtet, *Advanced Combinatorics* (D. Reidel, Dordrecht, 1974).
- [17] R.M. Corless, G.H. Gonnet, D.E.G. Hare, D.J. Jeffrey and D.E. Knuth, On the Lambert W function, *Adv. Comput. Math.* **5**, 329–359 (1996).
- [18] N.G. De Bruijn, *Asymptotic Methods in Analysis*, 2nd ed. (North-Holland, Amsterdam, 1961).
- [19] R. Donaghey and L.W. Shapiro, Motzkin numbers, *J. Combin. Theory A* **23**, 291–301 (1977).
- [20] J. Dubail, J.L. Jacobsen, and H. Saleur, Conformal two-boundary loop model on the annulus, *Nucl. Phys. B* **813**, 430–459 (2009), arXiv:0812:2746 at arXiv.org.
- [21] R.G. Edwards and A.D. Sokal, Generalization of the Fortuin-Kasteleyn-Swendsen-Wang representation and Monte Carlo algorithm, *Phys. Rev. D* **38**, 2009–2012 (1988).
- [22] I.G. Enting, Generalised Möbius functions for rectangles on the square lattice, *J. Phys. A: Math. Gen.* **11**, 563–568 (1978).
- [23] I.G. Enting, Series expansions from the finite lattice method, *Nucl. Phys. B – Proc. Suppl.* **47**, 180–187 (1996).
- [24] I.G. Enting, Inclusion-exclusion relations for series expansions of boundary effects using the finite lattice method, *J. Stat. Mech.* (2005), P12007.
- [25] I.G. Enting, Surface magnetisation of the 3-state Potts model with free and fixed boundaries on the square lattice, *J. Phys.: Conf. Ser.* **42**, 83–94 (2006).
- [26] R. Fernández and A. Procacci, Regions without complex zeros for chromatic polynomials on graphs with bounded degree, *Combin. Probab. Comput.* **17**, 225–238 (2008), arXiv:0704.2617 at arXiv.org.
- [27] C.M. Fortuin and P.W. Kasteleyn, On the random-cluster model. I. Introduction and relation to other models, *Physica* **57**, 536–564 (1972).
- [28] G.H. Golub and C.F. Van Loan, *Matrix Computations*, 3rd edition (The Johns Hopkins University Press, Baltimore, 1996).

- [29] D. Gouyou-Beauchamps and G. Viennot, Equivalence of the two-dimensional directed animal problem to a one-dimensional path problem, *Adv. Appl. Math.* **9**, 334–357 (1988).
- [30] R.L. Graham, D.E. Knuth and O. Patashnik, *Concrete Mathematics: A Foundation for Computer Science*, 2nd ed. (Addison-Wesley, Reading, Mass., 1994).
- [31] B. Jackson, A. Procacci and A.D. Sokal, Complex zero-free regions at large $|q|$ for multivariate Tutte polynomials (alias Potts-model partition functions) with general complex edge weights, preprint (October 2008), arXiv:0810.4703 at arXiv.org.
- [32] J.L. Jacobsen, Bulk, surface and corner free energy series for the chromatic polynomial on the square and triangular lattices *J. Phys. A: Math. Theor.* **43**, 315002 (2010), arXiv:1005.3609 at arXiv.org.
- [33] J.L. Jacobsen, J.-F. Richard and J. Salas, Complex-temperature phase diagram of Potts and RSOS models, *Nucl. Phys. B* **743**, 153–206 (2006), cond-mat/0511059 at arXiv.org.
- [34] J.L. Jacobsen and J. Salas, Transfer matrices and partition-function zeros for antiferromagnetic Potts models. II. Extended results for square-lattice chromatic polynomial, *J. Stat. Phys.* **104**, 701–723 (2001), cond-mat/0011456 at arXiv.org.
- [35] J.L. Jacobsen and J. Salas, Transfer matrices and partition-function zeros for antiferromagnetic Potts models. IV. Chromatic polynomial with cyclic boundary conditions, *J. Stat. Phys.* **122**, 705–760 (2006), cond-mat/0407444 at arXiv.org.
- [36] J.L. Jacobsen and J. Salas, Phase diagram of the chromatic polynomial on a torus, *Nucl. Phys. B* **783**, 238–296 (2007), cond-mat/0703228 at arXiv.org.
- [37] J.L. Jacobsen and J. Salas, Is the five-flow conjecture almost false?, preprint (September 2010), arXiv:1009.4062 at arXiv.org.
- [38] J.L. Jacobsen, J. Salas and A.D. Sokal, Transfer matrices and partition-function zeros for antiferromagnetic Potts models. III. Triangular-lattice chromatic polynomial, *J. Stat. Phys.* **112**, 921–1017 (2003), cond-mat/0204587 at arXiv.org.
- [39] J.L. Jacobsen and H. Saleur, Conformal boundary loop models, *Nucl. Phys. B* **788**, 137–166 (2008), math-ph/0611078 at arXiv.org.
- [40] J.L. Jacobsen and H. Saleur, Combinatorial aspects of boundary loop models, *J. Stat. Mech.* (2008), P01021, arXiv:0709.0812 at arXiv.org.
- [41] J.L. Jacobsen and H. Saleur, Boundary chromatic polynomial, *J. Stat. Phys.* **132**, 707–719 (2008), arXiv:0803.2665 at arXiv.org.
- [42] P.W. Kasteleyn and C.M. Fortuin, Phase transitions in lattice systems with random local properties, *J. Phys. Soc. Japan* **26** (Suppl.), 11–14 (1969).

- [43] D. Kim and I.G. Enting, The limit of chromatic polynomials, *J. Combin. Theory B* **26**, 327–336 (1979).
- [44] T. Kato, *Perturbation Theory for Linear Operators*, 2nd ed., corrected printing (Springer-Verlag, Berlin–New York, 1980).
- [45] M. Klazar, On trees and noncrossing partitions, *Discrete Appl. Math.* **82**, 263–269 (1998).
- [46] T. de Neef and I.G. Enting, Series expansions from the finite-lattice method, *J. Phys. A: Math. Gen.* **10**, 801–805 (1977).
- [47] R.B. Potts, Some generalized order-disorder transformations, *Proc. Cambridge Philos. Soc.* **48**, 106–109 (1952).
- [48] V. Privman, Finite-size scaling theory, in *Finite Size Scaling and Numerical Simulation of Statistical Physics*, V. Privman (editor), pp. 1–98 (World Scientific, Singapore, 1990).
- [49] A. Proccaci, B. Scoppola, and V. Gerasimov, Potts model on infinite graphs and the limit of chromatic polynomials, *Commun. Math. Phys.* **235**, 215–231 (2003), cond-mat/0201183 at arXiv.org.
- [50] R.C. Read and G.F. Royle, Chromatic roots of families of graphs, in *Graph Theory, Combinatorics and Applications*, vol. 2, Y. Alavi, G. Chartrand, O.R. Oellermann and A.J. Schwenk (editors), pp. 1009–1029 (Wiley, New York, 1991).
- [51] J. Riordan, Enumeration of plane trees by branches and endpoints, *J. Combin. Theory A* **19**, 214–222 (1975).
- [52] M. Roček, R. Shrock and S.-H. Tsai, Chromatic polynomials for $J(\prod H)I$ strip graphs and their asymptotic limits, *Physica A* **259**, 367–387 (1998), cond-mat/9807106 at arXiv.org.
- [53] J. Salas and A.D. Sokal, Transfer matrices and partition-function zeros for antiferromagnetic Potts models. I. General theory and square-lattice chromatic polynomial, *J. Stat. Phys.* **104**, 609–699 (2001), cond-mat/0004330 at arXiv.org.
- [54] J. Salas and A.D. Sokal, Transfer matrices and partition-function zeros for antiferromagnetic Potts models. V. Further results for the square-lattice chromatic polynomial, *J. Stat. Phys.* **135**, 279–373 (2009), arXiv:0711.1738 at arXiv.org.
- [55] R. Shrock, Exact Potts model partition functions on ladder graphs, *Physica A* **283**, 388–446 (2000), cond-mat/0001389 at arXiv.org.
- [56] R. Shrock, Chromatic polynomials and their zeros and asymptotic limits for families of graphs, *Discrete Math.* **231**, 421–446 (2001), cond-mat/9908387 at arXiv.org.

- [57] R. Shrock and S.-H. Tsai, Asymptotic limits and zeros of chromatic polynomials and ground state entropy of Potts antiferromagnets, *Phys. Rev. E* **55**, 5165–5178 (1997), cond-mat/9612249 at arXiv.org.
- [58] R. Shrock and S.-H. Tsai, Families of graphs with $W_r(\{G\}, q)$ functions that are nonanalytic at $1/q = 0$, *Phys. Rev. E* **56**, 3935–3943 (1997), cond-mat/9707096 at arXiv.org.
- [59] R. Shrock and S.-H. Tsai, Ground state degeneracy of Potts antiferromagnets: cases with non-compact W boundaries having multiple points at $1/q = 0$, *J. Phys. A: Math. Gen.* **31**, 9641–9665 (1998), cond-mat/9810057 at arXiv.org.
- [60] R. Simion and D. Ullman, On the structure of the lattice of noncrossing partitions, *Discrete Math.* **98**, 193–206 (1991).
- [61] N.J.A. Sloane, The On-Line Encyclopedia of Integer Sequences, <http://www.research.att.com/~njas/sequences/index.html>
- [62] A.D. Sokal, Bounds on the complex zeros of (di)chromatic polynomials and Potts-model partition functions, *Combin. Probab. Comput.* **10**, 41–77 (2001), cond-mat/9904146 at arXiv.org.
- [63] A.D. Sokal, Chromatic roots are dense in the whole complex plane, *Combin. Probab. Comput.* **13**, 221–261 (2004), cond-mat/0012369 at arXiv.org.
- [64] A.D. Sokal, The multivariate Tutte polynomial (alias Potts model) for graphs and matroids, in Bridget S. Webb (editor), *Surveys in Combinatorics, 2005*, pp. 173–226 (Cambridge University Press, Cambridge–New York, 2005), math.CO/0503607 at arXiv.org.
- [65] R.P. Stanley, *Enumerative Combinatorics*, vol. 1 (Wadsworth & Brooks/Cole, Monterey, CA, 1986). Reprinted by Cambridge University Press, 1999.
- [66] R.P. Stanley, *Enumerative Combinatorics*, vol. 2 (Cambridge University Press, Cambridge–New York, 1999).
- [67] W.T. Tutte, A ring in graph theory, *Proc. Cambridge Philos. Soc.* **43**, 26–40 (1947).
- [68] W.T. Tutte, A contribution to the theory of chromatic polynomials, *Canad. J. Math.* **6**, 80–91 (1954).
- [69] H. Whitney, A logical expansion in mathematics, *Bull. Amer. Math. Soc.* **38**, 572–579 (1932).
- [70] F.Y. Wu, The Potts model, *Rev. Mod. Phys.* **54**, 235–268 (1982); erratum **55**, 315 (1983).
- [71] F.Y. Wu, Potts model of magnetism (invited), *J. Appl. Phys.* **55**, 2421–2425 (1984).
- [72] C.N. Yang and T.D. Lee, Statistical theory of equations of state and phase transitions. I. Theory of condensation, *Phys. Rev.* **87**, 404–409 (1952)

m	B_m	C_m	M_{m-1}	SqFree(m)	$N_{\neq}(m-2)$	$N_{=}(m-2)$
1	1	1	1	1		
2	2	2	1	1		
3	5	5	2	2	1	1
4	15	14	4	3	2	1
5	52	42	9	7	4	3
6	203	132	21	13	9	4
7	877	429	51	32	21	11
8	4140	1430	127	70	49	21
9	21147	4862	323	179	124	55
10	115975	16796	835	435	311	124
11	678570	58786	2188	1142	815	327
12	4213597	208012	5798	2947	2132	815
13	27644437	742900	15511	7889	5712	2177
14	190899322	2674440	41835	21051	15339	5712
15	1382958545	9694845	113634	57192	41727	15465
16	10480142147	35357670	310572	155661	113934	41727

Table 1: Dimension of the transfer matrix. For each strip width m we give the number B_m of all partitions, the number C_m of non-crossing partitions, the number M_{m-1} of non-crossing non-nearest-neighbor partitions with free boundary conditions, and the number SqFree(m) of equivalence classes of non-crossing non-nearest-neighbor partitions modulo reflection in the center of the strip. The dimension of the transfer matrix $T''(m)$ associated to the strip $S_{m,n}$ is SqFree($m+2$). We also show the dimensionalities $N_{\neq}(m)$ and $N_{=}(m)$ of the transfer matrices $T''_{\neq}(m)$ and $T''_{=}(m)$, respectively.

m	b_0^\neq	b_1^\neq	b_2^\neq	b_3^\neq	b_4^\neq	b_5^\neq	b_6^\neq	b_7^\neq	b_8^\neq	b_9^\neq	b_{10}^\neq	b_{11}^\neq	b_{12}^\neq	b_{13}^\neq	b_{14}^\neq	b_{15}^\neq
1	1	3	0	0	0	0	0	0	0	0	0	0	0	0	0	0
2	1	5	8	2	-4	4	4	-24	40	0	-128	128	752	-3392	6624	-5184
3	1	7	19	23	7	-11	2	21	-19	-59	139	16	-347	62	335	6886
4	1	9	34	67	67	19	-21	-13	40	20	-75	-166	654	-754	245	1835
5	1	11	53	143	227	195	52	-45	-35	20	156	-110	-324	139	1833	-5085
6	1	13	76	259	556	749	570	138	-101	-78	-20	198	381	-975	-646	3534
7	1	15	103	423	1138	2056	2429	1666	367	-256	-127	-139	129	1064	-228	-3872
8	1	17	134	643	2073	4666	7345	7775	4870	965	-666	-223	-221	-485	1841	3088
9	1	19	169	927	3477	9337	18225	25582	24638	14219	2536	-1811	-350	-188	-1917	1550
10	1	21	208	1283	5482	17067	39600	68667	87380	77434	41471	6619	-4973	-559	426	-4676
11	1	23	251	1719	8236	29126	78121	160546	251621	293864	241705	120781	17181	-13789	-831	2878

Table 2: Coefficients $b_k^\neq(m)$ of the large- q expansion of the dominant eigenvalue $\lambda_{*,\neq}$. For each $1 \leq m \leq 11$, we include all coefficients $b_k^\neq(m)$ up to $k = 15$. For the whole data set up to $k = 40$, see the MATHEMATICA file `data_Neq.m` included in the on-line version of the paper at arXiv.org. Those data points below the staircase-like line satisfy $m \geq m_{\min}^\neq(k)$ [cf. (4.16)].

m	c_1^\neq	$2c_2^\neq$	$3c_3^\neq$	$4c_4^\neq$	$5c_5^\neq$	$6c_6^\neq$	$7c_7^\neq$	$8c_8^\neq$	$9c_9^\neq$	$10c_{10}^\neq$	$11c_{11}^\neq$	$12c_{12}^\neq$	$13c_{13}^\neq$	$14c_{14}^\neq$	$15c_{15}^\neq$
1	-3	-9	-27	-81	-243	-729	-2187	-6561	-19683	-59049	-177147	-531441	-1594323	-4782969	-14348907
2	-5	-9	-11	-9	-15	-57	-75	447	3085	10791	28309	71055	212077	720263	2329749
3	-7	-11	-13	-15	-7	103	588	1969	5387	14529	40286	106983	258381	554704	922742
4	-9	-13	-12	-1	36	128	320	943	3849	15852	58115	195236	623874	1913472	5551353
5	-11	-15	-11	9	59	171	500	1681	5488	16305	47487	147099	481457	1575678	4990814
6	-13	-17	-10	19	87	232	596	1683	5273	18063	63270	210208	644943	1849922	5061480
7	-15	-19	-9	29	115	287	678	1845	6012	20881	69692	219419	668588	2007980	5885716
8	-17	-21	-8	39	143	342	767	2015	6508	22629	76763	248394	766372	2251389	6294362
9	-19	-23	-7	49	171	397	856	2177	7004	24707	84890	274117	833229	2418344	6784758
10	-21	-25	-6	59	199	452	945	2339	7509	26775	92599	298952	906755	2626305	7326784
11	-23	-27	-5	69	227	507	1034	2501	8014	28833	100330	324291	980827	2823500	7820795

Table 3: Coefficients $kc_k^\neq(m)$ of the large- q expansion of $\log(q^{-m}\lambda_\star^\neq)$ where $\lambda_{\star,\neq}$ is the dominant eigenvalue for \neq boundary conditions. For each $1 \leq m \leq 11$, we include all coefficients $c_k^\neq(m)$ up to $k = 15$. For the whole data set up to $k = 40$, see the MATHEMATICA file **data_Neq.m** included in the on-line version of the paper at arXiv.org. Those data points below the staircase-like line satisfy $m \geq m_{\min}^\neq(k)$ [cf. (4.16)].

k	$C_k(m) = \alpha_k m + \beta_k$		$E_k(m) = \gamma_k m + \delta_k$		$F_k(m) = \epsilon_k m + \phi_k$	
	$k\alpha_k$	$k\beta_k$	$k\gamma_k$	$k\delta_k$	$k\epsilon_k$	$k\phi_k$
1	-2	-1	-3	4	1	-5
2	-2	-5	-13	12	11	-17
3	1	-16	-48	61	49	-77
4	10	-41	-181	264	191	-305
5	28	-81	-658	934	686	-1015
6	55	-98	-2164	2643	2219	-2741
7	89	55	-6142	5401	6231	-5346
8	162	719	-13989	4128	14151	-3409
9	505	2459	-19281	-26021	19786	28480
10	2058	6195	31592	-165918	-29534	172113
11	7742	15168	414158	-652120	-406416	667288
12	25291	46102	2389460	-2362893	-2364169	2408995
13	73552	171677	11542242	-9775073	-11468690	9946750
14	197755	647719				
15	508036	2234229				
16	1264258	6898415				
17	2984620	19118828				

Table 4: Polynomials $C_k(m)$, $E_k(m)$ and $F_k(m)$ representing for $m \geq k + 1$ the coefficients $c_k^\sharp(m)$ [cf. (4.3)], $e_k(m)$ [cf. (4.13)] and $f_k(m)$ [cf. (4.14)], respectively. All these polynomials are of degree 1 in m , and their coefficients multiplied by k are always integers.

m	Δ_1^\neq	Δ_2^\neq	Δ_3^\neq	Δ_4^\neq	Δ_5^\neq	Δ_6^\neq	Δ_7^\neq	Δ_8^\neq	Δ_9^\neq	Δ_{10}^\neq	Δ_{11}^\neq	Δ_{12}^\neq	Δ_{13}^\neq	Δ_{14}^\neq	Δ_{15}^\neq
1	0	-1	-4	$-\frac{25}{2}$	-38	$-\frac{343}{3}$	-333	$-\frac{3721}{4}$	$-\frac{7549}{3}$	$-\frac{33651}{5}$	-18187	$-\frac{301417}{6}$	-141504	$-\frac{5628443}{14}$	$-\frac{17091172}{15}$
2	0	0	1	3	2	$-\frac{23}{2}$	-44	$-\frac{149}{2}$	$-\frac{128}{3}$	48	-213	$-\frac{8543}{4}$	-8208	-23069	$-\frac{920552}{15}$
3	0	0	0	-1	-2	6	38	$\frac{191}{2}$	157	216	172	$-\frac{3748}{3}$	-10304	-49020	$-\frac{567119}{3}$
4	0	0	0	0	1	1	-13	-53	-70	$\frac{285}{2}$	1089	$\frac{7995}{2}$	12153	$\frac{67819}{2}$	$\frac{256996}{3}$
5	0	0	0	0	0	-1	0	19	56	-18	-581	$-\frac{4243}{2}$	-4460	-4344	14427
6	0	0	0	0	0	0	1	-1	-24	-48	150	1030	2458	$\frac{2239}{2}$	-14731
7	0	0	0	0	0	0	0	-1	2	28	30	-310	-1381	-1716	6349
8	0	0	0	0	0	0	0	0	1	-3	-31	-3	483	1545	-277
9	0	0	0	0	0	0	0	0	0	-1	4	33	-32	-655	-1453
10	0	0	0	0	0	0	0	0	0	0	1	-5	-34	74	813
11	0	0	0	0	0	0	0	0	0	0	0	-1	6	34	-122

Table 5: Coefficients $\Delta_k^\neq(m)$ for \neq boundary conditions [cf. (4.21)] for $1 \leq k \leq 15$ and $1 \leq m \leq 11$. Those data points below the lower staircase-like line satisfy $m \geq m_{\min}^\neq(k)$ [cf. (4.16)] and are therefore zero. Those data points between the two staircase-like lines can be fitted to a polynomial Ansatz [cf. (4.23)–(4.27)].

m	b_0^-	b_1^-	b_2^-	b_3^-	b_4^-	b_5^-	b_6^-	b_7^-	b_8^-	b_9^-	b_{10}^-	b_{11}^-	b_{12}^-	b_{13}^-	b_{14}^-	b_{15}^-
1	1	2	0	0	0	0	0	0	0	0	0	0	0	0	0	0
2	1	5	7	0	0	0	0	0	0	0	0	0	0	0	0	0
3	1	7	19	22	2	-10	20	-8	-59	111	226	-1478	3029	-1922	-359	-26461
4	1	9	34	67	66	11	-33	18	74	-109	-175	410	884	-3801	4508	-7375
5	1	11	53	143	227	194	41	-79	-25	166	92	-567	-49	1555	-957	-366
6	1	13	76	259	556	749	569	124	-166	-149	215	541	-495	-1832	2683	2725
7	1	15	103	423	1138	2056	2429	1665	350	-361	-366	1	1282	766	-4301	-1274
8	1	17	134	643	2073	4666	7345	7775	4869	945	-820	-744	-603	1495	4652	-4003
9	1	19	169	927	3477	9337	18225	25582	24638	14218	2513	-2023	-1294	-1843	-155	10811
10	1	21	208	1283	5482	17067	39600	68667	87380	77434	41470	6593	-5252	-2094	-3658	-6157
11	1	23	251	1719	8236	29126	78121	160546	251621	293864	241705	120780	17152	-14144	-3152	-5277
12	1	25	298	2243	11903	47088	143119	339167	628439	901807	975816	750058	351253	44217	-38862	-4178

Table 6: Coefficients $b_k^-(m)$ of the large- q expansion of the dominant eigenvalue $\lambda_{*,=}$. For each $1 \leq m \leq 12$, we include all coefficients $b_k^-(m)$ up to $k = 15$. For the whole data set up to $k = 40$, see the MATHEMATICA file `data_Eq.m` included in the on-line version of the paper at arXiv.org. Those data points below the staircase-like line satisfy $m \geq m_{\min}^-(k)$ [cf. (4.28)].

m	c_1^-	$2c_2^-$	$3c_3^-$	$4c_4^-$	$5c_5^-$	$6c_6^-$	$7c_7^-$	$8c_8^-$	$9c_9^-$	$10c_{10}^-$	$11c_{11}^-$	$12c_{12}^-$	$13c_{13}^-$	$14c_{14}^-$	$15c_{15}^-$
1	-2	-4	-8	-16	-32	-64	-128	-256	-512	-1024	-2048	-4096	-8192	-16384	-32768
2	-5	-11	-20	-23	25	286	1255	4273	12580	32989	76885	153502	229315	72061	-1244900
3	-7	-11	-10	-7	-37	-134	-63	1209	5732	17459	58194	250586	1073039	3960589	12879935
4	-9	-13	-12	-5	31	206	691	1491	2643	5947	17371	54094	211345	1009373	4696918
5	-11	-15	-11	9	64	171	367	1233	5650	22100	70983	202131	541595	1384095	3268114
6	-13	-17	-10	19	87	226	603	1875	5705	16563	51940	180694	630656	2058179	6217815
7	-15	-19	-9	29	115	287	685	1829	5760	20581	73102	235991	690896	1919073	5277046
8	-17	-21	-8	39	143	342	767	2007	6535	22939	76796	242598	746287	2255267	6547532
9	-19	-23	-7	49	171	397	856	2177	7013	24667	84527	274501	841744	2438686	6732003
10	-21	-25	-6	59	199	452	945	2339	7509	26765	92654	299360	905793	2614923	7310959
11	-23	-27	-5	69	227	507	1034	2501	8014	28833	100341	324219	980385	2825208	7834970
12	-25	-29	-4	79	255	562	1123	2663	8519	30891	108072	349582	1054405	3021143	8327541

Table 7: Coefficients $kc_k^-(m)$ of the large- q expansion of $\log(q^{-m}\lambda_\star^-)$ where $\lambda_{\star,=}$ is the dominant eigenvalue for $=$ boundary conditions. For each $1 \leq m \leq 12$, we include all coefficients $c_k^-(m)$ up to $k = 15$. For the whole data set up to $k = 40$, see the MATHEMATICA file `data_Eq.m` included in the on-line version of the paper at arXiv.org. Those data points below the staircase-like line satisfy $m \geq m_{\min}^-(k)$ [cf. (4.28)].

m	Δ_1^-	Δ_2^-	Δ_3^-	Δ_4^-	Δ_5^-	Δ_6^-	Δ_7^-	Δ_8^-	Δ_9^-	Δ_{10}^-	Δ_{11}^-	Δ_{12}^-	Δ_{13}^-	Δ_{14}^-	Δ_{15}^-
1	1	$\frac{3}{2}$	$\frac{7}{3}$	$\frac{15}{4}$	$\frac{21}{5}$	$-\frac{7}{2}$	$-\frac{272}{7}$	$-\frac{1137}{8}$	$-\frac{3476}{9}$	$-\frac{9277}{10}$	$-\frac{24958}{11}$	$-\frac{25163}{4}$	$-\frac{253421}{13}$	$-\frac{430929}{7}$	$-\frac{925011}{5}$
2	0	-1	-2	$-\frac{1}{2}$	10	$\frac{137}{3}$	146	$\frac{1615}{4}$	$\frac{3037}{3}$	$\frac{11339}{5}$	4203	$\frac{28409}{6}$	-6882	$-\frac{485584}{7}$	$-\frac{4495201}{15}$
3	0	0	1	1	-8	$-\frac{67}{2}$	-55	$\frac{1}{2}$	$\frac{586}{3}$	509	1800	$\frac{128611}{12}$	52362	$\frac{388515}{2}$	$\frac{9121598}{15}$
4	0	0	0	-1	0	14	40	$\frac{31}{2}$	-204	-848	-2615	$-\frac{23293}{3}$	-19580	-30669	28703
5	0	0	0	0	1	-1	-19	-37	74	$\frac{1123}{2}$	1555	$\frac{4929}{2}$	166	$-\frac{36057}{2}$	$-\frac{301259}{3}$
6	0	0	0	0	0	-1	2	23	24	-198	-880	$-\frac{2859}{2}$	1359	15995	62358
7	0	0	0	0	0	0	1	-3	-26	-2	340	1071	335	$-\frac{16133}{2}$	-34229
8	0	0	0	0	0	0	0	-1	4	28	-28	-486	-1062	1822	16601
9	0	0	0	0	0	0	0	0	1	-5	-29	65	623	798	-4970
10	0	0	0	0	0	0	0	0	0	-1	6	29	-108	-739	-242
11	0	0	0	0	0	0	0	0	0	0	1	-7	-28	156	823
12	0	0	0	0	0	0	0	0	0	0	0	-1	8	26	-208

Table 8: Coefficients $\Delta_k^-(m)$ for = boundary conditions [cf. (4.21)] for $1 \leq k \leq 15$ and $1 \leq m \leq 12$. Those data points below the lower staircase-like line satisfy $m \geq m_{\min}^-(k)$ [cf. (4.28)] and are therefore zero. Those data points between the two staircase-like lines can be fitted to a polynomial Ansatz [cf. (4.29d)–(4.31)].

m	d_1	d_2	d_3	d_4	d_5	d_6	d_7	d_8	d_9	d_{10}	d_{11}	d_{12}	d_{13}
1	0	0	0	0	0	0	0	0	0	0	0	0	0
2	2	-4	4	4	-24	40	0	-128	128	752	-3392	6624	-5184
3	5	-1	-18	29	40	-170	-87	1494	-3376	1984	694	33347	-197615
4	8	12	-31	-34	129	100	-576	-230	3047	-4263	9210	-64867	238639
5	11	34	-10	-146	64	457	-275	-1416	2790	-4719	5981	47388	-300709
6	14	65	71	-235	-343	876	857	-3329	809	13186	-49587	89187	-19
7	17	105	239	-140	-1153	298	4073	-2598	-12636	26869	5107	-135403	331386
8	20	154	521	382	-1980	-2811	7091	9054	-29248	-9219	120387	-160314	-41468
9	23	212	944	1655	-1762	-9261	2518	35377	-15992	-117784	152402	218878	-752711
10	26	279	1535	4084	1481	-17296	-21291	60152	83981	-236658	-170823	927069	-457202
11	29	355	2321	8155	10890	-20003	-74321	29922	301365	-105940	-1047643	906441	2674932

Table 9: Coefficients $d_\ell(m)$ [cf. (4.11)] for $1 \leq \ell \leq 13$ and $1 \leq m \leq 11$. For the whole data set up to $\ell = 20$, see the MATHEMATICA file `data_Diff.m` included in the on-line version of the paper at arXiv.org. Those data points below the lower staircase-like line satisfy $m \geq \ell + 1$.

m	e_1	$2e_2$	$3e_3$	$4e_4$	$5e_5$	$6e_6$	$7e_7$	$8e_8$	$9e_9$	$10e_{10}$	$11e_{11}$	$12e_{12}$	$13e_{13}$
1	0	0	0	0	0	0	0	0	0	0	0	0	0
2	-2	-12	-44	-128	-352	-1056	-3488	-11584	-36512	-109792	-326944	-993536	-3077440
3	-5	-27	-86	-251	-910	-3690	-13669	-44019	-125411	-312552	-557969	452254	12297228
4	-8	-40	-131	-456	-1753	-6283	-19874	-54888	-117392	-59295	1300181	10433589	57898495
5	-11	-53	-179	-641	-2361	-8087	-24847	-63873	-106973	100877	1976447	11655889	52017110
6	-14	-66	-227	-822	-3014	-10335	-31584	-80518	-146018	-21616	1451227	9451641	45388641
7	-17	-79	-275	-1003	-3672	-12505	-37600	-93611	-159962	63596	2351805	15369983	78870073
8	-20	-92	-323	-1184	-4330	-14669	-43735	-107776	-180512	85408	2646349	16541923	80306297
9	-23	-105	-371	-1365	-4988	-16833	-49877	-121773	-199559	118720	3077172	19166619	94490152
10	-26	-118	-419	-1546	-5646	-18997	-56019	-135762	-218831	150012	3489075	21529295	105609348
11	-29	-131	-467	-1727	-6304	-21161	-62161	-149751	-238112	181594	3903607	23921635	117192631

Table 10: Coefficients $\ell e_\ell(m)$ [cf. (4.13)] for $1 \leq \ell \leq 13$ and $1 \leq m \leq 11$. For the whole data set up to $\ell = 20$, see the MATHEMATICA file `data_Diff.m` included in the on-line version of the paper at arXiv.org. Those data points below the lower staircase-like line satisfy $m \geq \ell + 1$.

m	$\Delta_1^{(e)}$	$\Delta_2^{(e)}$	$\Delta_3^{(e)}$	$\Delta_4^{(e)}$	$\Delta_5^{(e)}$	$\Delta_6^{(e)}$	$\Delta_7^{(e)}$	$\Delta_8^{(e)}$	$\Delta_9^{(e)}$	$\Delta_{10}^{(e)}$	$\Delta_{11}^{(e)}$	$\Delta_{12}^{(e)}$	$\Delta_{13}^{(e)}$
1	-1	$\frac{1}{2}$	$-\frac{13}{3}$	$-\frac{83}{4}$	$-\frac{276}{5}$	$-\frac{479}{6}$	$\frac{741}{7}$	$\frac{9861}{8}$	$\frac{45302}{9}$	$\frac{67163}{5}$	$\frac{237962}{11}$	$-\frac{26567}{12}$	$-\frac{1767169}{13}$
2	0	1	-3	$-\frac{15}{2}$	6	$\frac{629}{6}$	485	$\frac{6133}{4}$	3119	$-\frac{3529}{5}$	-45740	$-\frac{1136521}{4}$	-1260527
3	0	0	-1	7	26	$\frac{53}{2}$	-92	$-\frac{1545}{2}$	$-\frac{13849}{3}$	-24141	-104393	$-\frac{4353233}{12}$	-965725
4	0	0	0	1	-11	-45	-101	$-\frac{765}{2}$	-1583	$-\frac{3949}{2}$	26879	$\frac{1619321}{6}$	1654200
5	0	0	0	0	-1	15	66	243	1717	$\frac{21767}{2}$	50707	$\frac{345247}{2}$	313921
6	0	0	0	0	0	1	-19	-89	-479	-4525	-34691	$-\frac{420371}{2}$	-1083826
7	0	0	0	0	0	0	-1	23	114	837	9529	83888	603804
8	0	0	0	0	0	0	0	1	-27	-141	-1345	-17572	-173582
9	0	0	0	0	0	0	0	0	-1	31	170	2031	29619
10	0	0	0	0	0	0	0	0	0	1	-35	-201	-2923
11	0	0	0	0	0	0	0	0	0	0	-1	39	234

Table 11: Coefficients $\Delta_\ell^{(e)}(m)$ [cf. (4.34)] for $1 \leq \ell \leq 13$ and $1 \leq m \leq 11$. For the whole data set up to $\ell = 20$, see the MATHEMATICA file `data_Diff.m` included in the on-line version of the paper at arXiv.org. Those data points below the lower staircase-like line satisfy $m \geq \ell + 1$ and are therefore zero. Those data points between the two staircase-like lines can be fitted to a polynomial Ansatz [cf. (4.35)].

m	f_1	$2f_2$	$3f_3$	$4f_4$	$5f_5$	$6f_6$	$7f_7$	$8f_8$	$9f_9$	$10f_{10}$	$11f_{11}$	$12f_{12}$
1	$-\frac{5}{2}$	$-\frac{77}{12}$	$-\frac{135}{8}$	$-\frac{32651}{720}$	$-\frac{35755}{288}$	$-\frac{20877127}{60480}$	$-\frac{3359377}{3456}$	$-\frac{10035074977}{3628800}$	$-\frac{426428659}{53760}$	$-\frac{2193911030309}{95800320}$	$-\frac{231533054159}{3483648}$	$-\frac{506578309836952357}{2615348736000}$
2	-3	2	$\frac{57}{2}$	$\frac{673}{6}$	$\frac{1433}{4}$	$\frac{2349}{2}$	$\frac{97907}{24}$	$\frac{5001829}{360}$	$\frac{3524187}{80}$	$\frac{9408107}{72}$	$\frac{542977339}{1440}$	$\frac{6664350307}{6048}$
3	-2	16	$\frac{149}{2}$	240	888	$\frac{14699}{4}$	$\frac{41798}{3}$	$\frac{136816}{3}$	$\frac{1047455}{8}$	$\frac{985253}{3}$	$\frac{1821506}{3}$	$-\frac{65347931}{240}$
4	-1	27	119	453	$\frac{3573}{2}$	6450	$\frac{40759}{2}$	$\frac{168316}{3}$	$\frac{482555}{4}$	$\frac{842209}{12}$	$-\frac{2524997}{2}$	-10308961
5	0	38	168	650	$\frac{4845}{2}$	8258	$\frac{50561}{2}$	65330	112542	$-\frac{980089}{12}$	-1917212	-11481293
6	1	49	217	841	3101	10564	$\frac{64367}{2}$	82297	151507	38929	-1393622	$-\frac{18512379}{2}$
7	2	60	266	1032	3787	12792	$\frac{76563}{2}$	95448	165848	-42865	-2280408	-15142278
8	3	71	315	1223	4473	15011	44502	109787	$\frac{374067}{2}$	-62624	$-\frac{5139139}{2}$	-16296427
9	4	82	364	1414	5159	17230	50733	123950	$\frac{413135}{2}$	-94033	$-\frac{5984927}{2}$	-18892310
10	5	93	413	1605	5845	19449	56964	138101	226340	-123242	$-\frac{6792897}{2}$	-21230139
11	6	104	462	1796	6531	21668	63195	152252	246126	-152761	$-\frac{7606543}{2}$	-23597380

Table 12: Coefficients $kf_\ell(m)$ [cf. (4.14)] for $1 \leq \ell \leq 12$ and $1 \leq m \leq 11$. For the whole data set up to $\ell = 20$, see the MATHEMATICA file `data_Diff.m` included in the on-line version of the paper at arXiv.org. Those data points below the lower staircase-like line satisfy $m \geq \ell + 1$.

m	$\Delta_1^{(f)}$	$\Delta_2^{(f)}$	$\Delta_3^{(f)}$	$\Delta_4^{(f)}$	$\Delta_5^{(f)}$	$\Delta_6^{(f)}$	$\Delta_7^{(f)}$	$\Delta_8^{(f)}$	$\Delta_9^{(f)}$	$\Delta_{10}^{(f)}$	$\Delta_{11}^{(f)}$	$\Delta_{12}^{(f)}$
1	$\frac{3}{2}$	$-\frac{5}{24}$	$\frac{89}{24}$	$\frac{49429}{2880}$	$\frac{58997}{1440}$	$\frac{10693433}{362880}$	$-\frac{6417937}{24192}$	$-\frac{49015644577}{29030400}$	$-\frac{3021208819}{483840}$	$-\frac{15853024855589}{958003200}$	$-\frac{1140319275215}{38320128}$	$-\frac{623813932276888357}{31384184832000}$
2	0	$-\frac{3}{2}$	$\frac{5}{2}$	$\frac{211}{24}$	$\frac{1}{4}$	$-\frac{1045}{12}$	$-\frac{10411}{24}$	$-\frac{3959651}{2880}$	$-\frac{639991}{240}$	$\frac{1268867}{720}$	$\frac{68414609}{1440}$	$\frac{20691736771}{72576}$
3	0	0	$\frac{3}{2}$	-7	-31	$-\frac{965}{24}$	$\frac{251}{3}$	$\frac{4921}{6}$	$\frac{114917}{24}$	$\frac{73472}{3}$	$\frac{316126}{3}$	$\frac{1058694949}{2880}$
4	0	0	0	$-\frac{3}{2}$	$\frac{23}{2}$	$\frac{105}{2}$	$\frac{229}{2}$	$\frac{8731}{24}$	$\frac{17353}{12}$	$\frac{38897}{24}$	$-\frac{55295}{2}$	$-\frac{815320}{3}$
5	0	0	0	0	$\frac{3}{2}$	-16	$-\frac{151}{2}$	-252	-1652	$-\frac{254681}{24}$	-50220	$-\frac{2069443}{12}$
6	0	0	0	0	0	$-\frac{3}{2}$	$\frac{41}{2}$	100	479	4402	34326	$\frac{5039659}{24}$
7	0	0	0	0	0	0	$\frac{3}{2}$	-25	-126	-824	-9344	$-\frac{167015}{2}$
8	0	0	0	0	0	0	0	$-\frac{3}{2}$	$\frac{59}{2}$	$\frac{307}{2}$	$\frac{2631}{2}$	$\frac{34655}{2}$
9	0	0	0	0	0	0	0	0	$\frac{3}{2}$	-34	$-\frac{365}{2}$	-1982
10	0	0	0	0	0	0	0	0	0	$-\frac{3}{2}$	$\frac{77}{2}$	213
11	0	0	0	0	0	0	0	0	0	0	$\frac{3}{2}$	-43

Table 13: Coefficients $\Delta_\ell^{(f)}(m)$ [cf. (4.37)] for $1 \leq \ell \leq 12$ and $1 \leq m \leq 11$. For the whole data set up to $\ell = 20$, see the MATHEMATICA file `data_Diff.m` included in the on-line version of the paper at arXiv.org. Those data points below the lower staircase-like line satisfy $m \geq \ell + 1$ and are therefore zero. Those data points between the two staircase-like lines can be fitted to a polynomial Ansatz [cf. (4.38)].

m	d_m	$X(m)$	$N_2(m)$	$N_3(m)$
1	1	1	1	1
2	1	1	1	1
3	1	1	1	1
4	3	1	2	3
5	6	2	4	4
6	15	3	9	11
7	36	6	21	21
8	91	7	49	55
9	232	16	124	124
10	603	19	311	327
11	1585	45	815	815
12	4213	51	2132	2177
13	11298	126	5712	5712
14	30537	141	15339	15465
15	83097	357	41727	41727
16	227475	393	113934	114291

Table 14: Counts of certain classes of non-crossing non-nearest-neighbor (ncnnn) partitions of the set $\{1, 2, \dots, m\}$ on a circle. For each m , we show the total number d_m of ncnnn partitions (which equals the Riordan number R_m when $m \geq 2$); the number $X(m)$ of ncnnn partitions that are invariant under reflection with respect an axis going between vertices 1 and m ; the number $N_2(m)$ of equivalence classes of ncnnn partitions modulo reflection with respect an axis going between vertices 1 and m ; and the number $N_3(m)$ of equivalence classes of ncnnn partitions modulo reflection with respect an axis going through vertex 1. Note that $R_0 = 1$ and $R_1 = 0$.

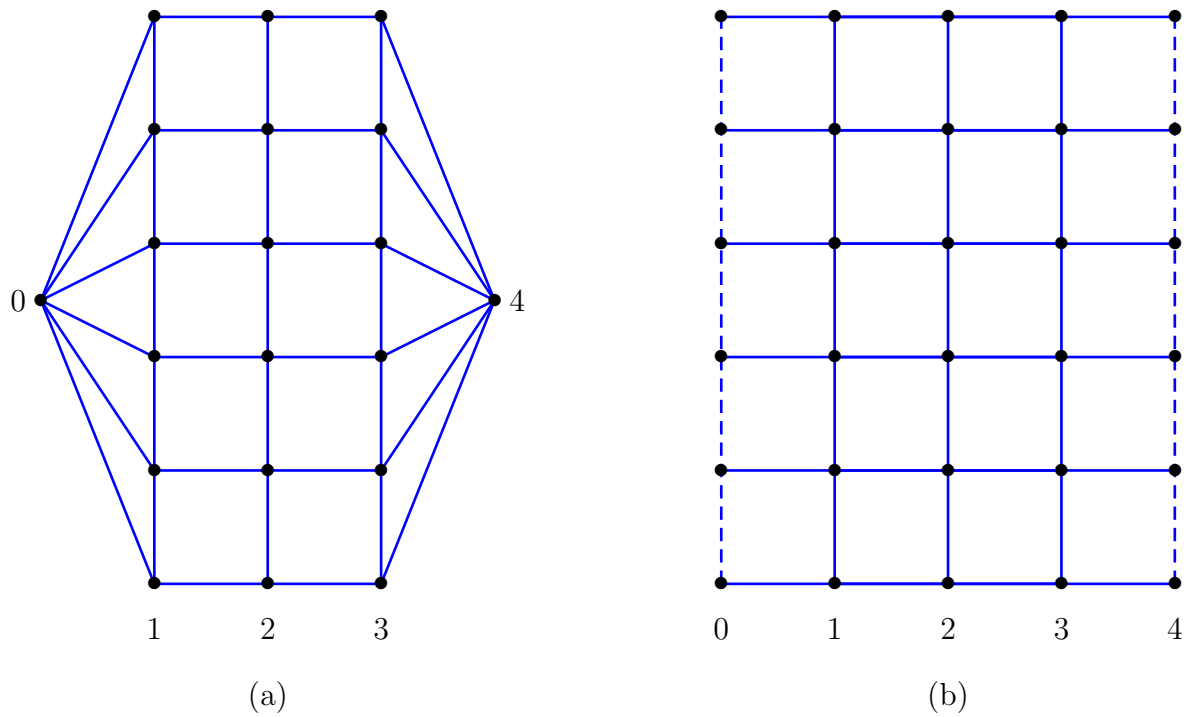


Figure 1: (a) Square-lattice strip $S_{3,6}$ of width $m=3$ and length $n=6$ with two extra sites. (b) Alternate representation of $S_{3,6}$ in terms of a square-lattice strip of width $m+2=5$, length $n=6$ and free boundary conditions, with edge weights $v \rightarrow +\infty$ on the dashed edges.

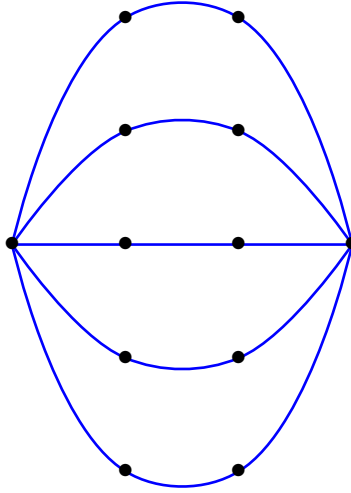


Figure 2: Generalized theta graph $\Theta^{(3,5)}$ formed by $p = 5$ chains in parallel, each consisting in $s = 3$ edges in series.

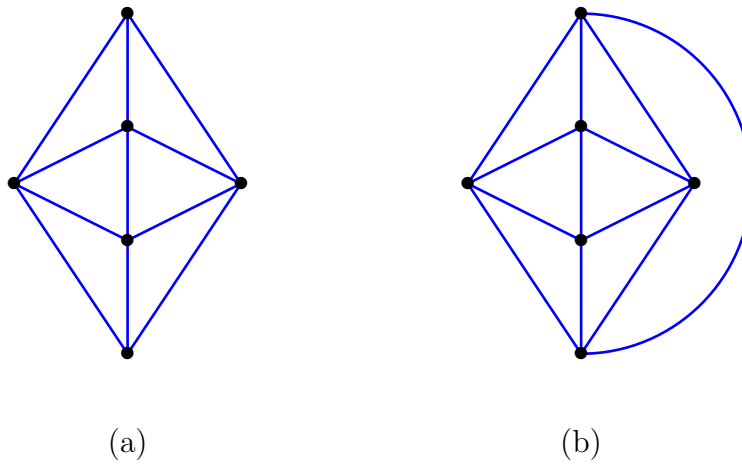


Figure 3: (a) Bi-fan $P_4 + \bar{K}_2$. (b) Bipyramid $C_4 + \bar{K}_2$.

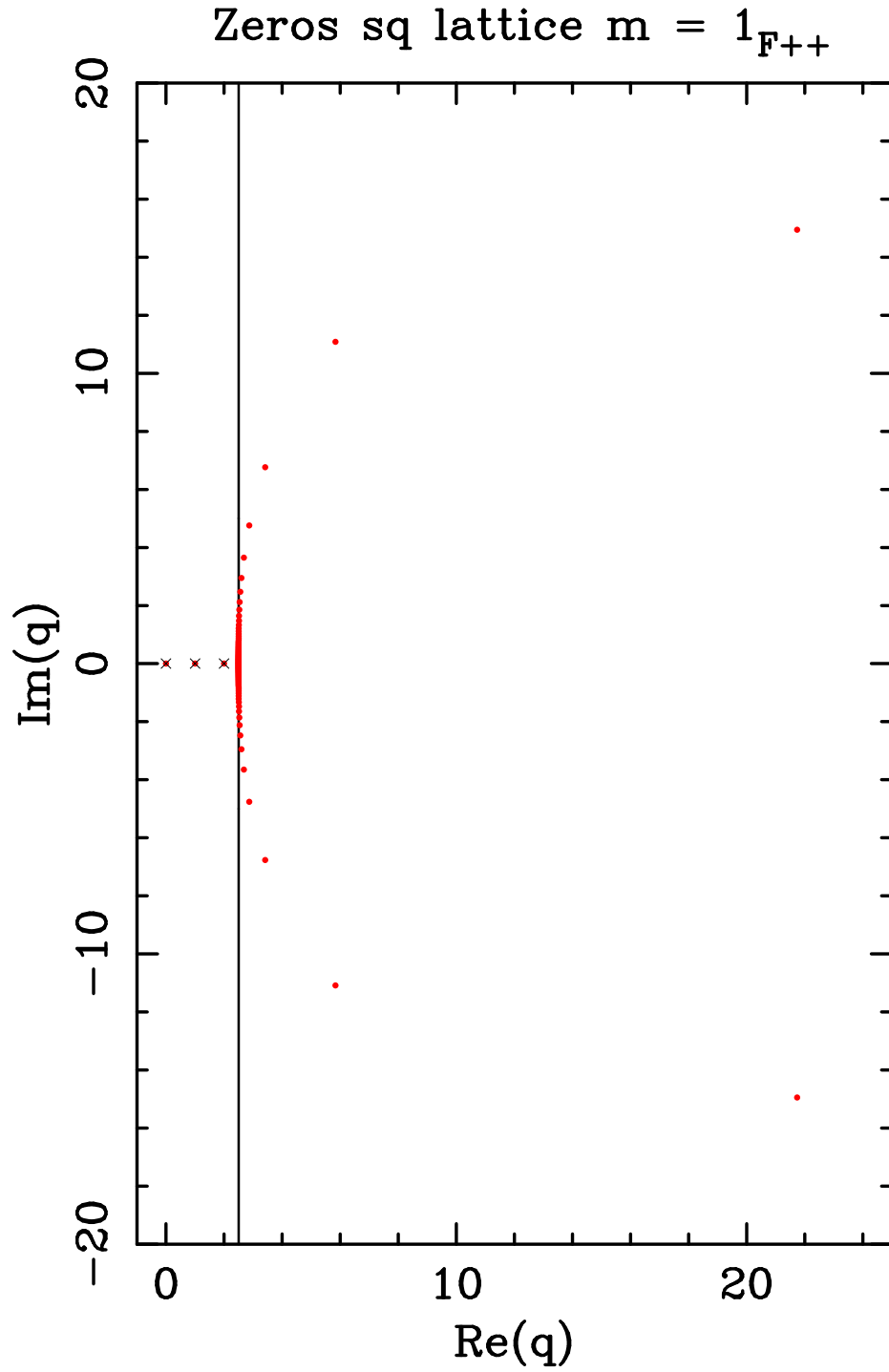


Figure 4: Chromatic roots for the bi-fan $P_{100} + \bar{K}_2 = S_{1,100}$ (red \bullet). We also show the limiting curve \mathcal{B}_1 , and the isolated limiting points (\times).

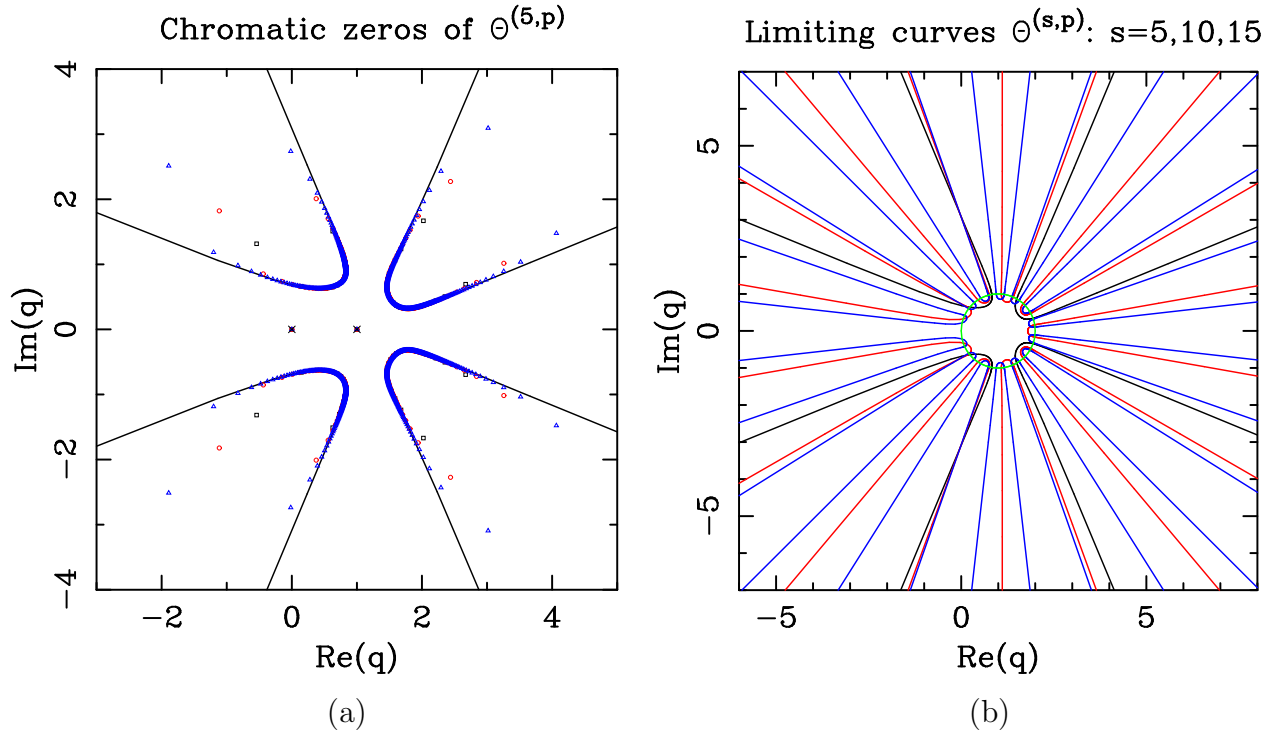


Figure 5: Chromatic roots for the generalized theta graphs $\Theta^{(s,p)}$. (a) Chromatic roots for the graphs $\Theta^{(5,p)}$ with $p = 25$ (black \square), $p = 100$ (red \bullet) and $p = 400$ (blue \triangle), and the limiting curve \mathcal{C}_5 [cf. (2.35)]. We also show the isolated limiting points for this family (black \times). (b) Limiting curves \mathcal{C}_s for $s = 5$ (black), $s = 10$ (red) and $s = 15$ (blue). The circle (depicted in green) is $|q - 1| = 1$.

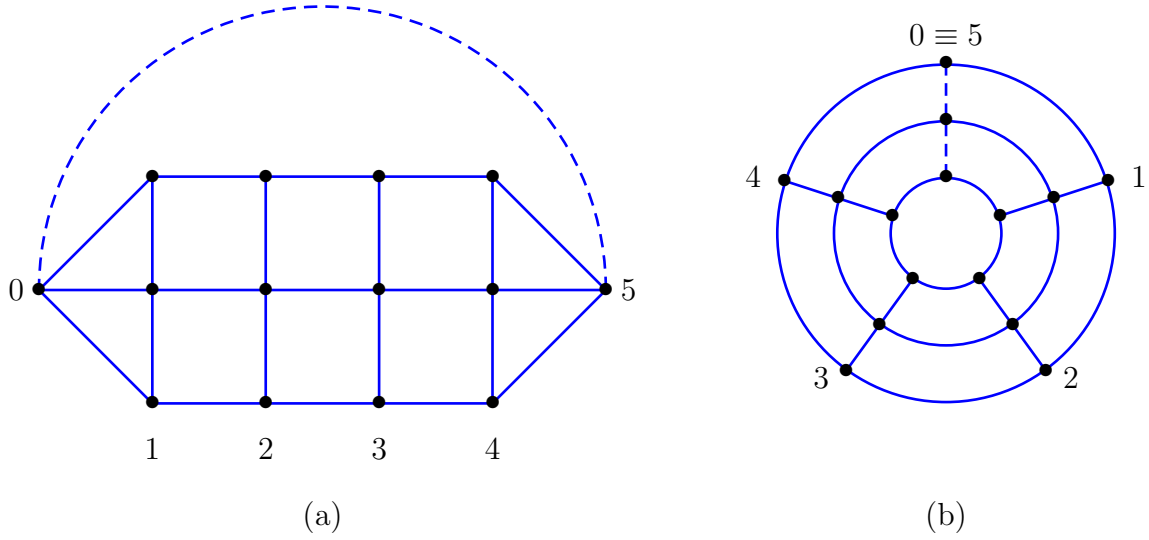


Figure 6: (a) Square-lattice strip $S_{4,3}^-$ of width $m = 4$ and length $n = 3$ with the two extra sites (0 and 5) contracted. This contraction is indicated by a dashed line. (b) Alternate representation of $S_{4,3}^-$ in terms of a square-lattice strip of width $m + 1 = 5$, length $n = 3$ and cylindrical boundary conditions, with edge weights $v \rightarrow +\infty$ on the dashed edges.

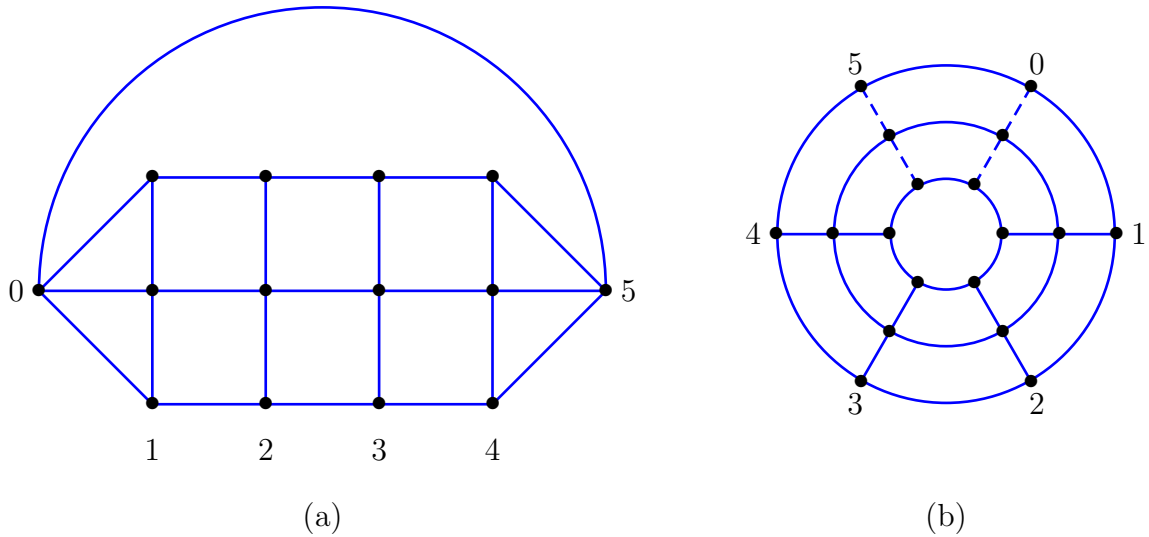


Figure 7: (a) Square-lattice strip $S_{4,3}^{\neq}$ of width $m = 4$ and length $n = 3$ with the two extra sites (0 and 5) joined by a $v = -1$ edge. (b) Alternate representation of $S_{4,3}^{\neq}$ in terms of a square-lattice strip of width $m + 2 = 6$, length $n = 3$ and cylindrical boundary conditions, with edge weights $v \rightarrow +\infty$ on the dashed edges.

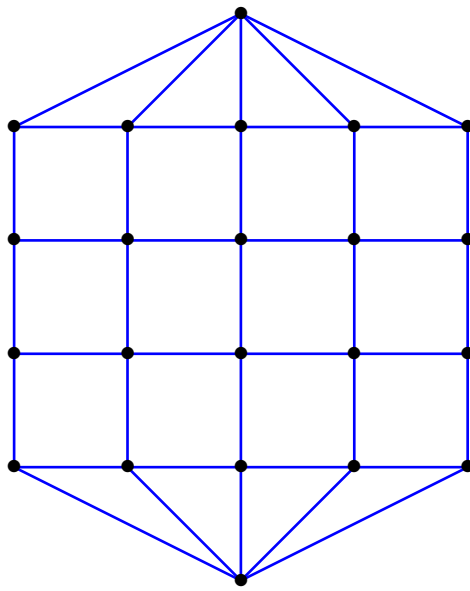


Figure 8: Square-lattice strip $\widehat{S}_{5,4}$ of width $m = 5$ and length $n = 4$ with extra sites at top and bottom.

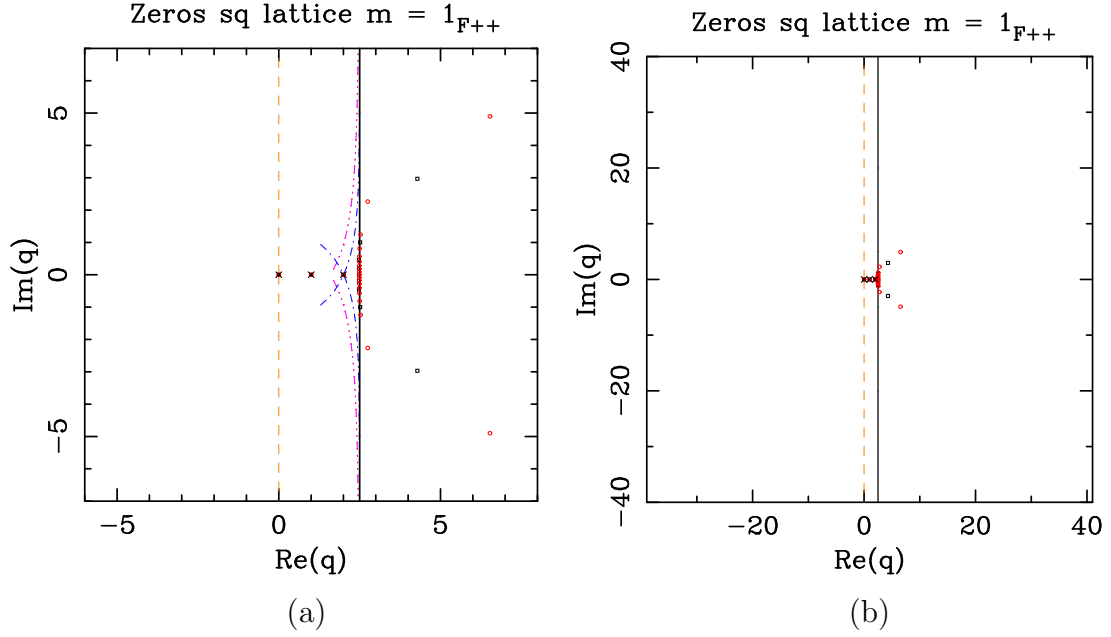


Figure 9: Limiting curves for square-lattice strips of width $m = 1$ with two extra sites. We also show the zeros for the strips $S_{1,10}$ (black \square) and $S_{1,20}$ (red \circ). We depict the isolated limiting points with the symbol \times . The zeroth-, first-, second- and third-order asymptotic expansions for the outward branches [cf. (7.14)] are depicted as dashed orange, dotted red, dot-dashed magenta, and dot-dot-dot-dashed blue curves, respectively. Please note that for $m = 1$ the first- and second-order asymptotics coincide, as the term of order q^{-2} has the factor $\sin[(2k - 1)\pi] = 0$.

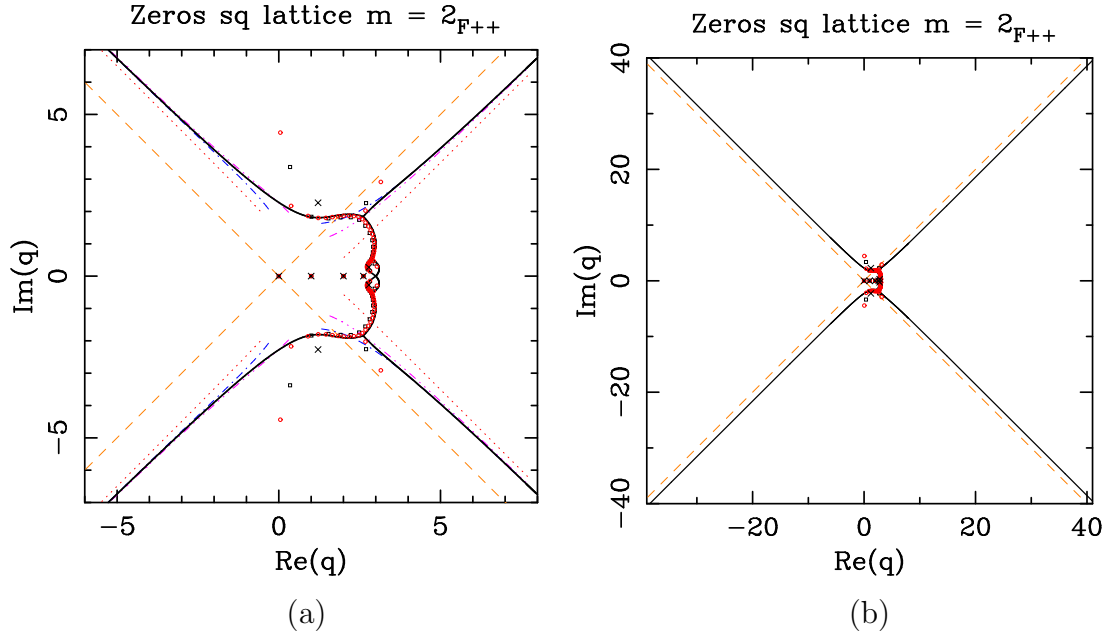


Figure 10: Limiting curves for square-lattice strips of width $m = 2$ with two extra sites. We also show the zeros for the strips $S_{2,20}$ (black \square) and $S_{2,40}$ (red \circ). We depict the isolated limiting points with the symbol \times . The zeroth-, first-, second- and third-order asymptotic expansions for the outward branches [cf. (7.14)] are depicted as dashed orange, dotted red, dot-dashed magenta, and dot-dot-dot-dashed blue curves, respectively.

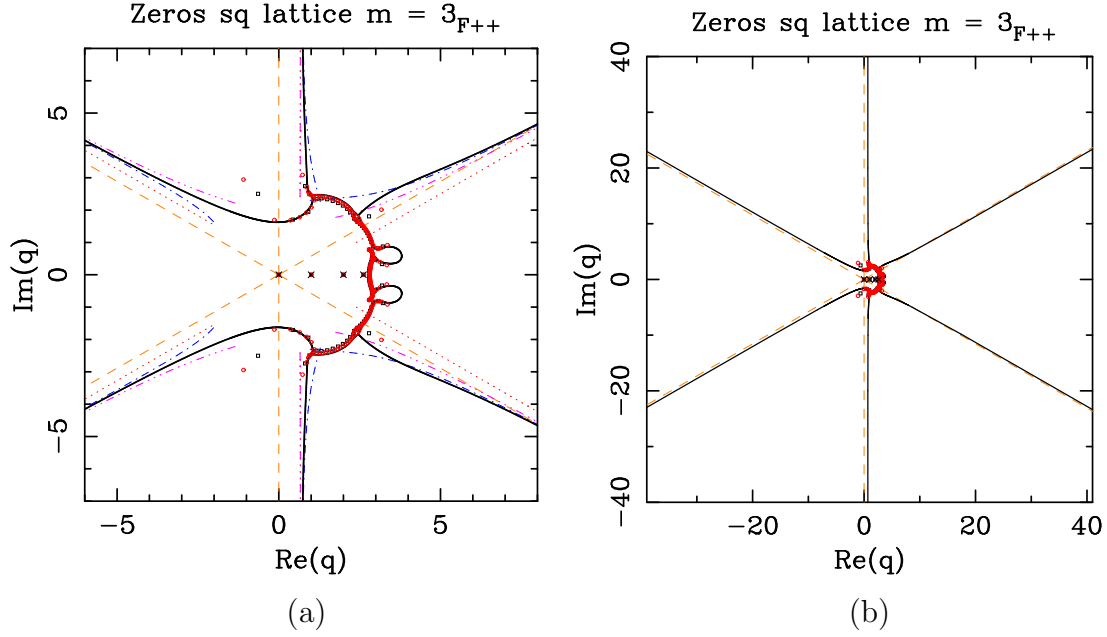


Figure 11: Limiting curves for square-lattice strips of width $m = 3$ with two extra sites. We also show the zeros for the strips $S_{3,30}$ (black \square) and $S_{3,60}$ (red \circ). We depict the isolated limiting points with the symbol \times . The zeroth-, first-, second- and third-order asymptotic expansions for the outward branches [cf. (7.14)] are depicted as dashed orange, dotted red, dot-dashed magenta, and dot-dot-dot-dashed blue curves, respectively. Please note that for $m = 3$ and $k = 2, 5$, the first- and second-order asymptotics coincide, as the term of order q^{-2} has the factor $\sin[(2k - 1)\pi/3] = 0$, which vanishes for $k = 2, 5$.

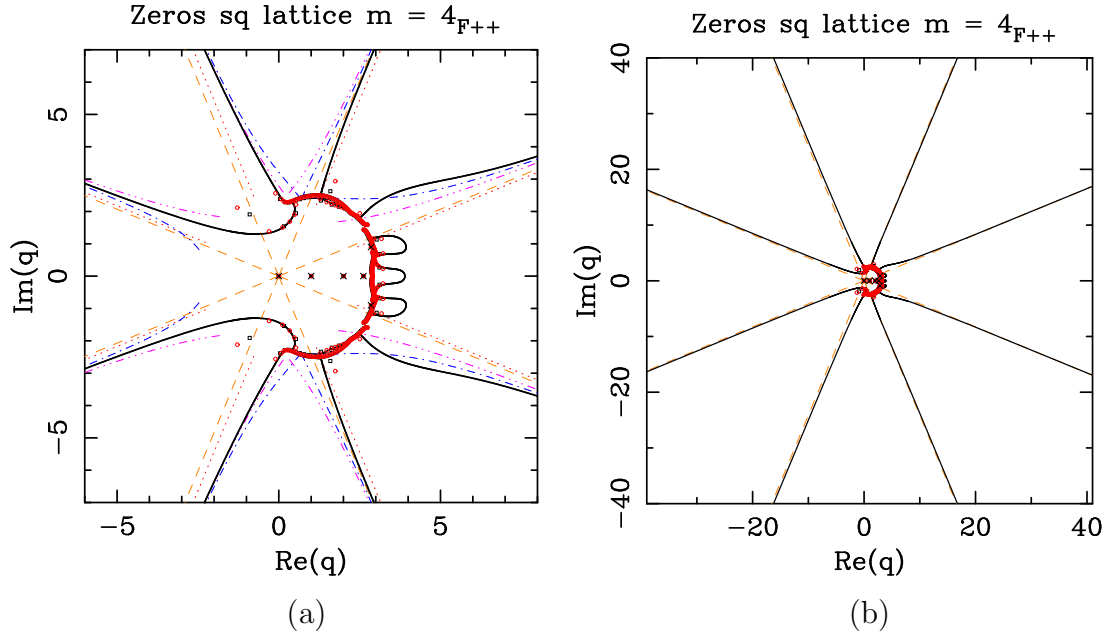


Figure 12: Limiting curves for square-lattice strips of width $m = 4$ with two extra sites. We also show the zeros for the strips $S_{4,40}$ (black \square) and $S_{4,80}$ (red \circ). We depict the isolated limiting points with the symbol \times . The zeroth-, first-, second- and third-order asymptotic expansions for the outward branches [cf. (7.14)] are depicted as dashed orange, dotted red, dot-dashed magenta, and dot-dot-dot-dashed blue curves, respectively.

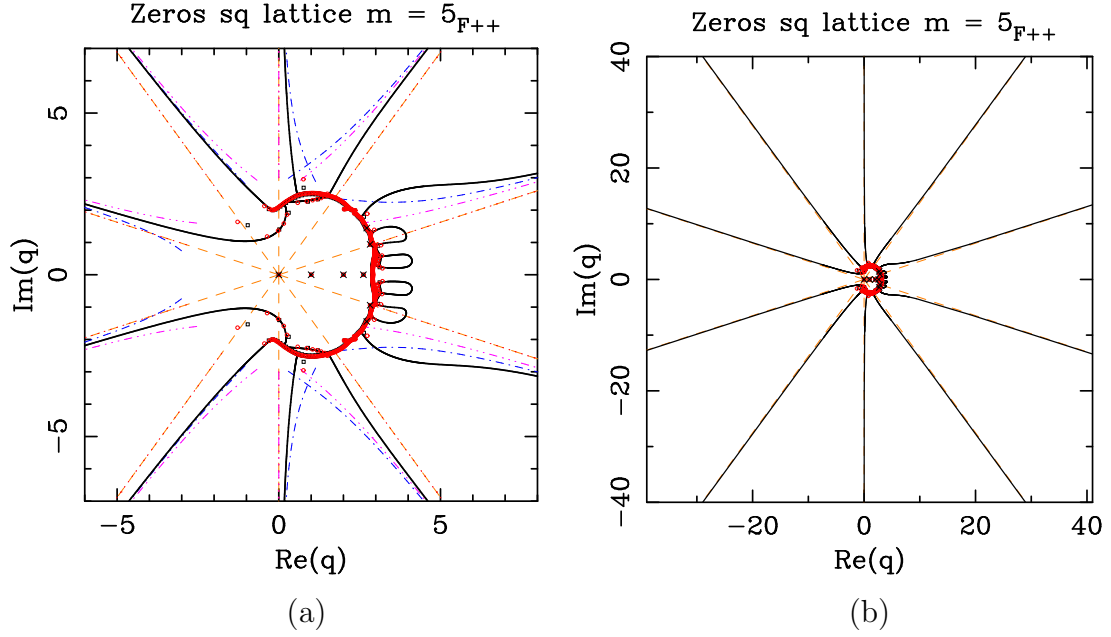


Figure 13: Limiting curves for square-lattice strips of width $m = 5$ with two extra sites. We also show the zeros for the strips $S_{5,50}$ (black \square) and $S_{5,100}$ (red \circ). We depict the isolated limiting points with the symbol \times . The zeroth-, first-, second- and third-order asymptotic expansions for the outward branches [cf. (7.14)] are depicted as dashed orange, dotted red, dot-dashed magenta, and dot-dot-dot-dashed blue curves, respectively. Please note that for $m = 5$ the zeroth- and first-order asymptotics coincide, as the term of order q^{-1} has the factor $f_1(5) = 0$.

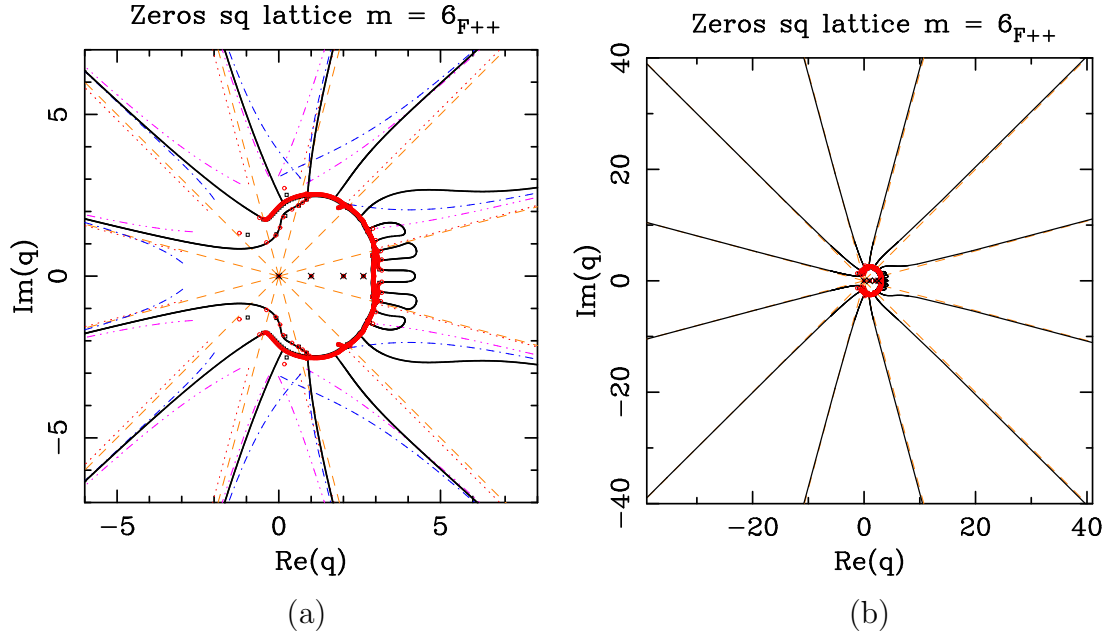


Figure 14: Limiting curves for square-lattice strips of width $m = 6$ with two extra sites. We also show the zeros for the strips $S_{6,60}$ (black \square) and $S_{6,120}$ (red \circ). We depict the isolated limiting points with the symbol \times . The zeroth-, first-, second- and third-order asymptotic expansions for the outward branches [cf. (7.14)] are depicted as dashed orange, dotted red, dot-dashed magenta, and dot-dot-dot-dashed blue curves, respectively.

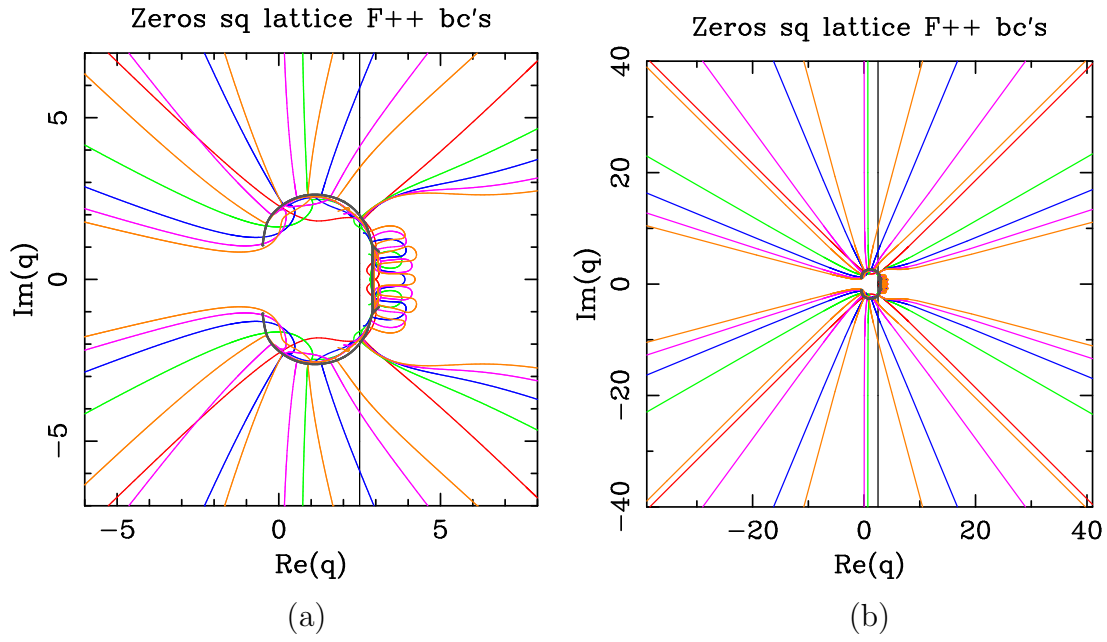


Figure 15: Limiting curves \mathcal{B}_m for square-lattice strips $S_{m,n}$ of widths $m = 1$ (black), $m = 2$ (red), $m = 3$ (green), $m = 4$ (blue), $m = 5$ (pink) and $m = 6$ (orange) with two extra sites. The solid dark gray curve corresponds to the limiting curve $\mathcal{B}_{11}^{\text{cyl}}$ for a strip of width $m = 11$ with *cylindrical* boundary conditions [34].

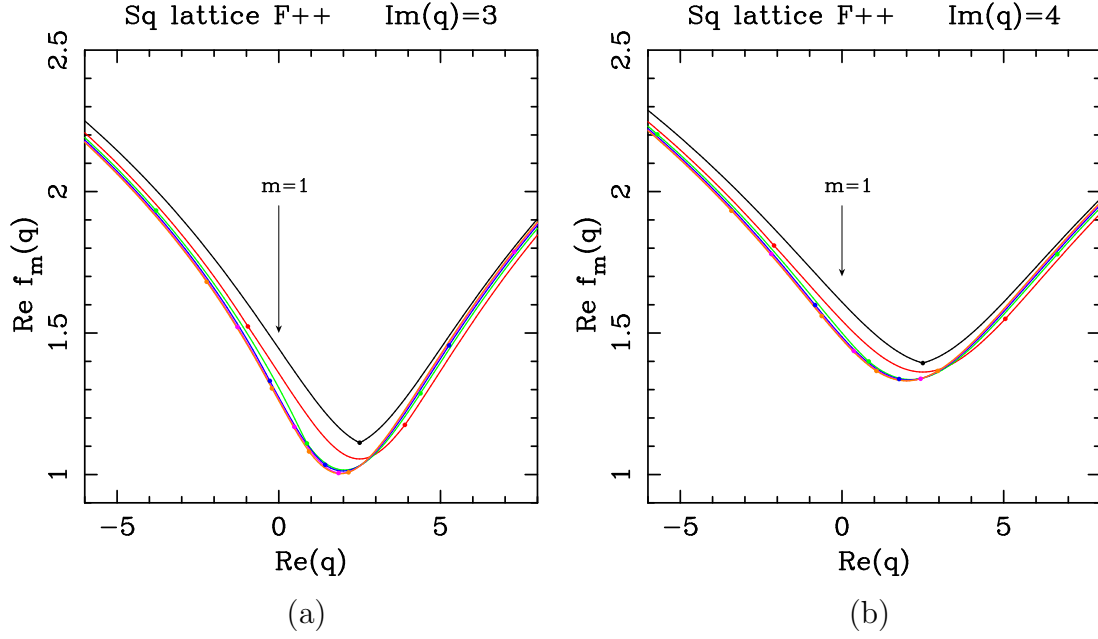


Figure 16: Real part of the free energy $\text{Re } f_m(q)$ [cf. (5.2)] for square-lattice strips $S_{m,n}$ of width m (and length $n \rightarrow \infty$) as a function of $\text{Re } q$, for (a) $\text{Im } q = 3$ and (b) $\text{Im } q = 4$. Widths are $m = 1$ (black), $m = 2$ (red), $m = 3$ (green), $m = 4$ (blue), $m = 5$ (pink) and $m = 6$ (orange). The solid dots show the points of discontinuity in the derivative of the free energy.

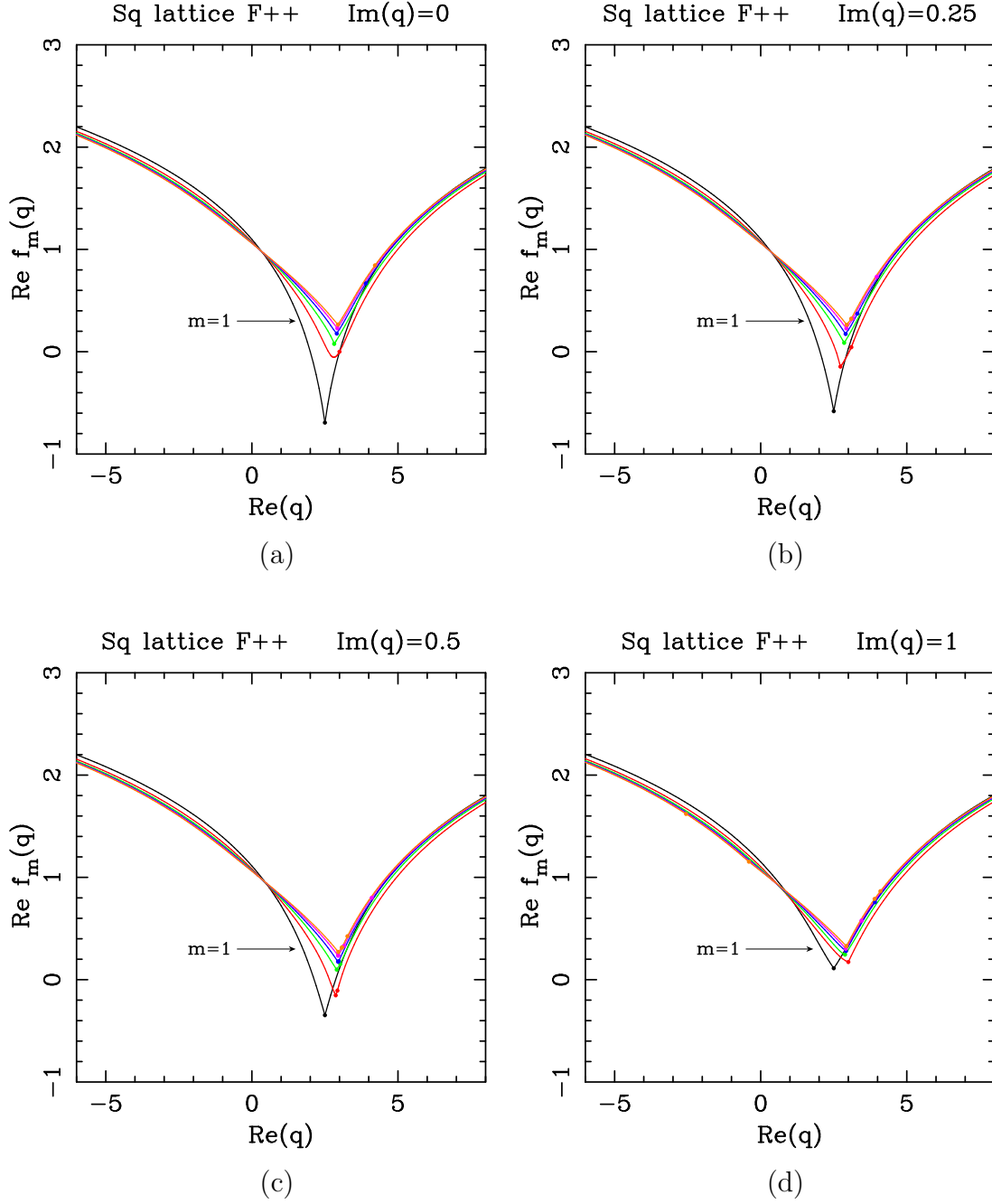


Figure 17: Real part of the free energy $\text{Re } f_m(q)$ [cf. (5.2)] for square-lattice strips $S_{m,n}$ of width m (and length $n \rightarrow \infty$) as a function of $\text{Re } q$, for (a) $\text{Im } q = 0$, (b) $\text{Im } q = 0.25$, (c) $\text{Im } q = 0.5$ and (d) $\text{Im } q = 1$. Widths are $m = 1$ (black), $m = 2$ (red), $m = 3$ (green), $m = 4$ (blue), $m = 5$ (pink) and $m = 6$ (orange). The solid dots show the points of discontinuity in the derivative of the free energy.

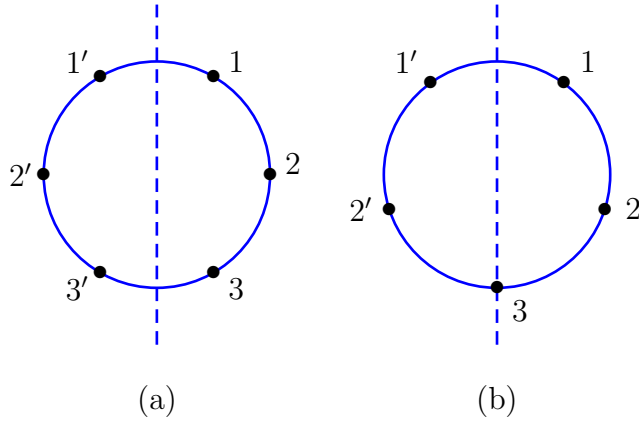


Figure 18: Vertex labels used in the proof of Proposition B.2, for (a) m even and (b) m odd. Vertices with a prime are obtained from the corresponding unprimed vertices by reflection \mathcal{R}_2 . When $m = 2\ell + 1$ is odd, the extra vertex (which is invariant under reflection) is denoted $\ell + 1$.